Molecular Basis for G-protein-Coupled Receptor (GPCR) Activation and Biased Signalling at the Platelet Thrombin Receptor Proteinase Activated Receptor-4 (PAR4).

Pierre E. Thibeault[1], Jordan C. LeSarge[2], D'Arcy Arends[1], Michaela Fernandes[2], Peter Chidiac[1], Peter B. Stathopulos[1], Leonard G. Luyt[2,3,4], and Rithwik Ramachandran[1*]

[1)] Department of Physiology and Pharmacology, University of Western Ontario, London, ON, N6A5C1, Canada.

[2)] Department of Chemistry, The University of Western Ontario, London, ON, N6A5C1, Canada.

[3)] Departments of Oncology, The University of Western Ontario, London, ON, N6A5C1, Canada.

[4)] London Regional Cancer Program, Lawson Health Research Institute, London, ON, N6C2R5, Canada.

* For correspondence:

Rithwik Ramachandran,
Department of Physiology and Pharmacology,
Schulich School of Medicine and Dentistry,
University of Western Ontario, London,
Ontario, Canada.
Phone: 519-661-2142
email: rramach@uwo.ca

Abstract:
Proteinase Activated Receptor-4 (PAR4) is a member of the proteolytically-activated PAR family of G-Protein-coupled Receptors (GPCRs). PARs are activated following proteolytic cleavage of the receptor N-terminus by enzymes such as thrombin, trypsin, and cathepsin-G to reveal the receptor-activating motif termed the tethered ligand. The tethered ligand binds intramolecularly to the receptor and triggers receptor signalling and cellular responses. In spite of this unusual mechanism of activation, PARs are fundamentally peptide receptors and can also be activated by exogenous application of short synthetic peptides derived from the tethered ligand sequence. In order to gain a better understanding of the molecular basis for PAR4-dependent signalling, we examined signalling responses to a library of peptides derived from the canonical PAR4 activating peptide (PAR4-AP), AYPGKF-NH_2. We examined peptide residues involved in activation of the $G\alpha_{q/11}$-coupled calcium signalling pathway, β-arrestin recruitment, and mitogen-activated protein kinase pathway activation. The peptide *N*-methyl-alanine-YPGKF-NH_2 was identified as a compound that is a poor activator of PAR4-dependent calcium signalling but was fully competent in recruiting β-arrestin-1 and -2. In order to gain a better understanding of the ligand-binding pocket, we used *in silico* docking to identify key residues involved in PAR4 interaction with AYPGKF-NH_2. The predicted interactions were verified by site-directed mutagenesis and analysis of calcium signalling and β-arrestin-1/-2 recruitment following proteolytic activation (with thrombin) or activation with the synthetic agonist peptide (AYPGKF-NH_2). We determined that a key extracellular loop-2 aspartic acid residue (Asp^{230}) is critical for signalling following both proteolytic and peptide activation of PAR4. Finally, we investigated platelet aggregation in response to A**y**PGKF-NH_2 (a peptide with D-tyrosine in position two) which is unable to activate calcium signalling, and AYPG**R**F-NH_2 a peptide that is equipotent to the parental peptide AYPGKF-NH_2 for calcium signalling but is more potent at recruiting β-arrestins. We found that A**y**PGKF-NH_2 fails to activate platelets while AYPG**R**F-NH_2 causes a platelet aggregation response that is greater than that seen with the parental peptide and is comparable to that seen with thrombin stimulation. Overall, these studies uncover molecular determinants for agonist binding and signalling through a non-canonically activated GPCR and provide a template for development of small molecule modulators of PAR4.

Introduction:

G-Protein-coupled receptors (GPCRs) are the largest family of cell surface receptors and regulate a host of important physiological responses (Fredriksson and Schioth, 2005; Pierce et al., 2002). GPCRs respond to a variety of extracellular signals and regulate cellular behaviour through engaging intracellular effector molecules to activate various cell-signalling pathways (Erlandson et al., 2018; Hilger et al., 2018). In drug discovery, GPCRs are a valuable and highly tractable class of drug targets with over 30% of all currently approved drugs acting on GPCRs (Sriram and Insel, 2018). GPCR activation occurs typically through binding of a soluble ligand and conformational changes that enable engagement of G-protein-dependent or β-arrestin-mediated signal transduction. The Proteinase Activated Receptors (PARs) are a four-member family of GPCRs with a distinct mechanism of activation that involves limited proteolysis and unmasking of a receptor activating motif called the tethered ligand. PARs were first discovered in an effort to identify the cellular receptors responsible for actions of thrombin that were independent from its role in the coagulation cascade (Vu et al., 1991). Various proteinases have now been described as activators of the different members of the PAR family, but canonically PAR1 and PAR4 are described as thrombin-activated receptors, while PAR2 is activated by trypsin and other trypsin-like serine proteinases. PAR4 can also be activated by trypsin. Whether PAR3 signals independently is unclear, though thrombin can cleave the PAR3 N-terminus to reveal a tethered ligand (Adams et al., 2011; Ishihara et al., 1997). Following the discovery of PARs it was quickly realized that two receptors, PAR1 and PAR4, serve as the thrombin receptors on human platelets (Coughlin, 2005, 1999). PAR1 and PAR4 both trigger platelet activation and aggregation. Given that anti-platelet agents are an important class of drugs for the treatment of various cardiovascular diseases, there has been a concerted effort aimed at understanding the role of these receptors in platelet activation and in identifying molecules that can act as PAR1 and PAR4 antagonists. A PAR1 antagonist was recently identified and approved for clinical use, however significant bleeding side effects were noted in patients administered this drug (Morrow et al., 2012, 2009; Scirica et al., 2012). While bleeding is a frequently encountered side effect of therapeutically targeting pathways involved in blood coagulation, it was hoped that targeting PAR1 would not present such liability. Much attention has now shifted to understanding and targeting the other thrombin receptor PAR4. Though both PAR1 and PAR4 are activated by thrombin, there are some key differences reported in the activation of these two receptors on platelets that argue for PAR4 being a better anti-platelet drug target than PAR1. PAR1 possesses a hirudin-like binding site that enables it to bind thrombin with relatively high affinity (Jacques et al., 2000; Liu et al., 1991). In lacking this thrombin-binding site, PAR4 can only be activated at much higher concentrations of thrombin, such as may be encountered on a growing platelet thrombus. There are also reported differences in the kinetics of PAR1 and PAR4-dependent calcium signalling, with PAR4 causing a delayed but more sustained signal compared to PAR1 (Shapiro et al., 2000). This is thought to be due to dual proline residues in the PAR4 exodomain that provide low-affinity interactions with the thrombin active site and an anionic cluster that slows dissociation from thrombin (Jacques and Kuliopulos, 2003). Overall, PAR1 is thought to initiate platelet activation in response to low concentrations of thrombin while PAR4 is engaged at higher concentrations to further consolidate and stabilize the clot.

102 Given the liabilities seen with targeting PAR1 as a platelet thrombin receptor there has been
103 renewed interest in developing small molecule PAR4 antagonists (Rwibasira Rudinga et al.,
104 2018; Wu et al., 2000; Young et al., 2010). Recently small molecule antagonists of PAR4 have
105 been described with efficacy in inhibiting injury induced thrombosis in both non-human
106 primates and humans (Miller et al., 2019; Wilson et al., 2017; Wong et al., 2017). Despite these
107 promising advances there remains the question of whether a complete inhibition of PAR4 might
108 also lead to bleeding liability. Our efforts have therefore focused on examining biased
109 signalling through PAR4 in order to identify pathways that are responsible for platelet
110 aggregation and that could be selectively manipulated for therapeutic efficacy. PAR4 can
111 activate multiple signalling pathways through coupling to $G\alpha_{q/11}$, $G\alpha_{12/13}$ and β-arrestin
112 (Holinstat et al., 2006; Li et al., 2011; Ramachandran et al., 2017). In previous work, we and
113 others showed that pepducins targeting different intracellular motifs in PAR4 could be
114 employed to differentially inhibit platelet activation by blocking G-protein-coupled or β-
115 arrestin-dependent signalling (Covic et al., 2002; Ramachandran et al., 2017). The ability to
116 selectively activate or inhibit GPCR signalling in a biased manner is of great interest and has
117 been proposed as a strategy for obtaining therapeutically superior drugs for a number of
118 conditions (Bar-Shavit et al., 2016; Hollenberg et al., 2014; Seyedabadi et al., 2019). In the
119 case of the finely balanced signalling systems involved in coagulation and platelet activation,
120 such subtle perturbations may be key to obtaining drugs which do not result in bleeding
121 liability.
122
123 Here we seek to gain an understanding of the molecular interactions responsible for agonist
124 docking to PAR4 and to identify interactions that can be manipulated to obtain biased ligands
125 for PAR4. By screening a peptide library derived from the most widely used PAR4 agonist
126 peptide, AYPGKF-NH_2, we have identified key residues that confer selective activation of
127 $G\alpha_{q/11}$ coupled calcium signalling and/or β-arrestin recruitment. Through *in silico* docking and
128 confirmatory mutagenesis experiments we further identify an extracellular loop 2 residue
129 (Asp^{230}) that is critical for receptor activation and signalling. We also examine platelet
130 activation by peptides that show differential activation of PAR4 signalling. Overall, these
131 studies advance our understanding of PAR4 activation and signalling and will help guide future
132 drug discovery efforts targeting this receptor.

133 **Results:**

134 **Experimental design and data analysis.** In order to understand the rules governing agonist
135 peptide activation of PAR4 we synthesized 37 hexapeptides through modification to the
136 synthetic PAR4 agonist peptide AYPGKF-NH_2. A number of different modifications were
137 examined at each of the six positions, including alanine, D-isomer, and *N*-methyl substitutions,
138 as well as other modifications aimed at further probing each of the six agonist peptide positions.
139 Henceforth, the parental PAR4 agonist peptide for this study, AYPGKF-NH_2 (Ala^1-Tyr^2-Pro^3-
140 Gly^4-Lys^5-Phe^6-NH_2; superscript denotes position from N-terminus), will be referred to as
141 PAR4-AP. $G\alpha_{q/11}$-coupled calcium signalling, β-arrestin-1/-2 recruitment (β-Arr-1-rluc, β-
142 Arrestin-2-rluc respectively), and p44/42 mitogen-activated protein kinase (MAPK) signalling
143 by each of these peptides was monitored and compared to responses triggered by PAR4-AP
144 (Table 1). Whereas PAR4-AP triggered $G\alpha_{q/11}$ signalling reached a clear plateau over the range
145 of concentrations tested (0.3 – 300 μM), β-arrestin recruitment did not and therefore the
146 effective concentration required to achieve half-maximal response (EC_{50}) values could not be
147 accurately assessed. In contrast, with the substituted peptides, $G\alpha_{q/11}$ signalling concentration-
148 effect curves in some cases did not clearly plateau, whereas β-arrestin recruitment did. Where
149 possible, EC_{50} values are compared between PAR4-AP and substituted peptides. However,
150 since clear maxima were not always obtained, comparisons of signal magnitude throughout the
151 present study are presented as the response elicited by a given compound at 100 μM, shown as
152 a percentage of responses elicited by PAR4-AP at the same concentration. Since the
153 concentration-effect curve for PAR4-AP exhibits a saturating calcium signal, peptides that
154 failed to saturate calcium signalling responses are depicted as having EC_{50} values that were
155 'not determined' (*n.d.*). Maximal calcium signal responses are shown as a percentage of the
156 response obtained with the calcium ionophore A23187 (Table 1, Max; % of A23187 calcium
157 ionophore) and are referred to throughout the results as a change in maximal calcium signalling
158 as a measure of the efficacy of the peptides. Throughout the results, β-arrestin recruitment
159 values are presented as a percentage (%) of the PAR4-AP-induced recruitment at 100 μM
160 concentration. For ease of comparison, concentration-effect curves for PAR4-AP-mediated
161 $G\alpha_{q/11}$ calcium signalling and β-arrestin recruitment are displayed as a repeated reference value
162 in each of the Figures 1 through 7.
163

164 **Effect of alanine substitution on PAR4-AP-mediated signalling responses.** Our first set of
165 changes involved alanine substitutions at positions 2-6 of the PAR4-AP (calcium EC_{50} = 12.1
166 ± 3.1 μM; β-arrestin-1 recruitment at 100 μM for comparison is considered 100 ± 3.9%, and
167 100 ± 3.5% for β-arrestin-2) (Fig. 1, Table 1). Potency was decreased with respect to calcium
168 signalling when $tyrosine^2$ was substituted with alanine and failed to reach a plateau over the
169 concentration range tested (A**A**PGKF-NH_2; EC_{50} = *n.d.*). Correspondingly, β-arrestin
170 recruitment was reduced compared to PAR4-AP at the same concentration (β-arr-1 47.3 ±
171 3.6%; β-arr-2 46.4 ± 3.2%). Substitution of $proline^3$ with alanine resulted in a significant
172 decrease in potency for calcium signalling (AY**A**GKF-NH_2 EC_{50} = 63.7 ± 20.8 μM) and yielded
173 reduced β-arrestin recruitment (β-arr-1 48.5 ± 7.9%; β-arr-2 43.4 ± 7.1%). Either $glycine^4$ or
174 $phenylalanine^6$ substitution to alanine resulted in modest decreases in maximal calcium

signalling compared to PAR4-AP at the same concentration, with no significant effect on potency (EC_{50} = 21.2 ± 6.6 μM; EC_{50} = 17.3 ± 5.0 μM, respectively). Additionally, alanine substitutions in these positions resulted in significantly reduced β-arrestin recruitment, to levels approximately half of those observed with PAR4-AP (AYP**A**KF-NH_2 β-arr-1 56.4 ± 5.6%, β-arr-2 54.6 ± 5.1%; AYPGK**A**-NH_2 β-arr-1 47.9 ± 3.8%, β-arr-2 52.6 ± 3.5%). Interestingly, we observed that lysine[5] to alanine substitution had no appreciable impact on potency with respect to calcium signalling (AYPG**A**F-NH_2 EC_{50} = 9.8 ± 2.9 μM); and modestly reduced recruitment of β-arrestin-1 (59.3 ± 7.2%) and -2 (70.8 ± 6.5%). Collectively, alanine substitutions of positions 2-6 resulted in decreased β-arrestin recruitment compared to the parental peptide (Fig. 1 B. and C.; Table 1). Interestingly, we observe differential effects on calcium signalling with significant detriment to potency attributed to tyrosine substitution (Fig. 1 A.). Additionally, substitution of glycine and phenylalanine moderately decreased maximal calcium signalling responses, perhaps indicating that these residues are important for full agonism of this pathway comparative to that achieved with the parental peptide. Notably, all single alanine substitutions of positions 2-6 of the PAR4-AP retained some agonist activity indicating that signalling is not wholly reliant on any single residue alone.

Effect of D-isomer amino acid substitutions on PAR4-AP-mediated signalling responses. To assess the impact of stereochemical inversion at each residue we generated five peptides with single amino acid substitutions to their respective D-isomers (Fig. 2, Table 1). Glycine possesses only one isomeric form and thus is not substituted. Both L-alanine to D-alanine (**a**YPGKF-NH_2) and L-lysine to D-lysine (AYPG**k**F-NH_2) substitutions resulted in significant losses of potency in calcium signalling assays compared to PAR4-AP. Consistent with calcium data, we observed a significant decrease in β-arrestin recruitment compared to the parental PAR4-AP (**a**YPGKF-NH_2 β-arr-1 48.7 ± 2.6%, β-arr-2 47.5 ± 2.4%; AYPG**k**F-NH_2 β-arr-1 47.4 ± 1.0%, β-arr-2 36.5 ± 0.9%). Interestingly, both D-tyrosine (A**y**PGKF-NH_2) and D-proline (AY**p**GKF-NH_2) substitutions completely abolished calcium signalling. Comparably, β-arrestin recruitment was significantly reduced with stimulation by either peptide (A**y**PGKF-NH_2 β-arr-1 50.7 ± 4.6%, β-arr-2 46.4 ± 4.2%; AY**p**GKF-NH_2 β-arr-1 45.2 ± 10.5%, β-arr-2 38.1 ± 9.5%). In keeping with what we observed with phenylalanine to alanine substitution (Fig. 1), D-phenylalanine substitution in position 6 (AYPGK**f**-NH_2) resulted in less efficacious agonism of both calcium (EC_{50} = 22.2 ± 4.7 μM) and β-arrestin recruitment (β-arr-1 80.3 ± 6.6%, β-arr-2 74.1 ± 6.0%). Overall, D-isomers substitutions of amino acids alanine[1], tyrosine[2], proline[3], and lysine[5] all result in significant reduction of (D-alanine, D-lysine) or abolition of (D-tyrosine, D-proline) calcium signalling while causing significant reductions in β-arrestin recruitment. Substitution of L-phenylalanine[6] for D-phenylalanine was the only D-isomer substitution that is somewhat tolerated, resulting in modest reductions in potency with respect to both calcium signalling and β-arrestin recruitment. These data reveal that the sidechain stereochemistry of residues within the AYPGKF-NH_2 peptide perform a role in agonism.

Effect of *N*-methylation on PAR4-AP-mediated signalling responses. We generated a series of peptides to investigate the pharmacological impact of *N*-methylation along the peptide backbone (Fig. 3, Table 1). In contrast to the parental PAR4-AP, all but one of the N-methylated peptides evaluated yielded clear plateaus and discernible EC_{50} values in β-arrestin

219 recruitment assays, and where applicable these are indicated below along with their relative
220 responses compared to PAR4-AP at 100 μM. Substitution of alanine[1] with *N*-methyl-alanine
221 [**(*N*-Me-A)**-YPGKF-NH_2] almost completely abolished calcium signalling (EC_{50} = *n.d.*).
222 Interestingly, this peptide was able to initiate β-arrestin-1/-2 recruitment comparable to levels
223 obtained with PAR4-AP (β-arr-1 119.2 ± 11.9%, EC_{50} = 6.8 ± 2.6 μM; β-arr-2 80.6 ± 10.8%;
224 EC_{50} = 2.0 ± 0.7 μM). These results suggest that increasing steric bulk and hydrophobicity of
225 the backbone at amide positions through the addition of an N-terminal methyl group drives
226 PAR4 signalling towards β-arrestin pathways and causes only modest activation of calcium
227 signalling. Substitution of tyrosine[2] for *N*-methyl-tyrosine [A-**(*N*-Me-Y)**-PGKF-NH_2]
228 abolished calcium signalling up to 300 μM (EC_{50} = *n.d.*). Consistent with calcium signalling,
229 we observed decreased signal magnitude in β-arrestin recruitment assays compared to PAR4-
230 AP (β-arr-1 71.4 ± 10.8%, EC_{50} = 14.2 ± 8.6 μM; β-arr-2 61.5 ± 9.8%, EC_{50} = 11.8 ± 5.7 μM).
231 Substitution of the PAR4-AP glycine[4] with sarcosine (Sar., a.k.a *N*-methyl-glycine; AYP-**Sar**-
232 KF-NH_2) resulted in significantly reduced calcium potency (EC_{50} = *n.d.*) and significantly
233 reduced β-arrestin-1/-2 recruitment (35.9 ± 4.3%, 36.1 ± 3.9% respectively). *N*-methylation of
234 the alpha (α) amine of lysine[5] [AYPG-**(N_α-Me-K)**-F-NH_2] resulted in significantly reduced
235 calcium signalling (EC_{50} = *n.d.*) with no significant effect on maximal β-arrestin recruitment
236 (β-arr-1 126.7 ± 18.6%, EC_{50} = 12.2 ± 4.3 μM; β-arr-2 77.1 ± 16.9%, EC_{50} = 2.5 ± 1.0 μM).
237 Substitution of phenylalanine[6] with *N*-methyl-phenylalanine [AYPGK-**(*N*-Me-F)**-NH_2] was
238 equipotent for calcium signalling compared to PAR4-AP (EC_{50} = 7.6 ± 1.9 μM). Interestingly,
239 this peptide showed increased recruitment of both β-arrestins (β-arr-1 136.9 ± 18.0%, EC_{50} =
240 10.4 ± 3.3 μM; β-arr-2 96.6 ± 16.4%, EC_{50} = 15.3 ± 4.6 μM). Together, these data reveal that
241 *N*-methylation of positions 1, 2, 4, and 5 are deleterious to calcium signalling.
242
243 We were excited to observe evidence of β-arrestin-biased peptides within this group, all of
244 which showed decreased calcium signalling and/or increased β-arrestin recruitment. Moreover,
245 the leftward shifts in their associated β-arrestin concentration-effect profiles imply that
246 substitution of *N*-methylated alanine[1], tyrosine[2], lysine[5], or phenylalanine[6] residues increases
247 peptide potency with respect to G-protein-independent signalling. Only *N*-methylation of
248 glycine[4] (sarcosine) resulted in a reduced overall ability to activate PAR4, with relative calcium
249 and β-arrestin signals being reduced by approximately 90% and 60%, respectively.
250
251 **Effect of N-terminal and position 1 modifications on PAR4-AP-mediated signalling**
252 **responses.** To further investigate the impact of *N*-terminal alterations to the PAR4-AP we
253 examined the impact of N-terminal acetylation and substitutions of position 1 (Fig. 4, Table 1).
254 Previously it was demonstrated that protonation of the N-terminus of the PAR1 tethered ligand
255 (SFLLRN) is critical for agonist function (Scarborough et al., 1992). Additionally, substitution
256 of glycine for mercaptoproprionic acid (Mpr), which lacks an amino-terminal protonated amine
257 found in the native tethered-ligand-mimicking peptide GYPGQV, resulted in complete loss of
258 agonist activity (Faruqi et al., 2000). Given the evidence for N-terminal protonation in PAR
259 agonism, we sought to determine the impact of N-terminal acetylation on PAR4-AP activity.
260 N-terminal acetylation of the PAR4-AP (**Ac**-AYPGKF-NH2) negatively impacted both
261 calcium signalling (EC_{50} = *n.d.*) as well as the magnitude of β-arrestin recruitment to PAR4 as

expected (β-arr-1 47.3 ± 3.1%, EC_{50} = 15.0 ± 4.3 μM; β-arr-2 45.5 ± 2.8%, EC_{50} = 26.7 ± 5.6 μM). In contrast to the previously reported complete loss of activity with Mpr-YPGQV peptide (Mpr = mercaptopropionic acid), we observed partial agonism with the loss of protonation through acetylation of PAR4-AP. This could also be influenced by the additional methyl group of the Ala in Ac-AYPGKF-NH2, which is not present in the Mpr-YPGQV peptide.

In both the native human PAR4 tethered-ligand sequence and the PAR4-AP, position 1 is occupied by small (tethered ligand – glycine, PAR4-AP – alanine) and non-polar (PAR4-AP – alanine) residues. To investigate the role of position 1 in the PAR4-AP, we generated seven peptides with position 1 substitutions. Introduction of steric bulk and increased hydrophobicity through substitution of alanine[1] for valine resulted in partial agonism of both calcium signalling and β-arrestin recruitment (**V**YPGKF-NH_2 EC_{50} = 22.9 ± 8.3 μM; β-arr-1 73.6 ± 13.0%, EC_{50} = 33.8 ± 13.7 μM; β-arr-2 55.2 ± 11.8%, EC_{50} = 13.7 ± 8.2 μM). Additionally, increasing hydrophobic bulk at position 1 through substitution with norleucine completely abolished calcium signalling (**Nle**-YPGKF-NH_2, EC_{50} = *n.d.*) and resulted in partial agonism of β-arrestin recruitment (β-arr-1 40.2 ± 9.7%; β-arr-2 36.5 ± 8.8%). Together, data from these substitutions indicate that the precise steric bulk of the side chain in position 1 is important for PAR4 agonism.

Next, we evaluated the impact of steric bulk relocation in position 1. Relocation of the methyl group in alanine to the N-terminus and loss of side chain through substitution with sarcosine (**Sar**-YPGKF-NH_2) resulted in poor agonism at both calcium signalling (EC_{50} = *n.d.*) and β-arrestin recruitment (β-arr-1 35.6 ± 2.0%, β-arr-2 39.8 ± 1.8%). Further, the addition of an α-methyl group through substitution of alanine[1] with 2-aminoisobutyric acid (**Aib**-YPGKF-NH_2) resulted in a significantly less potent partial agonist for calcium signalling (EC_{50} = 50.2 ± 15.3 μM) and also resulted in a significant reduction in β-arrestin recruitment (β-arr-1 38.6 ± 3.9%; β-arr-2 37.3 ± 3.6%). Similarly, replacement with *N*-methyl-serine [**(N-Me-S)**-YPGKF-NH_2] also caused a significant attenuation of calcium signalling (EC_{50} = *n.d.*), while also revealing a decrease in β-arrestin recruitment compared to PAR4-AP (β-arr-1 78.1 ± 6.9%, β-arr-2 51.7 ± 6.3%). Thus, it is apparent that the precise position of the side chain in position 1 is important for agonism.

To further probe the importance of charge localization at the N-terminal region of the peptide, we made several additional substitutions to position 1. Substitution of alanine with either beta-alanine or isonipecotic acid significantly reduced the potency and activity of the PAR4-AP, similar to the results with PAR4-AP N-terminal acetylation (**betaAla**-YPGKF-NH2 calcium EC_{50} = *n.d.*, β-arr-1 25.7 ± 4.8%, β-arr-2 31.8 ± 4.4%; **Inp**-YPGKF-NH_2 calcium EC_{50} = *n.d.*, β-arr-1 32.0 ± 3.3%, β-arr-2 26.9 ± 3.0%). Together these data suggest a role for N-terminal charge localization in agonist activity.

Effect of additional substitutions in positions 2-4 on PAR4-AP-mediated signalling. Previously, structure activity studies with PAR4 activating peptides revealed an apparent requirement for an aromatic residue in position 2 (tyrosine) and found that alterations to position 3 (proline) and position 4 (glycine) were not well tolerated (Faruqi et al., 2000). In the

306 present study, we observed that substitution of either tyrosine, proline, or glycine with alanine
307 reduced calcium signalling potency and β-arrestin recruitment, however none of these
308 substitutions completely abolished the activity of the peptide (Fig. 1). Interestingly, substitution
309 of either L-tyrosine or L-proline with the respective D-isomer significantly reduced the activity
310 of the PAR4-AP (Fig. 2, Table 1). Together, these data suggest that while no individual residue
311 is strictly required for agonist activity, the side chains of these residues and their positioning
312 are important for agonist function. To further probe the contribution of these residues to the
313 PAR4-AP, we generated peptides with alterations in the aromatic side chain of position 2, the
314 backbone conformation of position 3, or position 4 (Fig. 5, Table 1).
315
316 Peptides with substitution of tyrosine[2] with either 4-fluoro-L-phenylalanine [A-**F(4-fluoro)**-
317 PGKF-NH2] or *O*-methyl-tyrosine [A-**Tyr(Me)**-PGKF-NH_2] retained calcium signalling and
318 β-arrestin recruitment with no significant changes in potency compared to the PAR4-AP. These
319 data suggest that the side chain of tyrosine may be a site in which further modifications can be
320 made to the peptide without affecting agonist potential; however, by comparing A**A**PGKF-
321 NH_2 the presence of an aromatic ring in position 2 is of importance. Given the results obtained
322 with alanine or D-proline substitution of proline[3] (Fig. 1 & 2, respectively), we furthered
323 probed conformational contributions of this residue to the parental PAR4-AP. Proline was
324 substituted with pipecolic acid (2-piperidinecarboxylic acid; Pip) which is structurally similar
325 to proline but has an increased steric bulk and backbone elongation provided by a six-
326 membered ring compared to the five-membered ring of proline. We observed partial agonism
327 of calcium signalling in response to AY-**Pip**-GKF-NH_2 stimulation with no significant
328 difference in agonist potency (EC_{50} = 30.7 ± 4.9 μM) with a correlating partial agonism of β-
329 arrestin recruitment (β-arr-1 38.8 ± 3.0%; β-arr-2 44.0 ± 2.7%). Thus, it appears that increasing
330 steric bulk/backbone length may affect efficacy but still results in agonism. To further
331 investigate the role of backbone conformation provided at position 3, proline was substituted
332 with nipecotic acid (3-piperidinecarboxylic acid; Nip) which is similar to pipecotic acid,
333 however, results in change of the peptide backbone direction (AY-**Nip**-GKF-NH_2). With this
334 modification, both calcium signalling (EC_{50} = *n.d.*) and β-arrestin recruitment (β-arr-1 32.9 ±
335 4.9%; β-arr-2 30.9 ± 4.5%) were significantly decreased in response to PAR4 stimulation.
336 Elongation of the backbone in position four (glycine) by substitution with beta-alanine (AYP-
337 **betaAla**-KF-NH_2) was also significantly detrimental to both calcium signalling (EC_{50} = *n.d.*)
338 and β-arrestin recruitment (β-arr-1 42.5 ± 1.8%, β-arr-2 24.9 ± 1.6%). Together these data
339 suggest an important role for backbone conformation contributed by proline[3] and glycine[4]
340 compactness in the PAR4-AP. As well, these data suggest peptide backbone length at proline[3]
341 and glycine[4] has an important role; consistent with what we have observed with backbone
342 elongation modifications at position 1 (**Inp**-YPGKF-NH_2 and **betaAla**-YPGKF-NH_2; Fig. 4,
343 Table 1).
344
345 **Effect of additional substitutions in position 5 on PAR4-AP-mediated signalling**
346 **responses.** Previously, investigations into glutamine substitutions in the native tethered ligand
347 mimicking peptide, GYPGQV, revealed that agonism is maintained when this position is
348 substituted with a charged residue such as arginine or ornithine (Faruqi et al., 2000). In the

present study, we have identified that substitution of position 5 (lysine) of the PAR4-AP (AYPGKF-NH_2) with alanine does not significantly affect the agonist capacity of the peptide (Fig. 1). Further, we identified that substitution of L-lysine with D-lysine significantly decreases agonist stimulation of calcium signalling and β-arrestin recruitment (Fig. 2). To further probe the effect of positively charged residues in position 5, we generated several PAR4-AP analogues with lysine[5] substitutions by either arginine or ornithine (Fig. 6, Table 1). Substitution of lysine[5] with arginine resulted in a partial agonist with respect to calcium signalling but increased β-arrestin recruitment compared to the parental peptide (AYPG**R**F-NH_2 calcium EC_{50} = 4.0 ± 1.1 μM, β-arr-1 154.2 ± 10.3%, β-arr-2 140.1 ± 9.4%). This substitution delocalizes the positive charge of the side chain compared to lysine and increases steric bulk. Interestingly, substitution with ornithine, which is similarly charged but has a shortened distance between the charge and the peptide backbone compared to lysine, also resulted in partial agonism of PAR4-mediated calcium signalling accompanied by a modest increase in the recruitment of β-arrestins (AYPG**O**F-NH_2 calcium EC_{50} = 4.2 ± 1.1 μM, β-arr-1 121.7 ± 8.5%, β-arr-2 112.1 ± 7.7%). To further probe if steric bulk in the side chain of position 5 affects PAR4-AP potency, we increased steric bulk through methylation of the epsilon (ε) amine of lysine [AYPG-**(N_ε-Me-K)**-F-NH_2]. This substitution yielded a full agonist for calcium signalling (EC_{50} = 6.7 ± 1.9 μM) and a modestly more efficacious agonist for the recruitment of β-arrestins (β-arr-1 122.5 ± 12.4%; β-arr-2 116.7 ± 11.2%). All of these substitutions maintain a positive charge and are able to act as agonists for PAR4. To determine if charge in position 5 is required, we substituted lysine with citrulline, which maintains similar structure to arginine and lysine while removing a positive charge (AYPG-**Cit**-F-NH_2). Interestingly, we observed partial agonism with respect to calcium signalling (EC_{50} = 5.4 ± 0.8 μM) with equipotent β-arrestin recruitment compared to the PAR4-AP, consistent with the alanine scan data for this position. Thus, positively charged residues in position 5 seem to contribute to agonism. Interestingly, we observed similar increases in β-arrestin recruitment and equipotent calcium signalling when stericity was either increased (AYPG**R**F-NH_2) or decreased (AYPG**O**F-NH_2), suggesting that the positive charge in this position is more important than the size of the side chain. Finally, although both the charge and size of the size chain have an effect, all modifications to position 5, with the exception of D-lysine (Fig. 2, Table 1) and N_α-methyl-lysine (Fig. 3, Table 1) modifications, were generally well-tolerated and there appears to be modest freedom in the side-chain of this position. This makes the side chain a good candidate for further investigations of structure-activity relationships as well as a good region to label with an imagine modality.

Effect of additional substitutions in position 6 on PAR4-AP-mediated signalling responses. Through our initial investigations into position 6 substitutions, we observed that replacement of phenylalanine[6] with either alanine, D-phenylalanine, or *N*-methyl-phenylalanine had varied effects on PAR4-AP potency and efficacy. Previous investigations into position 6 substitutions in the native tethered ligand (GYPGQV) revealed the requirement for an aromatic residue, as substitution with non-aromatic residues such as lysine or ornithine significantly decreased or abolished the activity of the peptide (Faruqi et al., 2000). In addition to being an aromatic residue, phenylalanine is a hydrophobic residue so we investigated the

392 impact of altering the hydrophobicity/hydrophilicity and stericity while maintaining an
393 aromatic residue (Fig. 7, Table 1).
394
395 We investigated the effect of polar changes that decrease hydrophobicity. Substitution of
396 phenylalanine[6] with tyrosine results in the addition of a hydroxyl group to position 6
397 (AYPGK**Y**-NH_2). We observed partial agonism of calcium signalling with no significant
398 change in potency compared to the PAR4-AP (AYPGK**Y**-NH_2, EC_{50} = 5.2 ± 1.0 μM).
399 Interestingly, the peptide was able to recruit β-arrestins at least as well as the PAR4-AP (β-arr-
400 1 120.5 ± 12.5%; β-arr-2 109.9 ± 11.4%). Further, replacing the tyrosine hydroxyl group with
401 an electron withdrawing fluorine, by means of substitution with 4-fluoro-L-phenylalaine,
402 caused significant impairment of agonist activity, both decreasing calcium signalling and
403 significantly decreasing β-arrestin recruitment [AYPGK-**F(4-fluoro)**-NH_2, calcium EC_{50} =
404 *n.d.,* β-arr-1 25.2 ± 6.5%; β-arr-2 41.3 ± 5.9%]. The results of these two substitutions suggest
405 that altering the polarity, while maintaining aromaticity, in position 6 reduces efficacy
406 (Hoffmann et al., 2019). Since decreasing hydrophobicity did not increase PAR4-AP activity,
407 we next investigated alterations that increase stericity and hydrophobicity. Substitution with 4-
408 methyl-L-phenylalanine reduced the efficacy of the PAR4-AP to a partial agonist for both
409 calcium signalling and β-arrestin recruitment [AYPGK-**F(4-Me)**-NH_2 calcium EC_{50} = 9.4 ±3.0
410 μM, β-arr-1 56.4 ± 1.2%; β-arr-2 63.2 ± 1.1%]. Given these results, we wanted to assess the
411 pharmacological impact of substituting phenylalanine with (1-naphthyl)-L-alanine (1Nal) and
412 (2-naphthyl)-L-alanine (2Nal) which not only increase hydrophobicity but also have a modest
413 increase in steric bulk and π-stacking potential. Substitution of phenylalanine[6] with (1-
414 naphthyl)-L-alanine (1Nal; AYPGK-**1Nal**-NH_2) generated a partial agonist for both calcium
415 signalling (EC_{50} = 9.6 ±1.9 μM) and β-arrestin recruitment (β-arr-1 77.5 ± 2.3%; β-arr-2 64.1
416 ± 2.0%) compared to PAR4-AP. Notably, substitution to (2-naphthyl)-L-alanine (2Nal;
417 AYPGK-**2Nal**-NH_2), which differs in orientation compared to (1-naphthyl)-L-alanine such that
418 the alkyl chain is connected to position 2 of naphthyl group (instead of position one as in 1Nal),
419 restored potency of the peptide to the levels observed with PAR4-AP. AYPGK-**2Nal**-NH_2 was
420 an equipotent agonist for calcium signalling (EC_{50} = 11.1 ± 2.3 μM) and β-arrestin recruitment
421 (β-arr-1 77.0 ± 7.0%; β-arr-2 91.6 ± 6.4%). Together, these results indicate that hydrophobicity,
422 stericity, and side chain positioning of the C-terminal residue all contributes to agonist peptide
423 activity at PAR4.
424
425 **Probing antagonism of PAR4-AP-stimulated calcium signalling by calcium signalling null**
426 **peptides.** The failure of some substituted peptides to stimulate calcium signalling could reflect
427 either a failure to bind or a loss of efficacy. To determine if such peptides can act as antagonists
428 of PAR4-AP stimulated calcium signalling, we pre-incubated HEK-293 cells stably expressing
429 PAR4-YFP prior to stimulation with PAR4-AP. Pre-treatment and competition with 100 μM
430 of calcium null peptides were largely unable to affect the calcium response elicited by 30 μM
431 PAR4-AP (AYPGKF-NH_2) compared to vehicle treated controls. Interestingly, two calcium
432 null peptides with substitution in position 3 or 4 were able to decrease calcium signals elicited
433 by PAR4-AP. Calcium signalling in response to AYPGKF-NH_2 (30 μM) was significantly
434 reduced following pre-treatment with AY-**Nip**-GKF-NH_2 (10.6 ± 0.9% of A23187; $p<0.05$) or

435 AYP-**Sar**-KF-NH_2 (13.0 ± 1.5% of A23187; $p<0.05$) compared to non-pre-treated control (20.8
436 ± 1.3% of A23187; $p<0.05$) (Fig. 8).
437
438 **PAR4-dependent calcium signalling is $G\alpha_{q/11}$-dependent.** In order to verify that PAR4-
439 dependent calcium signalling was $G\alpha_{q/11}$-dependent, HEK-293 cells stably expressing PAR4-
440 YFP were stimulated with 100 µM AYPGKF-NH_2 following pre-incubation with selective
441 $G\alpha_{q/11}$-inhibitor YM254890. YM254890 inhibited AYPGKF-NH_2-stimulated calcium
442 signalling in a concentration-dependent manner, with complete inhibition observed at 100 nM
443 YM254890. The control vehicle (0.001% DMSO) had no effect on calcium signalling (Fig. 9).
444
445 **Calcium signalling-null peptides do not activate MAPK signalling.** Activation of G-protein
446 and β-arrestin pathways downstream of GPCRs often converge on the activation of the p44/42
447 MAP kinase-signalling pathway (Jean-Charles et al., 2017). We therefore monitored
448 phosphorylation of p44/42 MAPK in response to the 37 AYPGKF-NH_2 derivative peptides.
449 HEK-293 cells, stably expressing PAR4-YFP, were incubated with control vehicle (0.001%
450 DMSO), 100 µM of AYPGKF-NH_2, or derivative peptides (100 µM) for 10 minutes. Data were
451 normalized as a ratio of phosphorylated-p44/42 (p-p44/42) to total-p44/42 (p44/42).
452 Interestingly, we find that most peptides that were unable to stimulate calcium signalling were
453 also unable to activate p44/42 MAPK signalling (*i.e.* A**y**PGKF-NH_2, AY**p**GKF-NH_2, **(*N*-Me-**
454 **S)**-YPGKF-NH_2, **Inp**-YPGKF-NH_2, **Sar**-YPGKF-NH_2, AY-**Nip**-GKF-NH_2, AYP-**Sar**-KF-
455 NH_2). Similarly, peptides that perform as partial agonists of $G\alpha_{q/11}$-mediated calcium signalling
456 were also partial agonists for p44/42 phosphorylation. Several peptides were able to cause a
457 significantly greater increase in phosphorylation compared to the parental peptide (*i.e.* **Nle**-
458 YPGKF-NH_2, AYPG**O**F-NH_2, AYPG-**(N_ε-Me-K)**-F-NH_2, AYPG-**Cit**-F-NH_2, AYPGK**Y**-
459 NH_2, AYPGK-**1Nal**-NH_2,) (Fig. 10, Table 1).
460
461 **PAR4-mediated MAPK signalling is $G\alpha_{q/11}$-dependent and β-arrestin independent.**
462 In order to further probe the contribution of different pathways downstream of PAR4 to p44/42
463 phosphorylation, we examined the effective of blocking $G\alpha_{q/11}$-signalling with the specific
464 antagonist YM254890 and examined the role of β-arrestins using a β-arrestin-1/-2 double
465 knockout HEK-293 cell derived by CRISPR/Cas9 mediated targeting (Supp. Fig. 3). Pre-
466 treatment of PAR4-YFP HEK-293 cells with 100 nM YM254890 for 20 minutes abolished
467 PAR4-AP (30 µM) stimulated activation of MAP kinase signalling and subsequent
468 phosphorylation of p-p44/42 at five minutes time (Fig. 11 A.). In contrast, there was no
469 significant difference in the phosphorylation of p44/42 MAPK between wild-type HEK-293
470 and β-arrestin-1/-2 knockout HEK-293 cells stimulated with 30 µM PAR4-AP for 0-90 minutes
471 (Fig. 11 B.).
472
473 **Homology modelling of PAR4 and *in silico* docking of AYPGKF-NH_2.** In order to gain a
474 better understanding of the ligand-binding pocket in PAR4 we turned to homology modelling
475 and *in silico* docking experiments. A homology model of PAR4 was generated using known
476 coordinates of thermostabilized human PAR2 crystal structure in complex with AZ8838 (2.8Å
477 resolution, 5NDD.pdb, Cheng et al., 2017). Sequences of human PAR4 were aligned with the

478 structure-resolved residues of PAR2 using Clustal Omega (Madeira et al., 2019; Sievers et al.,
479 2011). We generated a homology model of wild-type PAR2 on the PAR2 structure, which
480 contained modifications necessary for crystallization. Twenty human PAR4 homology models,
481 using the wild-type human PAR2 model as a template, were generated in MODELLER (Webb
482 and Sali, 2014). The PAR4 model with the lowest discrete optimized protein energy (DOPE)
483 score was utilized for *in silico* analyses.
484
485 Docking AYPGKF-NH_2 to the PAR4 homology model (GalaxyPepDock; Lee et al., 2015)
486 revealed a number of highly predicted peptide-receptor interaction sites (Fig. 12 A.; Ser^{67},
487 Tyr^{157}, His^{229}, Asp^{230}, Leu^{232}, Leu^{234}, Asp^{235}, Ala^{238}, Gln^{242}, His^{306}, Tyr^{307}, Pro^{310}, Ser^{311}, Ala^{314},
488 Gly^{316}, Tyr^{319}, and Tyr^{322}). Of these, the most frequently predicted interactions were receptor
489 residues His^{229}, Asp^{230}, and Gln^{242}. In peptide-docked models, Gln^{242} made contact with
490 alanine, tyrosine, and lysine, with the most frequent prediction being with phenylalanine. His^{229}
491 was predicted to interact with lysine and phenylalanine. Asp^{230} was frequently predicted to
492 interact with lysine and phenylalanine and contacts with lysine appeared in 60% of predictions
493 (Fig. 12 B.). Interestingly, when visualizing receptor residues predicted to interact with the
494 peptide, we found that a large number of these residues were localized on extracellular loop 2
495 (ECL2) (Fig. 12 A. and B.).
496
497 **Calcium signalling and β-arrestin recruitment to predicted peptide binding-site mutant-**
498 **PAR4.** To experimentally examine *in silico* predictions, site-directed mutagenesis was
499 performed introducing alanine substitutions at the three most highly predicted interacting
500 residues, His^{229}, Asp^{230}, and Gln^{242}. Additionally, we generated a double mutation, $PAR4^{H229A,}$
501 ^{D230A}, to determine if combined loss of His^{229} and Asp^{230} would result in additive detriment to
502 receptor activation. We evaluated the functional consequences of these mutations by recording
503 calcium signalling in response to AYPGKF-NH_2 with all mutants. We observed no calcium
504 response in cells expressing $PAR4^{D230A}$-YFP or $PAR4^{H229A, D230A}$-YFP mutant receptors up to
505 300 μM AYPGKF-NH_2 (Fig. 13 A.). Similarly, peptide-induced β-arrestin-1/-2 recruitment to
506 $PAR4^{D230A}$-YFP and $PAR4^{H229A, D230A}$-YFP was significantly reduced compared to the wild-
507 type PAR4. Both $PAR4^{H229A}$ and $PAR4^{Q242A}$ mutations were fully able to recruit β-arrestin-1/-
508 2 to the same levels observed with wild-type PAR4-YFP (Fig. 13 B. and C.).
509
510 To investigate whether these sites are important for tethered ligand activation of the receptor,
511 we stimulated cells expressing wildtype and mutant constructs with thrombin. Thrombin
512 cleavage of the receptor reveals the native tethered ligand, GYPGQV (Xu et al., 1998).
513 Comparable to activation with AYPGKF-NH_2, we observed significantly diminished calcium
514 signalling in HEK-293 cells expressing $PAR4^{D230A}$-YFP and $PAR4^{H229A, D230A}$-YFP mutants,
515 even up to 10 units/mL thrombin (Fig. 13 D.). Additionally, β-arrestin-1/-2 recruitment was
516 also impaired to $PAR4^{D230A}$ and $PAR4^{H229A, D230A}$ mutants (Fig. 13 E. and F.). We observed no
517 appreciable difference in calcium signalling or β-arrestin recruitment when $PAR4^{H229A}$-YFP
518 and $PAR4^{Q242A}$-YFP mutants were stimulated with thrombin, with the exception of a modest
519 decrease in β-arrestin-1 recruitment to $PAR4^{Q242A}$-YFP mutant receptor. Thus, Asp^{230}
520 interactions with either PAR4-AP or the tethered ligand are critical for receptor activation.

521
522 **Platelet aggregation response to differential activation of PAR4 signalling.** To determine
523 the effects of targeted signalling observed with several peptides we investigated PAR4-
524 mediated platelet aggregation in response to the β-arrestin biased, calcium signalling-null
525 peptide, A**y**PGKF-NH_2, as well as a modestly more potent calcium agonist AYPG**R**F-NH_2
526 (compared to AYPGKF-NH_2). Thrombin (1 unit/mL) and 100 μM AYPGKF-NH_2 were used
527 as controls to ensure successfully washed platelet preparations. In response to thrombin
528 stimulation, we observed a characteristic aggregation trace resulting in 100% aggregation at 1
529 unit/mL. In agreement with previously published data, AYPGKF-NH_2 (100 μM) stimulation
530 resulted in approximately 50% platelet aggregation (Ramachandran et al., 2017). We observed
531 that platelet aggregation was not stimulated by 100 μM A**y**PGKF-NH_2. Interestingly, when
532 platelet preparations were stimulated with AYPG**R**F-NH_2, with which we observed a modest
533 increase in potency in calcium signalling assays, enhanced β-arrestin recruitment, and an
534 increased phosphorylation of p44/42, we observed platelet aggregation response comparable
535 to levels observed with thrombin (1 unit/mL) (Fig. 14).
536
537 **Discussion:**
538 PAR4 is emerging as a novel anti-platelet drug target. Here we examine structure activity
539 requirements for PAR4 activation of calcium signalling, β-arrestin recruitment and MAP
540 kinase activation. PAR cleavage by a number of different enzymes has been reported (Soh et
541 al., 2010). Canonically, thrombin has been described as a PAR1 and PAR4 activator while
542 trypsin is described as a PAR2 and PAR4 activator. While PAR3 can be cleaved by thrombin,
543 its ability to act as a signalling receptor remains ambiguous. In each case, cleavage by serine
544 proteases occurs at an arginine-serine site which reveals a unique tethered-ligand specific to
545 each PAR (Hollenberg, 2003) - human PAR1- SFLLRNP… (Liu et al., 1991; Vu et al., 1991),
546 human PAR2- SLIGKV… (Al-Ani et al., 2002; Nystedt et al., 1994) and human PAR4-
547 GYPGQV… (Kahn et al., 1998; Xu et al., 1998). While these tethered-ligand sequences are
548 diverse, they retain some highly-conserved properties including a highly-conserved charged
549 residue in position five of the revealed tethered-ligands (arginine in PAR1; lysine in PAR2).
550 Additionally, PAR2 and PAR4 have a conserved glycine in position three and valine in position
551 six of their tethered-ligands. The similarities of the proteolytically-revealed tethered ligands is
552 also observed in the optimized tethered-ligand-mimicking synthetic agonist peptides.
553 Hydrophobic residues leucine, isoleucine, and proline are preferred in position three of PAR1,
554 PAR2, and PAR4 agonist peptides, respectively. Additionally, there is a basic residue in
555 position five of the tethered ligand peptide in all three receptors (arginine in PAR1 and PAR2
556 and lysine in PAR4 activating peptides). These conserved residue properties highlight some of
557 the key requirements that a PAR4 agonist peptide must meet. Previous structure-activity work
558 starting with the proteolytically-revealed sequences of human (GYPGQV) and murine
559 (GYPGKF) PAR4 identified the hexapeptide AYPGKF-NH_2 or SYPGKF-NH_2 to be potent
560 and selective agonists for PAR4 (Faruqi et al., 2000). In this study we started with the
561 hexapeptide AYPGKF-NH_2, as our parental peptide agonist, and incorporated various
562 modifications at each of the six positions in this peptide to investigate determinants of agonist-

563 induced PAR4-coupling to $G\alpha_{q/11}$, MAP kinase and β-arrestin-1/-2 recruitment to guide
564 development of biased agonists of PAR4.
565
566 Previously, it was demonstrated that substitution of alanine or serine in position 1 of the
567 GYPGKF-NH_2 activating peptide retained the ability to trigger tritiated inositol 1,4,5-
568 triphosphate release to a level comparable to that observed with thrombin activation and much
569 higher than release caused by the GYPGKF-NH_2 (Faruqi et al., 2000). Interestingly,
570 substitution of position 1 with threonine was reported to significantly reduce the potency of the
571 activating peptide (Faruqi et al., 2000). In keeping with results from previous studies, we find
572 a requirement for small aliphatic side chains in position 1 of PAR4 activating peptides, with
573 substitutions that increased bulk in this position consistently resulting in poor agonists for both
574 calcium signalling and β-arrestin recruitment (*N*-Me-A Fig. 3; *N*-Me-S, Aib, Inp, V, Nle Fig 4;
575 Table 1). Additionally, we observed that both stereochemical inversion of L-alanine to D-
576 alanine (D-alanine, Fig. 2) and backbone elongation (betaAla., Fig. 4) were detrimental to both
577 calcium signalling and β-arrestin recruitment. Additionally, we observed that capping of the
578 N-terminal charge via acetylation significantly decreases agonist potency. Together these
579 results indicate that a positive charge and the localization of that charge in addition to precise
580 side-chain positioning at position 1 are critical to effective PAR4-agonism.
581
582 The aromatic sidechain, and to a lesser extent the hydroxyl group, of the tyrosine[2] residue of
583 the parental peptide also proved to be important for peptide activity with alanine or D-isomer
584 substitutions resulting in decreased activity of all pathways tested. These results are consistent
585 with previous reports that replacement of tyrosine with other aromatic residues, such as
586 phenylalanine, significantly reduced both the selectivity and the potency of the activating
587 peptide (Faruqi et al., 2000). Interestingly, substituting L-tyrosine[2] for either D-tyrosine (Fig.
588 2 A., Fig. 10) or *N*-methyl-tyrosine (Fig. 3 A. & 10) resulted in significant decreases in calcium
589 and p44/42 signalling, while having relatively modest effects on β-arrestin recruitment (Fig, 2
590 B. & C., Fig. 3 B. & C., respectively; Table 1). Also, substitution of tyrosine with either 4-
591 fluoro-phenylalanine or *O*-methyl-tyrosine did not significantly affect calcium transients,
592 p44/42 phosphorylation or β-arrestin recruitment in comparison to AYPGKF-NH_2 (Fig. 5 &
593 10; Table 1). Our findings, together with previously reported data (Faruqi et al., 2000), point
594 to the necessity of an aromatic residue in position 2 to maintain agonist potency. Further, our
595 data reveal that backbone orientation in position 2 is a key determinant of agonist potency.
596 Future experiments fine-tuning the aromatic substituents may be beneficial for peptide
597 analogue development.
598
599 Our data reveal that alterations affecting proline backbone conformation or glycine residue
600 compactness are not well-tolerated, as these decreased calcium signalling, p44/42 MAP kinase
601 signalling, and β-arrestin recruitment to PAR4. Calcium signalling has previously been
602 reported to be negatively impacted by alterations to either of these two residues (Faruqi et al.,
603 2000). Both proline and glycine residues are frequently found in β-turns, in which proline
604 provides a characteristic kink, and the available data support the notion that the conformation(s)
605 (proline[3] and glycine[4]) and rigidity (proline[3]) of PAR4 agonists permitted by these residues

606 is/are important for receptor activation. To test this hypothesis further, we made several
607 substitutions in position 3 (proline) aimed at evaluating favoured backbone conformations. We
608 observed that a return to a predominantly trans-amide conformation by substitution of proline
609 with alanine (Fig. 1), results in decreased potency in all pathways studied. Interestingly, this
610 substitution did not abolish signalling but did significantly decrease agonist potency, which
611 suggests that the backbone conformation of proline may be necessary for receptor binding but
612 not receptor activation. Substitution of proline to pipecolic acid (Pip., Fig. 5), which has a
613 similar peptide backbone orientation to proline with a six-membered aromatic ring, decreased
614 β-arrestin recruitment with relatively modest effects for calcium signalling activation.
615 Interestingly, substitution of proline with nipecotic acid (Nip., Fig. 5) abolished both calcium
616 signalling and p44/42 phosphorylation while also significantly reducing β-arrestin recruitment.
617 Nipecotic acid is similar to pipecolic acid with the exception that nipecotic acid changes the
618 direction of the peptide backbone compared to that adopted by proline, while pipecolic acid
619 favours a similar backbone directionality and conformation similar to proline. Interestingly, we
620 observed a similar pharmacological profile observed with AY-**Nip**-GKF-NH_2 when we
621 substituted D-proline in position 3, which also changes the backbone orientation from that of
622 the of the parent peptide. These findings demonstrate that the backbone conformation provided
623 by proline in position 3 of the parental peptide is necessary for agonism of PAR4 signalling
624 pathways. Further, substitution of a proline[3] with alanine (AY**A**GKF-NH_2, Fig. 2) significantly
625 and detrimentally altered the pharmacological profile compared to the parental peptide PAR4-
626 AP, suggesting the possibility that agonist competency contributed by position 3 is largely
627 conformational and not chemical. Substitution of sarcosine or beta-alanine at position 4 also
628 negatively affected all signalling pathways, while substitution of glycine[4] with alanine resulted
629 in a decrease in potency with calcium signalling as well as a reduction of β-arrestin recruitment.
630 Together these substitutions reveal the requirement for a small flexible residue in position 4,
631 consistent with previous reports (Faruqi et al., 2000).
632
633 It has been previously demonstrated that substitution of position 5 glutamine in the native
634 tethered ligand (GYPGQV) with arginine or ornithine results in decreased potency in the PAR4
635 agonist peptide for calcium signalling pathways (Faruqi et al., 2000). However, there is a basic
636 residue found in position 5 of PAR1 (arginine, TFLL**R**), PAR2 (arginine, SLIG**R**L), and PAR4
637 (lysine, AYPG**K**F) tethered-ligand mimicking peptides. Given the conservation of charged
638 residues in position 5 of PAR tethered-ligand mimicking peptides, we generated PAR4-AP
639 derivative peptides with lysine[5] substitutions that maintained or altered charge in this position
640 to determine if this is a requirement for activity at PAR4. Substitution of lysine[5] with alanine
641 had no appreciable effect on calcium or MAP kinase signalling, while resulting in decreased
642 β-arrestin recruitment (Fig. 1). Substitution of L-lysine[5] with D-lysine, however, significantly
643 reduced potency and efficacy in calcium signalling and β-arrestin recruitment assays and
644 furthermore resulted in a loss of stimulation of MAP kinase signalling (Fig. 2). We continued
645 our exploration of this position with an N_α-methyl-lysine substitution, which increases steric
646 bulk through the addition of a methyl group to the backbone while also removing a hydrogen
647 bond donor and increasing the amount of peptide in the cis-transformation of the amide bond
648 between position 4 and 5. We found this substitution detrimental to calcium signalling but

649 advantageous for β-arrestin recruitment, resulting in comparable maximal levels of recruitment
650 to those observed with PAR4-AP but at lower concentrations (Fig. 3). Thus, backbone
651 conformation and bulk at position 5 are important for agonism of calcium signalling and MAP
652 kinase activation, while possibly being an important site for modification in the search for β-
653 arrestin biased ligands.
654
655 We next turned our attention to analogues that resemble the side chain of lysine[5], with a specific
656 interest on structure-activity in addition to ascertaining the importance of charge in this residue.
657 In contrast to the observation with similar substitutions to the tethered-ligand-mimicking
658 peptide (GYPGQV) (Faruqi et al., 2000) wherein signalling was decreased compared to PAR4-
659 AP, we found that both calcium signalling and β-arrestin recruitment are only modestly
660 impacted by position 5 substitution to ornithine in the PAR4-AP, which decreases steric bulk
661 and shortens the distance between the backbone and the positively charged amine compared to
662 lysine (AYPG**O**F-NH_2; Fig. 6). Interestingly, however, we observed significantly increased
663 p44/42 phosphorylation in response to AYPG**O**F-NH_2 stimulation (Fig. 10). This is somewhat
664 puzzling since we found p44/42 phosphorylation to be $G\alpha_{q/11}$-dependent (Fig. 11); however, it
665 is important to note that MAP kinase and other cellular signalling pathways downstream of
666 receptor activation are subject to amplification/deamplification processes within the cell
667 (Chidiac, 2016) and these observations may point to additional differences in signalling
668 stimulated by this peptide that needs to be examined. We further probed stericity in this position
669 through increasing bulk with substitution of lysine[5] with arginine (AYPG**R**F-NH_2).
670 Interestingly, this substitution also results in a delocalization of charge compared to the charge
671 on the lysine[5] side chain. This modification provided a similar calcium signalling profile
672 compared to that observed with ornithine substitution, however, it also resulted in a significant
673 increase of β-arrestin recruitment compared to the parental PAR4-AP. Interestingly, there was
674 no significant change in p44/42 phosphorylation unlike what was observed with ornithine
675 substitution. Another peptide with increased steric bulk, N_ε-methyl-lysine substitution in
676 position 5, improved calcium signalling potency, modestly improved β-arrestin recruitment,
677 and significantly increased p44/42 phosphorylation [AYPG-**(N_ε-Me-K)**-F-NH_2, Fig. 6]. We
678 further investigated whether charge was a significant determinant of agonism by substituting
679 lysine[5] with citrulline (AYPG-**Cit**-F-NH_2), which lacks charge but retains a similar structure
680 compared to arginine and, to a lesser extent, lysine. We observed decreased calcium, equivalent
681 β-arrestin recruitment, and significantly increased p44/42 phosphorylation compared to the
682 parental peptide (Fig. 6 & 10). Together these data reveal that changes to side chain charge,
683 bond donors/acceptors, and steric bulk result in varied pharmacological responses that may be
684 exploited to bias signalling responses in favour of β-arrestin recruitment (AYPG**R**F-NH_2) or
685 p44/42 phosphorylation (AYPG**O**F-NH_2; AYPG-**(N_ε-Me-K)**-F-NH_2) with modest
686 improvements to potency in calcium signalling. Interestingly, we observed that charge is not
687 wholly required for receptor activation as both alanine and citrulline substitutions resulted in
688 agonism of PAR4.
689
690 Finally, our structure-activity investigation turned to position 6, phenylalanine, of the parental
691 peptide. Given the significant impact that alterations to position 2 (tyrosine) had on agonist

692 potency, we predicted that there may be a pi-pi (π-π) stacking interaction between tyrosine and
693 phenylalanine which is supported by the backbone kink provided by proline in position 3.
694 Substitution of position 6 with alanine or D-phenylalanine reduced calcium signalling potency
695 while reducing β-arrestin recruitment and p44/42 phosphorylation. These alterations suggest
696 that phenylalanine in position 6 is not essential for PAR4 activation by agonist peptide but is
697 important for agonist potency and full activation of all signalling pathways. Methylation of the
698 backbone nitrogen in phenylalanine (AYPGK-**(*N*-Me-F)**-NH_2) resulted in improved activation
699 of calcium signalling, β-arrestin recruitment, and p44/42 phosphorylation compared to
700 AYPGKF-NH_2 (Fig. 3). Addition of either methyl (AYPGK-**F(4-Me)**-NH_2; Fig. 7), fluorine
701 (AYPGK-**F(4-fluoro)**-NH_2; Fig. 7), or hydroxyl (AYPGK**Y**-NH_2; Fig. 7) off of the *para*-
702 position of the aromatic side chain of phenylalanine was deleterious to all signalling pathways
703 studied. Substitution of unnatural residues that increase the size of steric bulk and π-stacking
704 potential yielded mixed results based on the orientation of the naphthyl. Substitution of
705 phenylalanine with (1-naphthyl)-L-alanine (1Nal) increased p44/42 phosphorylation but
706 decreased both calcium signalling and β-arrestin recruitment (Fig. 7). Changing the alkyl chain
707 connection from position 1 to position 2 of the naphthyl (AYPGK-2Nal-NH_2; Fig 7) resulted
708 in activity similar to AYPGKF-NH_2. With (2-naphthyl)-L-alanine showing some flexibility in
709 the steric bulk of position 6, it would be interesting for future work to investigate increasing
710 the π-stacking potential at position 2 while simultaneously increasing the π-stacking potential
711 at position 6, since we hypothesize that these two residues' aromatic regions of the PAR4-AP
712 may interact.
713
714 To determine if any of the calcium signalling-null peptides were able to act as antagonists, cells
715 were pre-treated with calcium null peptides and subsequently stimulated with AYPGKF-NH_2
716 to see if the parental peptide was able to still elicit a signal. We observed that both AY-**Nip**-
717 GKF-NH_2 and AYP-**Sar**-KF-NH_2 were both able to significantly decrease the calcium signal
718 elicited by PAR4-AP (Fig. 8). Interestingly, each of these substitutions resulted in ablation of
719 both calcium and p44/42 signalling as well as significantly decreasing β-arrestin recruitment.
720 These results may indicate that targeting PAR4 with small molecules mimicking position 3 and
721 4 dipeptides may provide a starting place for the design of novel PAR4 antagonists.
722 Additionally, peptides that further explore modifications to position 3 and 4 could be
723 investigated for potent PAR4 antagonists.
724
725 In platelets, it has previously been demonstrated that PAR4-mediated calcium mobilization
726 induces activation and aggregation (Edelstein et al., 2014; Holinstat et al., 2006). Both
727 thrombin and AYPGKF-NH_2 initiated PAR4-dependent platelet aggregation to levels
728 comparable to those previously reported in the literature in the same rat platelet system
729 (Ramachandran et al., 2017). As was hypothesized, we observed that stimulation of washed
730 platelet samples with a calcium signalling null, β-arrestin biased peptide, A**y**PGKF-NH_2 (100
731 μM) did not stimulate platelet aggregation (Fig. 14). Further, stimulation of washed platelets
732 with the agonist peptide, AYPG**R**F-NH_2 (Fig. 6), enhanced platelet aggregation to levels
733 comparable to those observed with thrombin activation of PAR4 (Fig. 14). AYPG**R**F-NH_2
734 stimulates calcium signalling to levels comparable to those seen with PAR4-AP but triggers

more β-arrestin-1 recruitment than the parental peptide. These data suggest that calcium signalling is essential for triggering platelet activation, but arrestin recruitment may also play a role.

Having ascertained some of the governing peptide residue characteristics enabling PAR4 activation and validated their signalling consequences in an *ex vivo* system, we turned our attention to investigating the binding site of the receptor. The extracellular loops of many GPCRs have been demonstrated to be important facilitators of ligand entry into the orthosteric site, with ECL2 possessing the most diversity in sequence and structure (Venkatakrishnan et al., 2014; Woolley and Conner, 2017). Analysis of common mechanisms of GPCR ligand interaction derived from crystal structure and biochemical experiments reveal a possible role of ECL2 secondary loop in binding and facilitating entry, while the diversity of residue sequences across class A GPCRs is thought to confer their ligand specificity (Venkatakrishnan et al., 2014; Woolley and Conner, 2017). In many class A GPCRs, a disulfide bond between ECL2 and a transmembrane 3 cysteine ($Cys^{3.25}$, Ballesteros-Weinstein numbering) is thought to stabilize the extracellular topology such that ligand recognition at ECL2 and subsequent orthosteric binding can occur (Wheatley et al., 2012). All PAR receptors possess this canonical TM3 $Cys^{3.25}$ (PAR1 $Cys175^{3.25}$, PAR2 $Cys148^{3.25}$, PAR3 $Cys166^{3.25}$, PAR4 $Cys149^{3.25}$) and residues adjacent to this conserved cysteine are important for ligand binding and receptor activation. Investigations into the role of PAR ECL2 domains have previously demonstrated that all PAR receptors possess a homologous CHDxL motif (…CHDVL… - $PAR1^{C254\text{-}L258}$ and $PAR2^{C226\text{-}L230}$; …CHDVH… $PAR3^{C245\text{-}L249}$ …CHDAL; … $PAR4^{C226\text{-}L230}$) in their ECL2 (Al-Ani et al., 1999; Xu et al., 1998). Given that the activating peptides of PAR1 and PAR2 (Al-Ani et al., 1999; Lerner et al., 1996) are similar (SFLLRN, PAR1; SLIGRL, PAR2), additional studies were conducted that revealed that ligand specificity is conferred by acidic residues distal to the CHDxL motif (PAR1, $N^{259}ETL^{261}$; PAR2 $P^{231}EQL^{234}$; (Gerszten et al., 1994; Lerner et al., 1996; Nanevicz et al., 1995). Interestingly, the equivalent human PAR4 ECL2 residues distal to the CHDAL domain, $P^{233}LDA^{236}$, share sequence homology with those distal to the human PAR2 CHDVL domain ($P^{231}EQL^{234}$), both of which contain an acidic residue. Al-Ani *et al.* (1999) demonstrated that glutamic acid residues in the rat PAR2 ECL2 (PEEVL) conferred specificity to PAR2 ligands. In previous studies, a series of aspartic acids in the PAR4 extracellular loop 2 (ECL2) and amino terminal (N)-tail were proposed to be key for thrombin binding to PAR4 (Nieman, 2008; Nieman and Schmaier, 2007; Sánchez Centellas et al., 2017). Mutations of ECL2 aspartic acid residues $D^{224}A$, $D^{230/235}A$ (double mutation), and $D^{224/230/235}A$ mutants were all found to decrease thrombin cleavage of PAR4 and activation in yeast models (Sánchez Centellas et al., 2017). Further, the activity of the PAR4 agonist peptide AYPGKF-NH_2 was also abolished in PAR4 mutants containing ECL2 single mutant D224A, double mutant $D^{230/235}A$, or triple mutant $D^{224/230/235}A$ aspartic acid mutations to alanine which the authors posit indicates that these aspartic acid residues may be important for both agonist peptide and tethered ligand bindings and activation of PAR4. The $D^{230/235}A$ mutation to alanine removed two acidic residues in the highly conserved …$CHD^{230}AL$ domain (PAR1 Asp^{256}; PAR2 Asp^{228}) as well as the homologous $PLD^{235}A$… specificity conferring domain observed in PAR1 (Glu^{260}) and PAR2 (Glu^{232}) making it difficult to assess whether the loss of cleavage and activation is due to the $CHD^{230}AL$ or $PLD^{235}A$ aspartic acid.

779
780 In the present study, *in silico* docking to a homology model of PAR4 revealed 17 predicted
781 sites of interaction with AYPGKF-NH_2 (Ser^{67}, Tyr^{157}, His^{229}, Asp^{230}, Leu^{232}, Leu^{234}, Asp^{235},
782 Ala^{238}, Gln^{242}, His^{306}, Tyr^{307}, Pro^{310}, Ser^{311}, Ala^{314}, Gly^{316}, Tyr^{319}, Tyr^{322}; Fig. 12 A.).
783 Interestingly, these predicted sites reveal residues that have been shown or predicted to have a
784 role in PAR4 activation by thrombin or agonist peptide. These sites include aspartic acid
785 residue Asp^{230} found in the highly conserved CHDxL domain in PARs as well as Asp^{235} in the
786 downstream region that is homologous to the specificity conferring motif found in PAR1 and
787 PAR2 (Sánchez Centellas et al., 2017). Additionally, previous *in silico* docking revealed a role
788 for aspartic acid and histidine in this motif in binding of AYPGKF-NH_2 to PAR4 (Moschonas
789 et al., 2017). We generated mutations of the most frequently predicted interaction sites (His^{229},
790 Asp^{230}, Gln^{242}, His^{229}/Asp^{230}) to alanine which revealed that Asp^{230} is essential for productive
791 interaction of the peptide with the receptor, as mutation to alanine abolished calcium signal
792 potentiation as well as β-arrestin recruitment. Interestingly, this loss of activity was observed
793 with both peptide agonist AYPGKF-NH_2 as well as with thrombin stimulated activation of
794 PAR4, which agrees with previous reports of the importance of these sites while also
795 elucidating the importance of the conserved $CHD^{230}AL$ motif in PAR4 activation, consistent
796 with the role of this domain in PAR1 and PAR2 (Al-Ani et al., 1999; Blackhart et al., 1996;
797 Gerszten et al., 1994; Lerner et al., 1996; Nanevicz et al., 1995; Sánchez Centellas et al., 2017).
798 Another frequently predicted residue belonging to the CHDAL domain, His^{229}, when mutated
799 to alanine did not alter the ability of either AYPGKF-NH_2 or the tethered ligand as revealed by
800 thrombin to activate calcium signalling or β-arrestin recruitment pathways. Further, we
801 observed that a double mutation of both of these sites to alanine (H229A, D230A) did not result
802 in any additive detriment to PAR4 activation; therefore, we conclude that Asp^{230} interaction
803 with PAR4 peptide and tethered ligand agonist performs an essential role in activation of
804 PAR4.
805
806 Finally, in the context of platelet activation we find that our modified peptides that are able to
807 cause a greater level of calcium signalling and β-arrestin recruitment than PAR4-AP could also
808 trigger greater platelet aggregation. In our hands, PAR4-AP was un able to elicit greater than
809 50% of the aggregation observed in response to 1 unit/mL of thrombin, while the peptide
810 AYPG**R**F-NH_2 was able to trigger aggregation comparable to that seen with thrombin. A role
811 for PAR4-dependent calcium signalling is well established (Edelstein et al., 2014; French and
812 Hamilton, 2016; Tourdot et al., 2018), and consistent with this, our calcium signalling-null
813 peptide A**y**PGKF-NH_2 failed to induce aggregation. A role for β-arrestin mediated PAR4
814 signalling in platelets has also been demonstrated (Khan et al., 2014; Ramachandran et al.,
815 2017). Together these data suggest that calcium signalling is critical for initiating PAR4
816 mediated platelet aggregation, but the precise role hierarchy of the different PAR4 signalling
817 pathways in platelet responses remains to be fully established.
818
819 In summary, the present studies identify key mechanisms involved in PAR4 activation and
820 signalling. We also present and characterize a novel toolkit of PAR4 agonist peptides that could
821 be used to study biased signalling through PAR4 in platelets as well as other physiological

822 systems. We further show that platelet activation by PAR4 critically depends on the $G\alpha_{q/11}$
823 pathway, and selective targeting of this pathway might yield a useful anti-platelet agent.
824 Overall, our work advances our understanding of agonist binding to PAR4 and will support
825 future efforts aimed at defining signalling contribution in homeostatic signalling and the
826 discovery of novel therapeutics targeting PAR4.

827 **Materials and Methods:**
828 All chemicals were purchased from Millipore-Sigma (Burlington, Massachusetts, United
829 States), Thermo Fisher Scientific (Hampton, New Hampshire, United States), or BioShop
830 Canada Inc. (Burlington, Ontario, Canada) unless otherwise stated. AYPGKF-NH_2 was
831 purchased from and synthesized by Genscript (Piscataway, New Jersey, United States).
832 Thrombin from human plasma was obtained from Millipore-Sigma (Cat. # 605195, 5000 units;
833 Burlington, Massachusetts, United States).
834
835 ***Molecular Cloning and Constructs.*** The plasmid encoding PAR4-YFP was described
836 previously (Ramachandran et al., 2017). Plasmid DNA mutations in the predicted orthosteric
837 binding site of PAR4 were generated using the QuikChange XL Multi Site-Directed
838 Mutagenesis Kit (Agilent Technologies, Mississauga, ON, Canada) to generate all mutants
839 described in this study. All constructs were verified by sanger sequencing (Robarts DNA
840 sequencing facility, University of Western Ontario). Renilla luciferase-tagged β-arrestin-1/-2
841 constructs were a kind gift from Michel Bouvier (Université de Montréal). PX458 vector for
842 CRISPR/Cas9 targeting was a kind gift from Feng Zhang (Massachusetts Institute of
843 Technology; Addgene # 48138) *Site-directed mutagenesis of predicted PAR4 receptor-peptide*
844 *interaction sites.* Site-directed mutagenesis using Agilent QuikChange-XL was undertaken to
845 generate mutations in highly predicted receptor residues to validate GalaxyPepDock model and
846 determine key binding site residues for the native PAR4 tethered ligand and PAR4 agonist
847 peptide AYPGKF-NH_2. Residues were mutated by single-nucleotide substitutions replacing
848 native residues with alanine. Successful mutations were confirmed by DNA sequencing
849 (London Regional Genomics Centre, London, ON).
850
851 ***Cell Lines and Culture Conditions.*** All media and cell culture reagents were purchased from
852 Thermo Fisher Scientific (Hampton, New Hampshire, United States). HEK-293 cells (ATCC;
853 Manassas, Virginia, United States) and CRISPR/Cas9 HEK-293 β-arrestin double knockout
854 (β-arr knockout) cell lines were maintained in Dulbecco's modified Eagle's medium
855 supplemented with 10% fetal bovine serum, 1% sodium pyruvate, and 1% streptomycin
856 penicillin. Cells stably transfected with PAR4-YFP vector was routinely cultured in the above
857 media supplemented with 600 µg/mL G418 sulfate (Geneticin; ThermoFisher Scientific
858 Waltham, Massachusetts, United States). Since trypsin activates PAR4, cells were routinely
859 sub-cultured using enzyme-free isotonic phosphate-buffered saline (PBS), pH 7.4, containing
860 1 mM EDTA followed by centrifugation to remove PBS-EDTA and plated in appropriate
861 culture plates for further experimentation. Cells were transiently transfected with appropriate
862 vectors using a modified calcium phosphate transfection (Nuclease free water, 2.5M $CaCl_2$,
863 and 2x HEPES Buffered Saline). Transient transfections were rinsed with phosphate buffered
864 saline (PBS) 24 hours post-transfection and replaced with growth media. Transiently
865 transfected cells were assayed or imaged at 48 hours post-transfection. *Generation of β-*
866 *arrestin-1/-2 double knockout HEK-293 cells using CRISPR/Cas9*. A β-arrestin-1/-2 double
867 knockout HEK-293 cells cell line (β-arr. knockout) was generated using CRISPR/Cas9
868 mediated gene targeting. Guides sequences targeted to β-arrestin-1 or β-arrestin-2 were
869 designed using the design tool at http://crispr.mit.edu. Gene targeting guides (β-arrestin 1;

870 TGTGGACCACATCGACCTCG, β-arrestin 2; GCGGGACTTCGTAGATCACC, were
871 ligated into the PX458 vector (Kind gift from Dr. Feng Zhang, MIT, Addgene plasmid #48138),
872 verified by direct sequencing and transfected in HEK-293 cells via calcium phosphate
873 transfection (Ferguson and Caron, 2004; Graham and van der Eb, 1973). GFP expressing cells
874 were single-cell selected by flow cytometry (FACSAria III; London Regional Flow Cytometry
875 Facility) into wells of a 96-well plate. Clonal cell populations were expanded and screened by
876 western blot to identify successful knockout (anti-β-arrestin-1/-2 antibody, rabbit mAb D24H9;
877 Cell Signalling Technologies, Danvers, Massachusetts, United States; anti-β-actin antibody,
878 mouse mAb 8H10D10; Cell Signalling Technologies; Supplemental Figure 3).
879
880 ***General Methods for Peptide Synthesis***
881 All reagents were purchased from Sigma-Aldrich, ChemImpex, or Thermo Fisher Scientific
882 and used without further purification. Peptides were synthesized using standard Fmoc-solid
883 phase peptide synthesis (SPPS) on Rink amide MBHA resin (256 mg, 0.1 mmol, 0.39 mmol/g)
884 with a Biotage® Syrowave™ automated peptide synthesizer (0.4 mmol of HCTU, 0.4 mmol
885 of Fmoc-amino acids, 0.6 mmol of DIPEA, 1 h coupling). Some peptides also involved
886 additional manual synthesis (see procedures below). Following automated and manual
887 synthesis, peptides were cleaved off the resin by being shaken in a cleavage cocktail solution
888 of 95% TFA, 2.5% TIPS, and 2.5% H_2O (4 mL, 5 h), precipitated in ice cold *tert*-butyl methyl
889 ether, lyophilized, purified by preparative RP-HPLC, and further lyophilized to obtain a dry
890 powder. Purity was assessed by analytical RP-HPLC and characterized by mass spectrometry
891 (MS). The analytical RP-HPLC was performed on a system consisting of an analytical Agilent
892 Zorbax SB-C8 column (4.6 x 150 mm, 5 µm), Waters 600 controller, Waters in-line degasser,
893 and Waters Masslynx software (version 4.1). Two mobile phases were used; eluent A (0.1%
894 TFA in acetonitrile) and eluent B (0.1% TFA in MilliQ water). The flow rate was set at 1.5
895 $mLmin^{-1}$ over 10 minutes with an additional 5-minute wash (95% solvent A in solvent B). A
896 Waters 2998 Photodiode array detector (200-800 nm) and an ESI-MS (Waters Quattro Micro
897 API mass spectrometer) were used to monitor the column eluate. The preparative RP-HPLC
898 used the same system, eluents, and detection method as mentioned above for the analytical RP-
899 HPLC, except that a preparative Agilent Zorbax SB-C8 column (21.2 x 150 mm, 5 µm) at a
900 flow rate of 20 $mLmin^{-1}$ was used. The mass spectra for all peptides were determined in positive
901 mode using an ESI ion source on either a Bruker micrOToF II mass spectrometer or a Xevo
902 QToF mass spectrometer (Table S1). All peptides had purity >95% as determined by analytical
903 HPLC (see supplemental information, Figure S1).
904
905 ***Synthesis of Ac-AYPGKF-NH_2.*** The hexapeptide (AYPGKF) was synthesized using the
906 standard automated Fmoc-SPPS discussed in the general methods for peptide synthesis. While
907 still on resin, with all of the side chains protected, and with the N-terminal Fmoc-deprotection
908 completed, the N-terminus of this peptide was acetylated by being shaken in a solution of acetic
909 anhydride and DMF (v/v 1:4, 5 mL, 30 min). Following this, the peptide was cleaved, purified,
910 and analyzed as mentioned in the general methods for peptide synthesis.
911

912 ***Synthesis of Peptides Involving N-methylation of the Peptide Backbone*** Peptides [(*N*-Me-A)-
913 YPGKF-NH_2, (*N*-Me-S)-YPGKF-NH2, A-(*N*-Me-Y)-PGKF-NH2, AYPG-(N_α-Me-K)-F-
914 NH2, and AYPGK-(*N*-Me-F)-NH_2] were synthesized using abovementioned automated Fmoc-
915 SPPS up to the desired amino acid that was *N*-methylated (e.g. KF-resin for AYPG-(N_α-Me-
916 K)-F-NH_2). Following Fmoc-deprotection of the resin-bound N-terminal amino acid (e.g.
917 lysine for AYPG-(N_α-Me-K)-F-NH_2), site selective *N*-methylation of the N-terminal amino
918 acid was completed as follows: First, protection of the primary amine was completed to favour
919 monomethylation by adding 2-nitrobenzenesulfonyl chloride (110.8 mg, 0.5 mmol) and 2,4,6-
920 trimethylpyridine (132 µL, 1.0 mmol) in NMP (4 mL) to the on-resin peptide (0.1 mmol) and
921 shaken (15 min). Following completion of the protection reaction, the resin was washed thrice
922 with NMP (3X 5 mL) and dry THF (3X 5 mL). Second, *N*-methylation was completed through
923 Mitsunobu conditions by adding triphenylphosphine (131.2 mg, 0.5 mmol), diisopropyl
924 azodicarboxylate (98 µL, 0.5 mmol), and methanol (41 µL, 1.0 mmol) in dry THF (4 mL) to
925 the on-resin peptide and shaken under N_2 (10 min). Following completion of the *N*-methylation
926 reaction, the resin was washed thrice with dry THF (3X 5mL) and NMP (3X 5 mL). Third, the
927 methylated N-terminal amine was then deprotected by adding 2-mercaptoethanol (70 µL, 1.0
928 mmol) and 1,8-diazabicyclo(5.4.0)undec-7-ene (75 µL, 0.5 mmol) in NMP (4 mL) to the on-
929 resin peptide and shaken (5 min). The solution turned bright yellow as expected. The solution
930 was removed and then this third step was repeated, followed by being washed five times with
931 NMP (5X 5 mL) and thrice with DMF (3X 5 mL). Addition of the next sequential amino acid
932 (except for inapplicable peptides i.e. (*N*-Me-A)-YPGKF-NH_2 and (*N*-Me-S)-YPGKF-NH_2)
933 was added manually [0.3 mmol of HATU, 0.3 mmol of Fmoc-amino acid (e.g. Fmoc-Gly-OH
934 for AYPG-(N_α-Me-K)-F-NH_2), 0.6 mmol of DIPEA, 4 mL of DMF, 3 h coupling]. Following
935 completion of the sequential amino acid reaction, the resin was washed 5 times with DMF (5X
936 5mL) and then the next sequential amino acid was added (on applicable peptides i.e AYPG-
937 (N_α-Me-K)-F-NH_2 and AYPGK-(*N*-Me-F)-NH_2) using the automated procedure mentioned in
938 the general methods for peptide synthesis. Following completion of the synthesis, the peptide
939 was cleaved, purified, and analyzed as mentioned in the general methods for peptide synthesis.
940 The amino acid *N*-methylglycine, commonly known as sarcosine, was obtained from a
941 commercial source, and therefore, *N*-methylglycine containing peptides (i.e. Sar-YPGKF-NH_2
942 and AYP-Sar-KF-NH_2) were synthesized solely by the standard automated Fmoc-SPPS
943 discussed in the general methods for peptide synthesis.
944
945 ***Synthesis of AYPG-(N_ε-Me-K)-F-NH_2.*** The hexapeptide (AYPGKF) was synthesized using
946 the standard automated Fmoc-SPPS discussed in the general methods for peptide synthesis,
947 except that Fmoc-Lys(Alloc)-OH was used in place of standard Fmoc-Lys(Boc)-OH. While
948 still on resin, with all of the side chains protected, and with the N-terminal Fmoc-deprotection
949 completed, the N-terminus of this peptide was Boc protected by adding Boc-ON (98.5 mg, 0.4
950 mmol) and DIPEA (70 µL, 0.4 mmol) in DMF (4 mL) and shaken (4 hours). The solution was
951 removed and this Boc protection was repeated overnight (20 hours) to ensure reaction
952 completion. The resin was washed thrice with DMF (3X 5 mL) and dry DCM (3X 5 mL) and
953 was placed under N_2 for site selective Alloc deprotection of the on-resin lysine side chain.
954 Phenylsilane (296 µL, 2.4 mmol) in dry DCM (2 mL) was added to the resin.
955 Tetrakis(triphenylphosphine) palladium(0) (23.1 mg, 20 µmol) was dissolved in dry DCM (1

956 mL) and added to the resin. The peptide column was flushed with N_2 (2 min) followed by being
957 shaken (5 min). The resin was washed thrice with dry DCM (3X 5 mL). The procedure was
958 repeated and shaken again (30 min). The resin was washed four times with DCM (4X 5 mL)
959 and DMF (4X 5 mL). Following this N-terminal Boc protection and subsequent side chain
960 Alloc deprotection, *N*-methylation of the on-resin lysine side chain was completed through the
961 site selective *N*-methylation procedure mentioned above. Following completion of the
962 synthesis, the peptide was cleaved, purified, and analyzed as discussed in the general methods
963 for peptide synthesis.
964
965 ***SPPS Reaction Monitoring.*** Three methods were used to monitor SPPS reactions. Two
966 methods (the Kaiser Test and the small-scale resin cleavage) were used to monitor general
967 peptide synthesis. Three methods (the Kaiser Test, the small-scale resin cleavage, and the
968 Chloranil Test) were used to monitor synthesis of peptides involving *N*-methylation. For the
969 Kaiser Test, several resin beads were placed in a test tube followed by the addition of 42.5 mM
970 phenol in ethanol (50 µL), 20 µM potassium cyanide in pyridine (50 µL), and 280.7 mM
971 ninhydrin in ethanol (50 µL). The mixture was then heated (100 °C, 5 min); where a positive
972 test indicates the presence of a free primary amine. For the small-scale resin cleavage method,
973 several beads and cleavage cocktail (500 µL) are shaken, worked up as per the full cleavage of
974 the resin procedure described above, and the desired peptide was confirmed through HPLC-
975 MS. For the Chloranil Test, several resin beads were placed in a test tube followed by the
976 addition of 357.8 mM acetaldehyde in DMF (50 µL) and 81.3 mM *p*-chloranil in DMF (50 µL)
977 and allowed to stand at room temperature (5 min); where a positive test indicates the presence
978 of a free secondary amine.
979
980 ***Calcium Signalling Assay.*** HEK-293 cells or HEK-293 cells stably expressing PAR4-YFP
981 were loaded with calcium sensitive dye (Fluo-4 NW, F36206, Life Technologies, Thermo
982 Fisher) and aliquoted into cuvettes with Hanks buffered salt solution (HBSS containing Ca^{2+}
983 and Mg^{2+}). Samples were excited at 480nm and emission recorded at 530nm. Baseline
984 fluorescence from PAR4-YFP excitation remains constant throughout experiment. Following
985 baseline recording, agonist induced changes in fluorescence was recorded. Change in
986 fluorescence from baseline to maximum response at a given agonist concentration (delta) were
987 expressed as a percentage of maximum cellular response elicited by calcium ionophore
988 (A23187, Sigma-Aldrich). *Calcium Signalling Assay with PAR4 orthosteric site-directed*
989 *mutants.* HEK-293 cells were transiently transfected with 2µg of wild-type YFP tagged PAR4
990 or PAR4 mutant receptors (described above) using the calcium phosphate transfection protocol
991 as described above. Calcium signalling was investigated as described above for the wild type
992 receptor.
993
994 ***β-arrestin Recruitment - Bioluminescence Resonance Energy Transfer (BRET).*** HEK-293
995 cells were co-transfected with PAR4-YFP (2µg) or mutant PAR4-YFP and β-arrestin-1- or -2-
996 renilla luciferase (rluc, 0.2µg) using modified calcium phosphate transfection. Cells were re-
997 plated (24 hours post-transfection) into white 96-well plates (Corning). At 48-hours post-
998 transfection, agonist-stimulated β-arrestin recruitment to PAR4 was detected by measuring

999 BRET following 20 minutes of agonist stimulation. Coelenterazine (5μM; Nanolight
1000 Technology, Pinetop, AZ) was added ten minutes prior to BRET collection using a Berthold
1001 Mithras LB 940 plate reader.
1002
1003 ***Testing Peptide library specificity for PAR4*** Previous studies have pointed to the possibility
1004 of PAR agonist peptides cross activating other members of this family. For example, the PAR1
1005 tethered ligand peptide SFLLRN is able to activate PAR2 and substitution of a phenylalanine
1006 residue in certain PAR4 agonist peptides confers PAR1 activity (Boitano et al., 2011; Faruqi
1007 et al., 2000; Lerner et al., 1996). Activating peptides typically require an aromatic sidechain in
1008 position 2 (F in PAR1) and we wondered if substitution of tyrosine for phenylalanine may
1009 decrease selectivity at PAR4 and increase crosstalk with PAR1. We examined whether
1010 substitutions made to AYPGKF-NH_2 affected their selectivity using a calcium signalling assay
1011 in HEK-293 cells that endogenously express PAR1 and PAR2. None of the peptides tested
1012 elicited a signalling greater than 5% of the calcium ionophore A23187 showing that they retain
1013 selectivity towards PAR4 (Supp. Fig. 4). Additionally, we investigated specificity using BRET
1014 for β-arrestin-2 recruitment to cells expressing PAR4-YFP or PAR2-YFP. None of the peptides
1015 were able to induce β-arrestin recruitment in PAR2-YFP expressing HEK-293 cells (NET
1016 BRET of 0.05 and over) with the exception of AYPGK-1Nal-NH_2 (Supp. Fig. 5).
1017
1018 ***PAR4-stimulated Mitogen-activated Protein Kinase (MAPK) signalling*** *HEK-293 and*
1019 *CRISPR/Cas9 β-arrestin-1/-2 double knockout HEK-293.* Agonist-stimulated mitogen-
1020 activated protein kinase (MAPK) signalling in CRISPR/Cas9 HEK-293 β-arrestin double
1021 knockout cells (β-arr. knockout) and wild-type HEK-293 cells transfected with PAR4-YFP
1022 were analysed by western blot. Cells were placed in serum free media (serum-free DMEM,
1023 Gibco) for 3 hours before beginning experiment. Cells were then stimulated with 30μM
1024 AYPGKF-NH_2 for varying time periods (0, 2, 5, 10, 20, 30, 60, 90 minutes) at 37 ˚C. Treated
1025 cells were placed on ice following stimulating period. Total protein was extracted adding kinase
1026 lysis buffer with phosphatase and protease inhibitors (20 mM Tris-HCl, pH 7.5, 100 mM NaCl,
1027 10 mM $MgCl_2$, 1 mM EDTA, 1 mM EGTA, 0.5% NP-40, 2.5 mM sodium pyrophosphate, 1
1028 mM b-glycerophosphate, 1 mM Na_3VO_4, 25 mM NaF, 1 mg/mL leupeptin, 1 mg/m aprotinin,
1029 1 mM phenylmethylsulfonyl fluoride, and 1mM dithiothreitol) for 20 minutes and cell
1030 membranes were cleared by centrifugation (13,300g for 3 minutes). Protein concentrations
1031 were measured using the Pierce BCA Protein Assay (Thermo Fisher Scientific). Protein
1032 samples were heat-denatured at 98°C for 8 minutes in denaturing Laemmli buffer (containing
1033 2-mercaptoethanol) and resolved on 4–12% gradient Invitrogen Bolt Bis-Tris Plus gels
1034 (Thermo Fisher Scientific). The resolved proteins were transferred via wet transfer in buffer
1035 (1X Tris-glycine, 20% methanol) to a polyvinylidene difluoride membrane and blocked in
1036 TBST buffer (TBS with 0.1% (v/v) Tween-20) supplemented with 1% ECL Advance Blocking
1037 Agent (GE Healthcare, Waukesha, WI) for 40 minutes at room temperature. p44/42
1038 (Thr202/Tyr204) phosphorylation was detected with specific antibodies (Cell Signalling
1039 Technology, Danvers, MA; diluted 1:1000 in TBST) overnight at 4°C. phospho-p44/42
1040 immunoreactivity was detected using the horseradish peroxidase-conjugated anti-rabbit
1041 secondary antibody (Cell Signalling Technology; 1:10,000 in TBST for 1 hour). After washing

1042 the membrane with TBST (3 x 10-minute washes), the peroxidase activity was detected with
1043 the chemiluminescence reagent ECL Advance (GE Healthcare) on iBright image Station
1044 (Invitrogen, Burlington, ON). Membranes were then stripped with blot stripping buffer
1045 (Thermo Fisher Scientific) at room temperature and blocked in TBST with 1% ECL Advance
1046 Blocking Agent before incubation with the p44/42 (1:1000 in TBST with 1% ECL Advance
1047 Blocking Agent) overnight at 4°C. Following incubation with primary antibody, blots were
1048 rinsed in TBST and incubated with appropriate horseradish peroxidase -conjugated anti-rabbit
1049 or anti-mouse secondary antibody (1:10,000 in TBST for 1 hour). Membranes were washed
1050 and imaged as previously described. Band intensities representing activated MAPK were
1051 quantified using FIJI (Schindelin et al., 2012). Phospho-kinase levels were normalized for
1052 differences in protein loading by expressing the data as a ratio of the corresponding total-p44/42
1053 signal. Data are expressed as a fold increase over unstimulated baseline control. *PAR4-*
1054 *stimulated MAPK signalling in HEK-293 +/- YM254890.* Agonist-stimulated MAPK signalling
1055 in wild-type HEK-293 cells transfected with PAR4-YFP were analysed by western blot. Cells
1056 were placed in serum free media (serum-free DMEM, Gibco) for 3 hours before beginning
1057 experiment. Prior to agonist stimulation cells were treated with either control (0.001% DMSO)
1058 or YM254890 (100nM) for 20 minutes. Cells were then stimulated with 30µM AYPGKF-NH_2
1059 for varying time periods (0, 2, 5, 10, 20, 30, 60, 90 minutes) at 37 degrees Celsius. Cells were
1060 lysed, protein quantified, and samples run and imaged as previously described. *MAPK*
1061 *signalling in PAR4-YFP stable cells with peptide library.* Agonist-stimulated mitogen-
1062 activated protein kinase (MAPK) signalling in HEK-293 cells stably expressing PAR4-YFP
1063 were analysed by western blot following stimulation with PAR4 peptide agonists. Cells were
1064 placed in serum free media (serum-free DMEM, Gibco) for 3 hours before beginning
1065 experiment. Cells were stimulated with either control (no agonist), AYPGKF-NH_2 or agonist
1066 peptides described at 100µM concentration. Cells were stimulated for 10 minutes with agonist
1067 and lysed, quantified, and blot as previously described.
1068
1069 ***Preparation of washed platelets and light-transmission aggregometry.*** Blood was drawn from
1070 the abdominal aorta or heart of Sprague-Dawley rats into trisodium citrate (3.4% w.v). The
1071 blood was centrifuged at 200g for 15 minutes at 22 degrees Celsius to isolate platelet-rich
1072 plasma (PRP). PRP was transferred to a 14 mL polypropylene round-bottom tube (Falcon) and
1073 centrifuged at 1800 rotations per minute (rpm.; 594g) for 10 minutes at 22˚C to pellet platelets
1074 and obtain platelet-poor plasma (PPP). PPP was decanted and used for 100% light transmission
1075 control. To obtain washed platelet sample, platelets were washed twice in Tyrode's buffer (12
1076 mM $NaHCO_3$, 127 mM NaCl, 5 mM KCl, 0.5 mM NaH_2PO_4, 1 mM $MgCl_2$, 5 mM glucose,
1077 and 10 mM HEPES; Ramachandran et al., 2017) and resuspended to a volume equivalent to
1078 that of the initial blood draw. Washed platelet sample was equilibrated for one hour at ambient
1079 temperature following the addition of 1M $CaCl_2$ (1 µl/mL). 400 µl of this washed platelet
1080 suspension was used for light transmission aggregometry on a platelet aggregometer (Model
1081 700; Chrono-Log Corp, Havertown, PA).
1082
1083 ***Structural homology modelling of PAR4.*** Residues resolved in the PAR2 crystal (5NDD.pdb)
1084 were used to generate a homology model of wild-type human PAR2. Homology model of wild-
1085 type human PAR2 was then aligned with the wild-type human PAR4 amino acid sequence

[National Center for Biotechnology Information (NCBI) accession number NM_003950) using Clustal Omega (Madeira et al., 2019; Sievers et al., 2011). Only residues resolved in the crystal structure of PAR2 were used as template coordinates for PAR4 homology modelling. Twenty human PAR4 homology models were generated using the human PAR2 crystal structure coordinates (5NDD.pdb; Cheng et al., 2017) as a template in MODELLER (version 9.16, Webb and Sali, 2017). The model with the lowest DOPE score was taken as the best structure and visualized using PyMOL (version 1.7.4, Schrödinger, LLC). Electrostatic surface potential was calculated after assignment of partial charges using PDB2PQR and using the Adaptive Poisson-Boltzmann Solver plugin in PyMOL (Dolinsky et al., 2004).

In silico docking of AYPGKF-NH$_2$ to the PAR4 homology model. *in silico* docking of PAR4 agonist peptide, AYPGKF-NH$_2$, to PAR4 homology model was undertaken using GalaxyPepDock (Lee et al., 2015). The lowest energy PAR4 homology model PDB file was loaded into GalaxyPepDock along with a text file of the PAR4 agonist peptide sequence which GalaxyPepDock uses to predict a peptide structure for docking analyses (Ala-Tyr-Pro-Gly-Lys-Phe; amidation is not included in the structure prediction). Ten models of PAR4-AP docking were generated. Frequency of receptor-peptide residue interactions, taken as atom-atom distances of less than 3 Angstroms, was quantified manually to determine highly recurrent interactions.

Data analysis and statistical tests. Data are shown as mean ± SEM. Calcium signalling and β-arrestin-1/-2 recruitment concentration effect curves were calculated using nonlinear regression curve fitting (three parameter; Prism7). EC_{50} values are reported (Table 1) where signal has saturated. Where signalling is not saturated EC_{50} is reported for calcium as not determined (*n.d.*). The F-statistic calculated to compare EC_{50} values was calculated using the extra sum-of-squares analysis (Kim et al., 2019). For table 1, values comparing percentage of signalling or recruitment at 100 μM to values obtained from the parental PAR4-AP, AYPGKF-NH$_2$, are shown. Significance was determined for comparisons with 100 μM AYPGKF-NH$_2$ and p44/42 phosphorylation by one-way analysis of variance (ANOVA). Western blot protein densitometry was quantified using FIJI. Transformation and analysis were conducted on raw data and significance is indicated by '*' ($p < 0.05$).

Acknowledgements and Funding. These studies were funded by a Canadian Institutes of Health Research (CIHR) grant (RR) and grants from the Natural Sciences and Engineering Research Council of Canada (LL and PS). PT is the recipient of a doctoral QEII Graduate Scholarships in Science and Technology. JCL is the recipient of a Canada Graduate Scholarship and an Ontario Graduate Scholarship.

Competing interests. The authors declare that no competing interests exist.

				% of AYPGKF-NH_2 Response (100μM)			
	Peptide (alterations shown in red)	**Ca^{2+} EC_{50} (μM)**	**Ca^{2+} Max. (% of A23187)**	**Ca^{2+} signaling**	**β-Arr-1 recruitment**	**β-Arr-2 recruitment**	**p-p44/42 (fold over baseline; 100 μM)**
PAR4-AP	**AYPGKF-NH_2**	12.1 ± 3.1	27.4 ± 1.7	100.0 ± 8.2	100.0 ± 3.9	100 ± 3.5	5.9 ± 1.5
Alanine	A**A**PGKF-NH_2	*n.d.*	51.8 ± 25.4	52.9 ± 12.4*	47.3 ± 3.6*	46.4 ± 3.2*	0.8 ± 0.1
	AY**A**GKF-NH_2	63.7 ± 20.8*	29.7 ± 3.4	75.4 ± 11.1	48.5 ± 7.9*	43.4 ± 7.1*	1.2 ± 0.3
	AYP**A**KF-NH_2	21.2 ± 6.6	22.4 ± 1.9	72.2 ± 6.3	56.4 ± 5.6*	54.6 ± 5.1*	1.0 ± 0.2
	AYPG**A**F-NH_2	9.8 ± 2.9	25.7 ± 1.8	96.7 ± 17.8	59.3 ± 7.2*	70.8 ± 6.5	6.5 ± 2.7
	AYPGK**A**-NH_2	17.3 ± 5.0	20.0 ± 1.5	69.4 ± 4.1	47.9 ± 3.8*	52.6 ± 3.5*	3.8 ± 2.2
D-isomer	**a**YPGKF-NH_2	*n.d.*	19.2 ± 4.8	24.0 ± 4.4*	48.7 ± 2.6*	47.5 ± 2.4*	0.8 ± 0.2
	A**y**PGKF-NH_2	*n.d.*	1.1 ± 0.5	3.9 ± 2.8*	50.7 ± 4.6*	46.4 ± 4.2*	0.6 ± 0.1
	AY**p**GKF-NH_2	*n.d.*	1.2 ± 0.4	6.1 ± 3.4*	45.2 ± 10.5*	38.1 ± 9.5*	0.7 ± 0.2
	AYPG**k**F-NH_2	*n.d.*	16.9 ± 5.3	25.2 ± 5.2*	47.4 ± 1.0*	36.5 ± 0.9*	1.0 ± 0.3
	AYPGK**f**-NH_2	22.2 ± 4.7	21.9 ± 1.2	76.7 ± 5.2	80.3 ± 6.6	74.1 ± 6.0	6.5 ± 2.9
***N*-methyl.**	**(*N*-Me-A)**-YPGKF-NH_2	*n.d.*	15.0 ± 7.5	13.3 ± 1.3*	119.2 ± 11.9	80.6 ± 10.8	1.3 ± 0.3
	A-**(*N*-Me-Y)**-PGKF-NH_2	*n.d.*	2.7 ± 0.2	9.8 ± 2.9*	71.4 ± 10.8	61.5 ± 9.8*	2.2 ± 0.2
	AYP-**Sar**-KF- NH_2	*n.d.*	2.4 ± 0.3	8.8 ± 1.5*	35.9 ± 4.3*	36.1 ± 3.9*	1.4 ± 0.2
	AYPG-**(N_α-Me-K)**-F-NH_2	*n.d.*	9.6 ± 1.9	18.3 ± 1.5*	126.7 ± 18.6	77.1 ± 16.9	1.8 ± 0.9
	AYPGK-**(*N*-Me-F)**-NH_2	7.6 ± 1.9	26.3 ± 1.4	99.4 ± 7.8	136.9 ± 18.0*	96.6 ± 16.9	15.7 ± 4.6
N-terminal	**Ac**-AYPGKF-NH_2	*n.d.*	11.0 ± 3.3	49.9 ± 16.5*	47.3 ± 3.1*	45.5 ± 2.8*	1.2 ± 0.4
Position 1	**V**YPGKF-NH_2	22.9 ± 8.3	16.8 ± 1.7	48.5 ± 4.6*	73.6 ± 13.0	55.2 ± 11.8*	2.3 ± 0.7
	Nle-YPGKF-NH_2	*n.d.*	1.1 ± 0.1	4.0 ± 1.1*	40.2 ± 9.7*	36.5 ± 8.8*	21.4 ± 7.0*
	Sar-YPGKF- NH_2	*n.d.*	1.6 ± 0.6	9.7 ± 8.5*	35.6 ± 2.0*	39.8 ± 1.8*	1.6 ± 1.1
	Aib-YPGKF-NH_2	50.2 ± 15.3*	25.1 ± 2.5	72.9 ± 12.0	38.6 ± 3.9*	37.3 ± 3.6*	7.8 ± 3.5
	(*N*-Me-S)-YPGKF-NH_2	*n.d.*	2.2 ± 0.5	8.8 ± 1.8*	78.1 ± 6.9	51.7 ± 6.3*	1.8 ± 0.4
	betaAla-YPGKF- NH_2	*n.d.*	1.9 ± 0.4	10.3 ± 3.9*	25.7 ± 4.8*	31.8 ± 4.4*	9.1 ± 3.4
	Inp-YPGKF-NH_2	*n.d.*	3.4 ± 0.8	18.9 ± 7.3*	32.0 ± 3.3*	26.9 ± 3.0*	1.3 ± 0.3
Position 2	A-**Tyr(Me)**-PGKF-NH_2	15.7 ± 4.0	25.7 ± 1.6	91.1 ± 10.1	77.9 ± 3.8	85.8 ± 3.4	12.7 ± 5.8
	A-**F-(4-fluoro)**-PGKF-NH_2	19.9 ± 5.4	35.1 ± 2.5	105.4 ± 9.0	72.1 ± 9.0	86.9 ± 8.1	10.1 ± 3.9
Position 3	AY-**Pip**-GKF- NH_2	30.7 ± 4.9	23.3 ± 1.1	74.2 ± 4.8	38.8 ± 3.0*	44.0 ± 2.7*	1.3 ± 0.3
	AY-**Nip**-GKF- NH_2	*n.d.*	2.5 ± 0.3	10.0 ± 1.8*	32.9 ± 4.9*	30.9 ± 4.5*	1.0 ± 0.3
Position 4	AYP-**betaAla**-KF- NH_2	*n.d.*	9.7 ± 2.4	19.8 ± 5.8*	42.5 ± 1.8*	24.9 ± 1.6*	1.8 ± 0.6
Position 5	AYPG**O**F- NH_2	4.2 ± 1.1	20.7 ± 1.1	77.3 ± 7.9	121.7 ± 8.5	112.1 ± 7.7	23.4 ± 7.2*
	AYPG**R**F-NH_2	4.0 ± 1.1	21.3 ± 1.2	82.0 ± 8.3	154.2 ± 10.3*	140.1 ± 9.4*	3.0 ± 0.3
	AYPG-**(N_ε-Me-K)**-F-NH_2	6.7 ± 1.9	23.8 ± 1.5	88.9 ± 9.3	122.5 ± 12.4	116.7 ± 11.2	20.5 ± 5.3*
	AYPG-**Cit**-F-NH_2	5.4 ± 0.8	18.2 ± 0.6	65.5 ± 1.3	94.1 ± 10.1	87.7 ± 9.2	25.1 ± 7.5*
Position 6	AYPGK**Y**-NH_2	5.2 ± 1.0	16.9 ± 0.7	61.2 ± 4.3*	120.5 ± 12.5	109.9 ± 11.4	20.2 ± 9.7*
	AYPGK-**F(4-Me)**-NH_2	9.4 ± 3.0	17.8 ± 1.3	62.0 ± 5.5*	56.4 ± 1.2*	63.2 ± 1.1*	0.9 ± 0.4
	AYPGK-**F(4-fluoro)**-NH_2	*n.d.*	*n.d.*	16.5 ± 10.2*	25.2 ± 6.5*	41.3 ± 5.9*	1.1 ± 0.5
	AYPGK-**1Nal**-NH_2	9.6 ± 1.9	18.7 ± 0.9	65.4 ± 7.4	77.5 ± 2.3	64.1 ± 2.0*	21.3 ± 10.8*
	AYPGK-**2Nal**-NH_2	11.1 ± 2.3	25.3 ± 1.3	93.9 ± 4.2	77.0 ± 7.0	91.6 ± 6.4	4.3 ± 1.7

Table 1. Summary table of all calcium, β-arrestin, and p44/42 data. Calcium data is displayed as EC_{50} or not determined (*n.d.*) if EC_{50} could not be calculated. Maximum calcium response achieved with each peptide is shown as a percentage of the maximum calcium response achievable in a given experiment revealed by calcium ionophore (% of A23187 calcium ionophore). Statistically significant shifts in EC_{50} compared to PAR4-AP, AYPGKF-NH_2, were found using the F-statistic (*$p < 0.05$). Given that saturation did not always occur, all peptides are compared to the parental PAR4-AP, AYPGKF-NH_2, and shown as a percent of

1133 the response obtained with PAR4-AP at a given concentration (100 μM). Finally, fold increase
1134 over unstimulated baseline is shown for phosphorylation of p44/42 MAP kinase activation.
1135 Statistical significance for comparisons at 100 μM and p44/42 phosphorylation are calculated
1136 using one-way ANOVA of response compared to PAR4-AP (*$p < 0.05$).

1137 **Figure 1. Calcium and β-**
1138 **arrestin recruitment in**
1139 **response to alanine**
1140 **substitutions in the PAR4-AP.**
1141 **(A) Agonist-stimulated**
1142 **calcium signalling.** Calcium
1143 signalling is shown as a
1144 percentage of the maximum
1145 calcium signalling obtained by
1146 application of calcium
1147 ionophore (A23187, 3 µM). (*n*
1148 = *3-7*) **Agonist-stimulated**
1149 **recruitment of β-arrestin-1**
1150 **(B) and β-arrestin-2 (C) to**
1151 **PAR4.** Concentration effect
1152 curves of BRET values from
1153 cells treated increasing
1154 concentrations of peptide are
1155 presented as normalized net
1156 BRET ratio. (*n* = *3*).

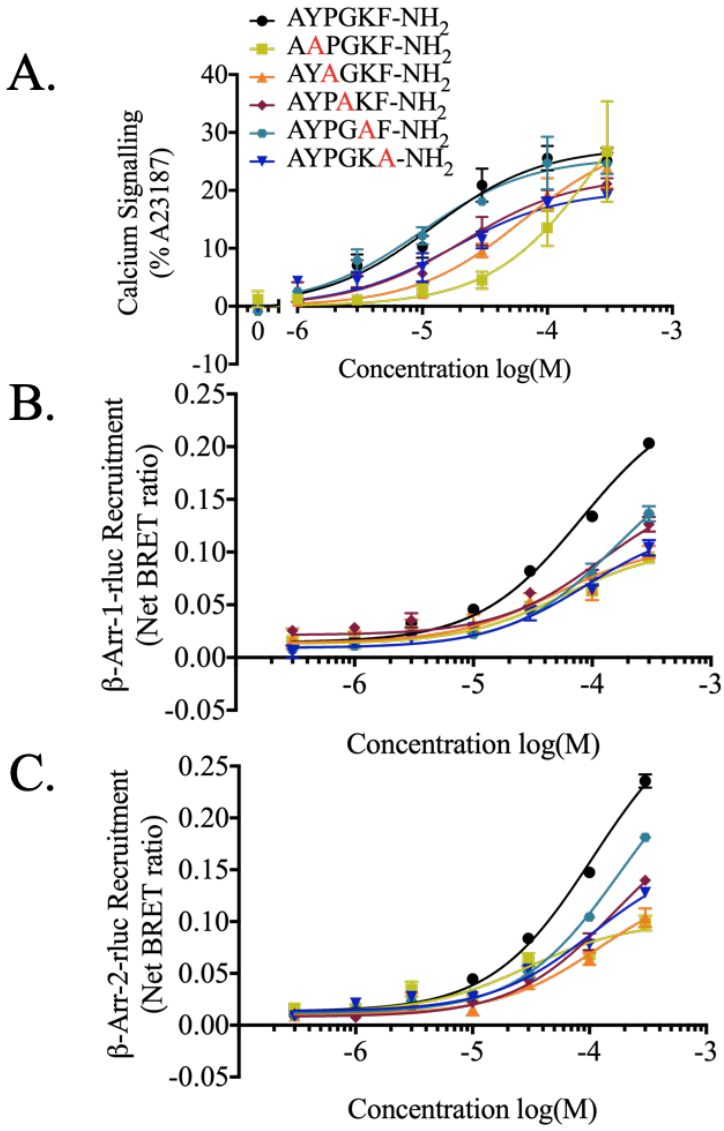

1157 **Figure 2. Calcium and β-**
1158 **arrestin recruitment in**
1159 **response to D-isomer**
1160 **substitutions in the PAR4-AP.**
1161 **(A) Agonist-stimulated**
1162 **calcium signalling.** Calcium
1163 signalling is shown as a
1164 percentage of the maximum
1165 calcium signalling obtained by
1166 application of calcium
1167 ionophore (A23187, 3 µM). (*n* =
1168 *3-4*) **Agonist-stimulated**
1169 **recruitment of β-arrestin-1 (B)**
1170 **and β-arrestin-2 (C) to PAR4.**
1171 Concentration effect curves of
1172 BRET values from cells treated
1173 increasing concentrations of
1174 peptide are presented as
1175 normalized net BRET ratio. (*n* =
1176 *3*).
1177

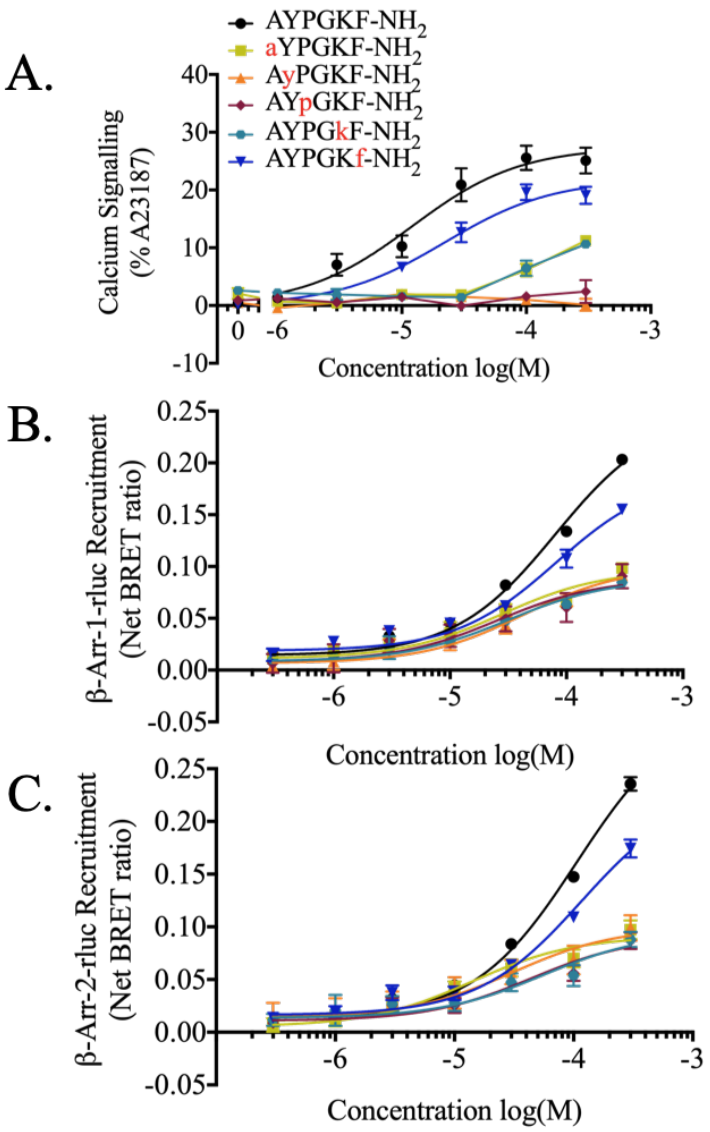

1178 **Figure 3. Calcium and β-arrestin**
1179 **recruitment in response to *N*-**
1180 **methylation substitutions in the**
1181 **PAR4-AP. (A) Agonist-stimulated**
1182 **calcium signalling.** Calcium
1183 signalling is shown as a percentage
1184 of the maximum calcium signalling
1185 obtained by application of calcium
1186 ionophore (A23187, 3 μM). (*n = 3-*
1187 *7)* **Agonist-stimulated recruitment**
1188 **of β-arrestin-1 (B) and β-arrestin-**
1189 **2 (C) to PAR4.** Concentration effect
1190 curves of BRET values from cells
1191 treated increasing concentrations of
1192 peptide are presented as normalized
1193 net BRET ratio. (*n = 3*).

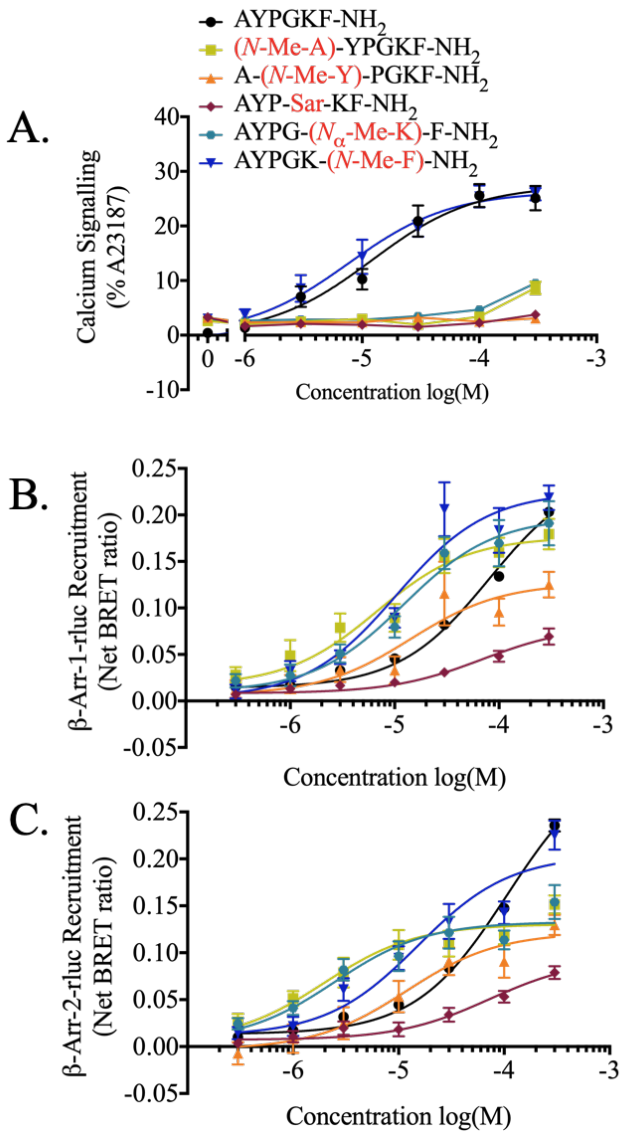

1194 **Figure 4. Calcium signalling and**
1195 **β-arrestin recruitment to PAR4 in**
1196 **response to AYPGKF-NH₂ or**
1197 **peptides with N-terminal**
1198 **acetylation or additional**
1199 **substitutions in position 1**
1200 **(alanine). (A) Agonist-stimulated**
1201 **calcium signalling.** Calcium
1202 signalling is shown as a percentage
1203 of the maximum calcium signalling
1204 obtained by application of calcium
1205 ionophore (A23187, 3 µM). (*n = 3-*
1206 *7)* **Agonist-stimulated recruitment**
1207 **of β-arrestin-1 (B) and β-arrestin-**
1208 **2 (C) to PAR4.** Concentration effect
1209 curves of BRET values from cells
1210 treated increasing concentrations of
1211 peptide are presented as normalized
1212 net BRET ratio. (*n = 3*).
1213

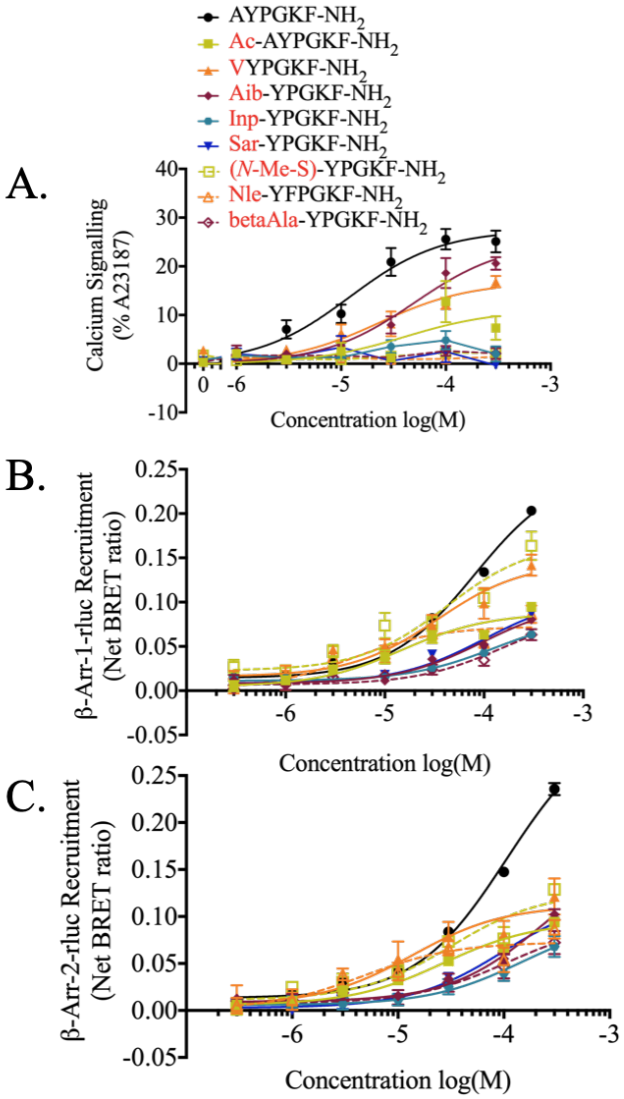

1214 **Figure 5. Calcium and β-arrestin**
1215 **recruitment to PAR4 in response**
1216 **to AYPGKF-NH_2 or peptides with**
1217 **additional substitutions in**
1218 **tyrosine[2], proline[3], or glycine[4]. (A)**
1219 **Agonist-stimulated calcium**
1220 **signalling.** Calcium signalling is
1221 shown as a percentage of the
1222 maximum calcium signalling
1223 obtained by application of calcium
1224 ionophore (A23187, 3 μM). (*n = 3-*
1225 *7)* **Agonist-stimulated recruitment**
1226 **of β-arrestin-1 (B) and β-arrestin-**
1227 **2 (C) to PAR4.** Concentration effect
1228 curves of BRET values from cells
1229 treated increasing concentrations of
1230 peptide are presented as normalized
1231 net BRET ratio. (*n = 3*).

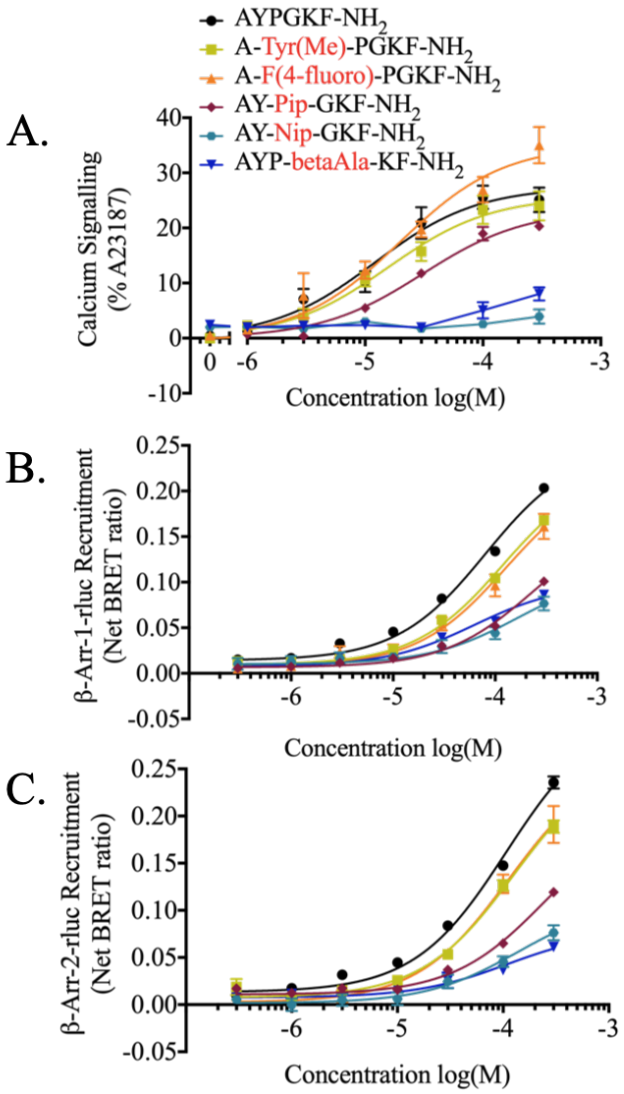

1232 **Figure 6. Calcium and β-arrestin**
1233 **recruitment to PAR4 in response**
1234 **to AYPGKF-NH$_2$ or peptides with**
1235 **additional substitutions in lysine[5].**
1236 **(A) Agonist-stimulated calcium**
1237 **signalling.** Calcium signalling is
1238 shown as a percentage of the
1239 maximum calcium signalling
1240 obtained by application of calcium
1241 ionophore (A23187, 3 μM). (*n = 3-*
1242 *7)* **Agonist-stimulated recruitment**
1243 **of β-arrestin-1 (B) and β-arrestin-**
1244 **2 (C) to PAR4.** Concentration effect
1245 curves of BRET values from cells
1246 treated increasing concentrations of
1247 peptide are presented as normalized
1248 net BRET ratio. (*n = 3*).
1249

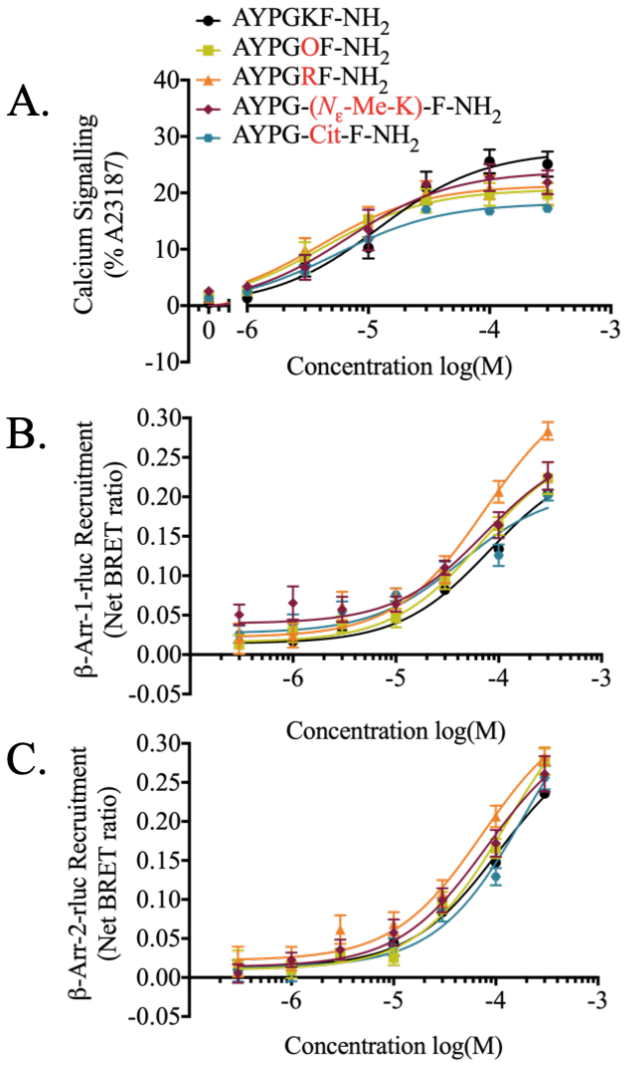

1250 **Figure 7. Calcium and β-arrestin**
1251 **recruitment to PAR4 in response**
1252 **to AYPGKF-NH_2 or peptides with**
1253 **additional substitutions in**
1254 **phenylalanine[6]. (A) Agonist-**
1255 **stimulated calcium signalling.**
1256 Calcium signalling is shown as a
1257 percentage of the maximum calcium
1258 signalling obtained by application of
1259 calcium ionophore (A23187, 3 μM).
1260 (*n = 3-7)* **Agonist-stimulated**
1261 **recruitment of β-arrestin-1 (B)**
1262 **and β-arrestin-2 (C) to PAR4.**
1263 Concentration effect curves of
1264 BRET values from cells treated
1265 increasing concentrations of peptide
1266 are presented as normalized net
1267 BRET ratio. (*n = 3*).

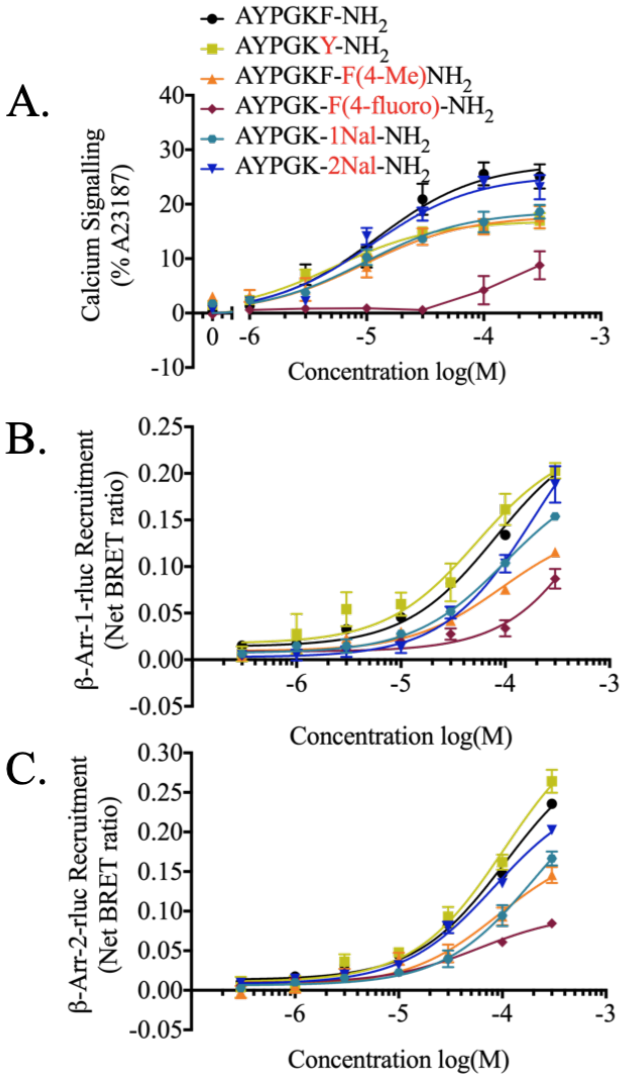

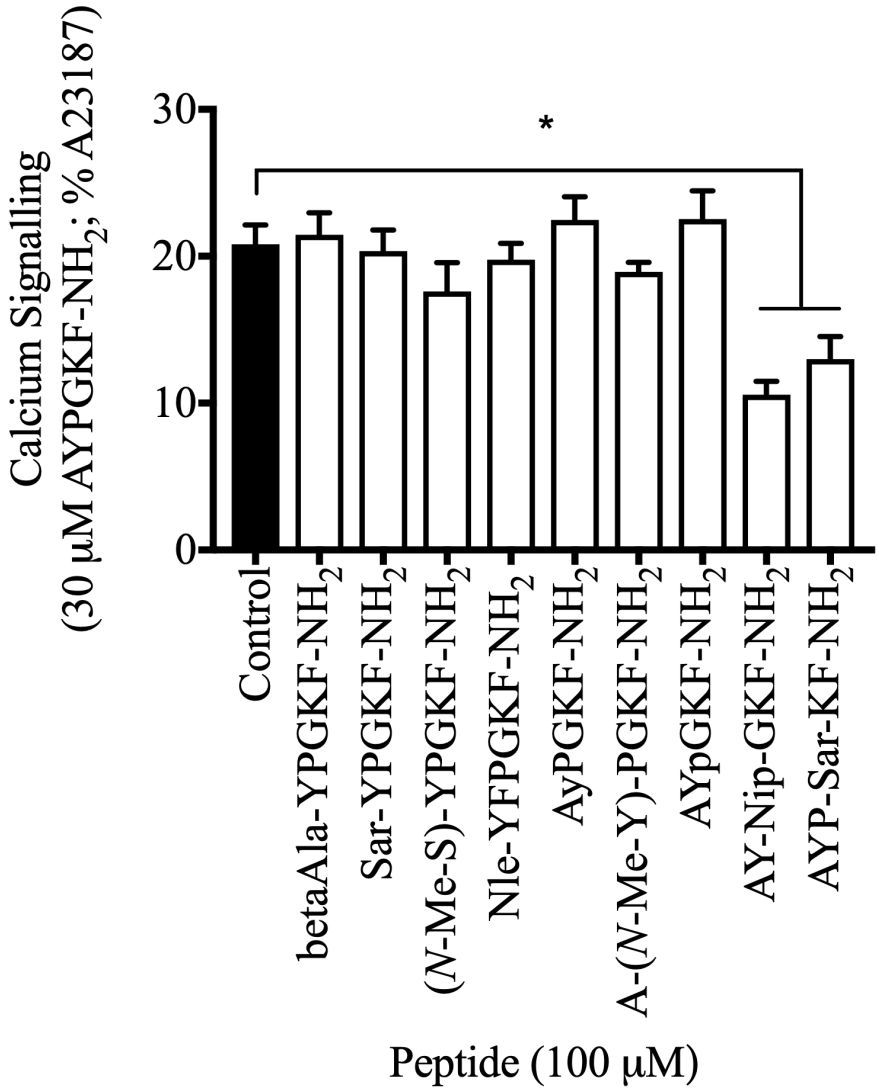

Figure 8. PAR4-AP (AYPGKF-NH_2) stimulated calcium signalling responses following pre-treatment with calcium signalling null peptides. Calcium signalling (Fluorescence Em: 530) in HEK-293 cells stably expressing PAR4-YFP were recorded following 30 μM AYPGKF-NH_2 addition after 30-minute pre-treatment incubation with 100 μM of calcium signalling-null peptides. Data are shown as a percentage of maximum response obtained in cells treated with the calcium ionophore A23187 (3 μM). Agonist peptide concentrations are in M. Pre-treatment with calcium-null peptides did not affect AYPGKF-NH_2-stimulated calcium signalling in most cases with the exception of AY-Nip-GKF-NH_2 and AYP-Sar-KF-NH_2, which significantly decreased AYPGKF-NH_2 stimulated calcium signalling compared to vehicle treated control. (*$p > 0.05$; $n = 3$)

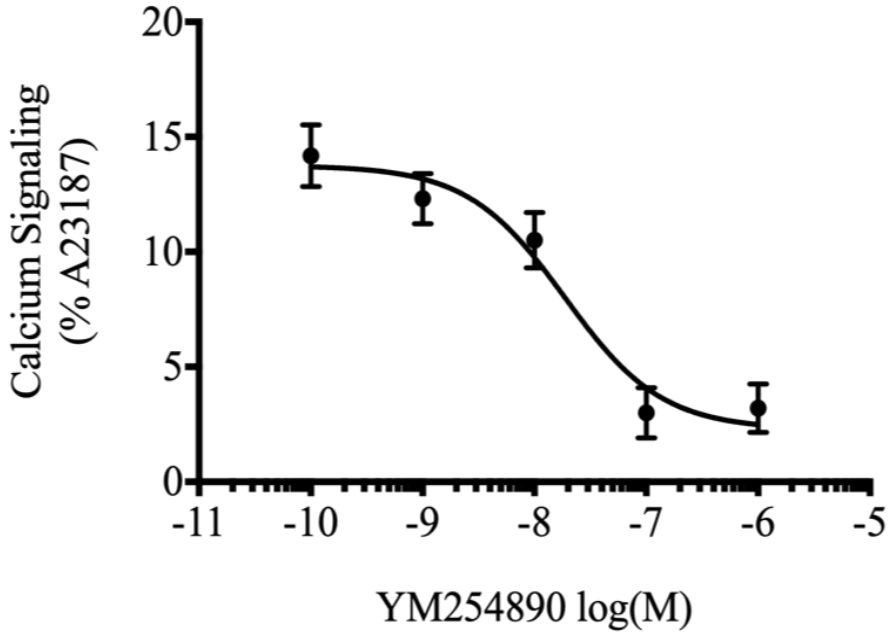

1278 **Figure 9. PAR4-mediated calcium signalling is $G\alpha_{q/11}$-dependent.** HEK-293 cells stably
1279 expressing PAR4 were pre-treated with either DMSO vehicle control (0.001%) or increasing
1280 concentration of the selective $G\alpha_{q/11}$ inhibitor YM254890. Calcium signalling following
1281 stimulation with AYPGKF-NH_2 (100µM) was recorded. PAR4-mediated calcium signalling
1282 was blocked by YM254890 at concentrations greater than 100 nM. (*n = 4*)
1283

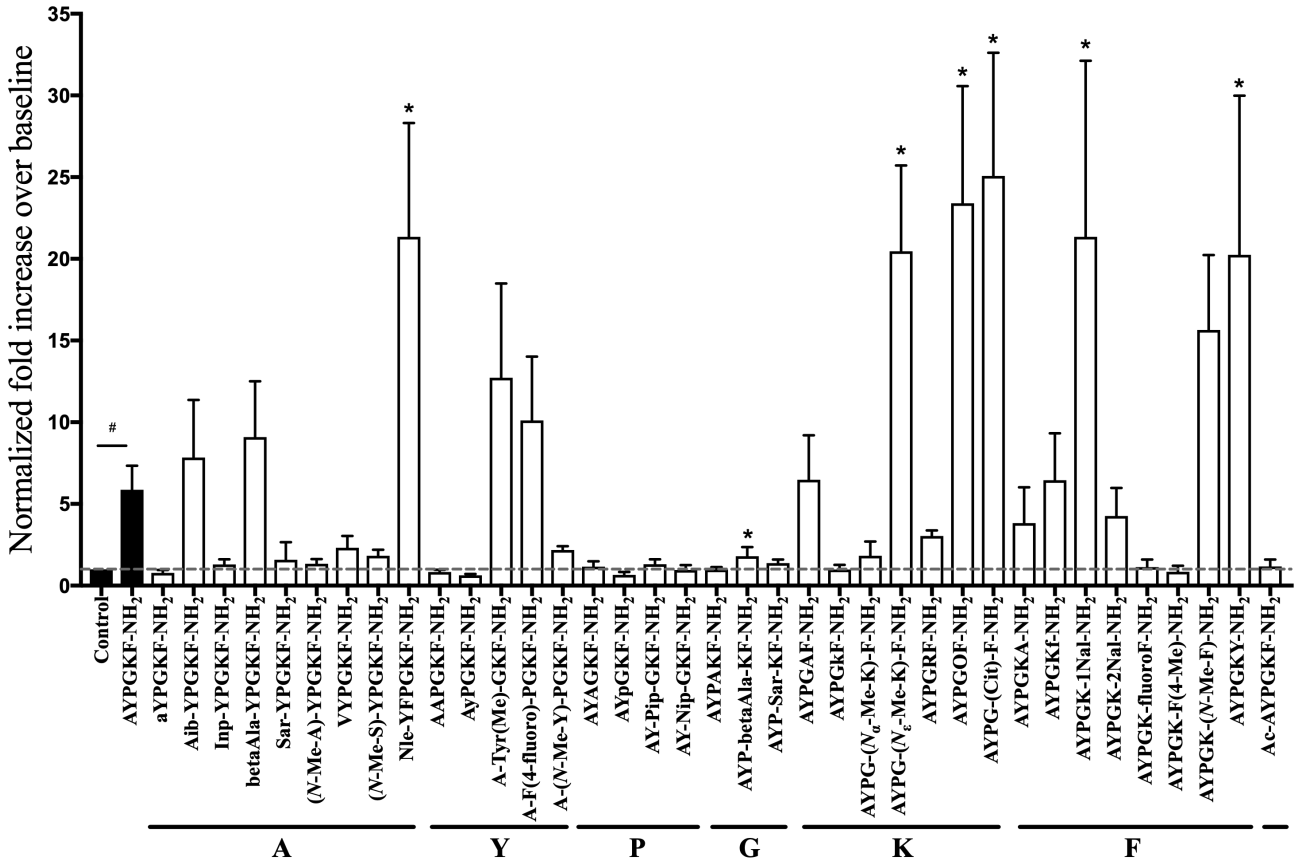

Figure 10. PAR4-mediated phosphorylation of p44/42(ERK) is attenuated upon stimulation of PAR4 with calcium-null peptide. HEK-293 cells stably expressing PAR4-YFP were stimulated with AYPGKF-NH_2 (30 μM) or peptide (30 μM) from library of compounds and Western blot for p44/42 phosphorylation (p-p44/42). Data are shown as normalized fold increase over unstimulated control cells. Dashed baseline shows mean of unstimulated baseline for comparison. Dotted baseline shows mean response achieved following AYPGKF-NH_2 stimulation. (# $p > 0.05$ AYPGKF-NH_2 compared to untreated control; *$p > 0.05$ AYPGKF-NH_2 compared to other peptide agonists; one-way ANOVA). Peptides that were unable to stimulate calcium signalling were also generally unable to stimulate phosphorylation of p44/42. Interestingly, several peptides were able to significantly increase phosphorylation of p44/42 compared to AYPGKF-NH_2. (Representative blots shown in supplemental figure S2; *n = 4-5*)

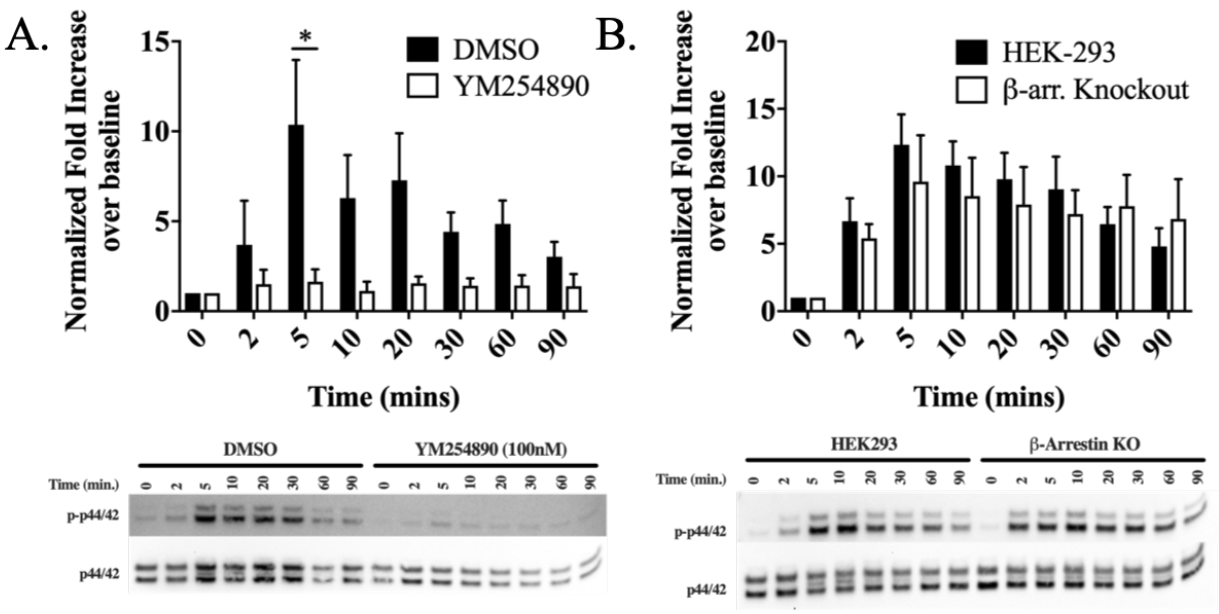

1296 **Figure 11. PAR4-mediated phosphorylation of p44/42 (ERK) is $G\alpha_{q/11}$-dependent and β-**
1297 **arrestin-independent.** To evaluate contribution of $G\alpha_{q/11}$ and β-arrestin to p44/42
1298 phosphorylation, p-p44/42 was monitored with western blot following stimulation with
1299 AYPGKF-NH_2 (30 μM) for various time points. To evaluate contribution of $G\alpha_{q/11}$-signalling
1300 cells were incubated with vehicle control (0.001% DMSO) or $G\alpha_{q/11}$-inhibitor, YM254890 (100
1301 nM) prior to agonist stimulation (A). To determine contribution of β-arrestin-signalling to
1302 p44/42 phosphorylation, HEK-293 and β-arrestin-1/2 CRISPR knockouts were assayed
1303 following agonist stimulation (B). Values are expressed as fold increase over unstimulated 0-
1304 minute time [(p-p44/22 / total p44/42) / (baseline p-p44/42 / total p44/42)]. Data are analysed
1305 with two-way ANOVA (*$p > 0.05$). We find that $G\alpha_{q/11}$ inhibition with YM254890 results in
1306 a significant reduction of p44/42 phosphorylation. We observe no statistical difference in ERK
1307 activation between HEK-293 and β-arrestin-1/2 knockouts HEK-293 cells. (Representative
1308 blots shown; *n = 4*)

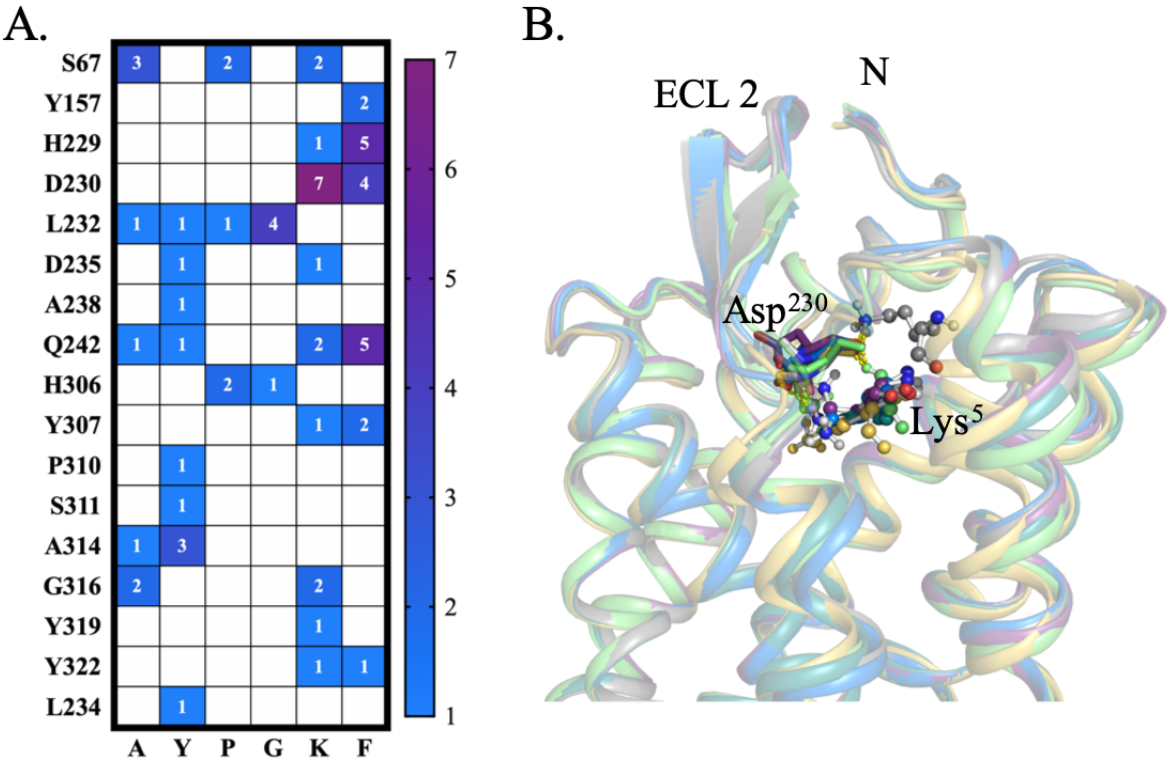

Figure 12. (A) Frequency table of PAR4/AYPGKF-NH_2 interactions as predicted by *in silico* peptide docking (GalaxyPepDock). Numbers represent the frequency with which an atom in a PAR4-AP residue was predicted to interact with an atom of a PAR4 residue. **(B) Representation of the most highly predicted AYPGKF-NH_2 binding site (Asp^{230}, shown as sticks) interacting (shown as yellow dashed lines) with position 5 (Lys^5; shown as ball and sticks) of AYPGKF-NH_2.** Interaction of Lys^5 and Asp^{230} was highly predicted in 7/10 models (B). Alignment of the receptor backbone (shown as transparent cartoon) reveals similar binding poses adopted by the side chain position of Asp^{230} and the position of Lys^5 of AYPGKF-NH_2.

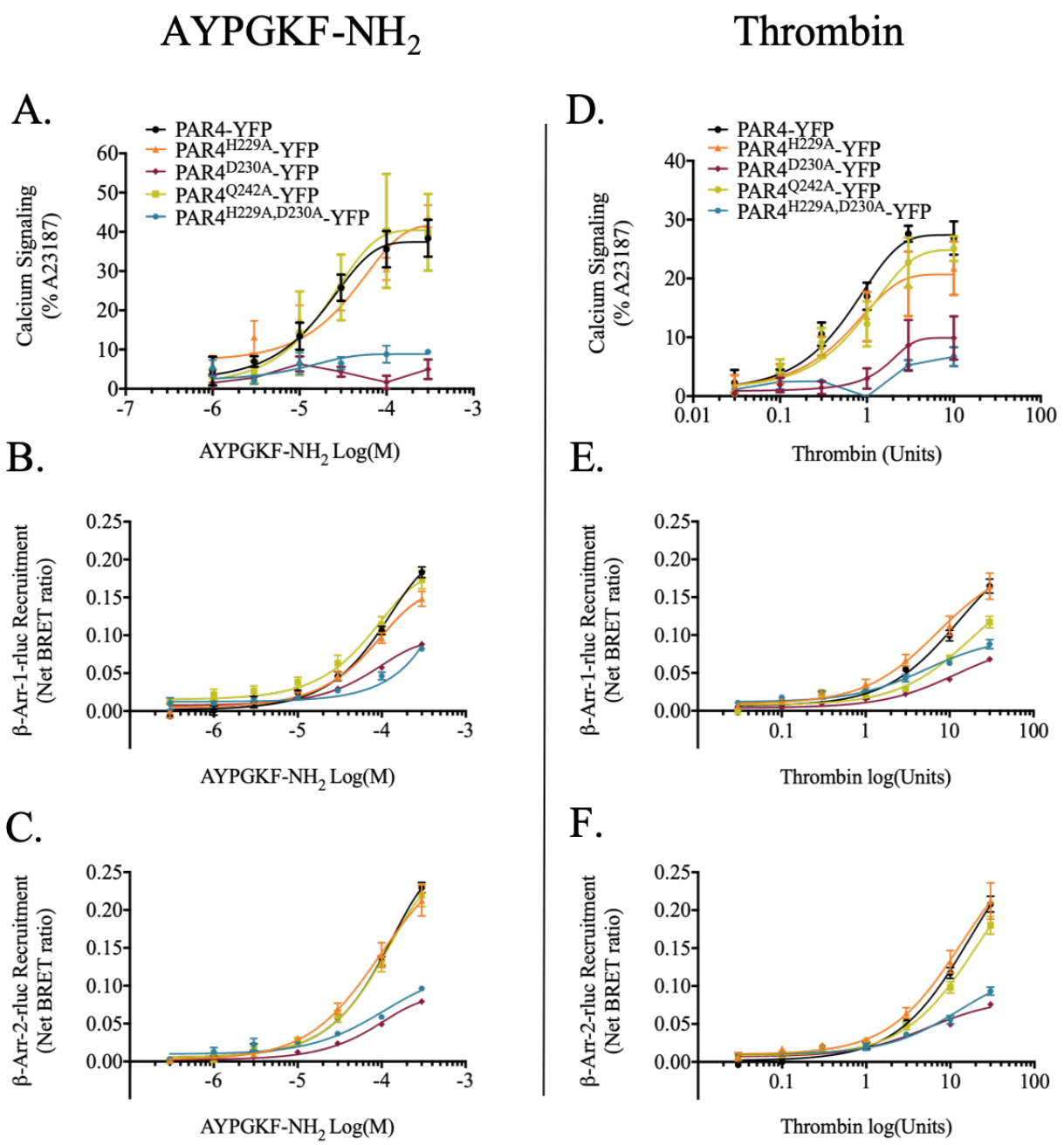

Figure 13. AYPGKF-NH$_2$-stimulated calcium signalling and β-arrestin-1/-2 recruitment in PAR4 extracellular loop 2 mutants. Agonist-stimulated Calcium signalling Calcium signalling in response to AYPGKF-NH$_2$ (A) or thrombin (D) was recorded in HEK-293 cells transiently expressing PAR4-YFP, single site-directed mutant PAR4-YFP (PAR4^{H229A}-YFP, PAR4^{D230A}-YFP, PAR4^{Q242A}-YFP), or double site-directed mutant PAR4-YFP (PAR4$^{H229A, D230A}$-YFP, PAR4$^{H229D, A231D}$-YFP). Data are shown as a percentage of maximum response obtained in cells treated with the calcium ionophore A23187 (3 μM) for each transient cell line, per experimental day. AYPGKF-NH$_2$ concentration is in M and thrombin concentration is shown as units. (N=3-5) **Agonist-stimulated β-arrestin-1/-2 recruitment** HEK-293 cells were transiently transfected with BRET pair of either β-arrestin-1-rluc or -2-rluc and PAR4-YFP or site-directed mutant PAR4-YFP (described above) and agonist-stimulated arrestin recruitment to PAR4 was monitored. Cells were incubated with increasing concentration of

1330 either AYPGKF-NH_2 (B, C) or thrombin (E, F) for 20 minutes and BRET values were recorded.
1331 BRET values from cells treated with HBSS were also collected to normalize the data. Renilla-
1332 luciferase substrate coelenterazine-h (5 μM) was added 10 minutes prior to data collection.
1333 Data are presented as the normalized net BRET ratio [eYFP/rluc - baseline (HBSS control)].
1334 AYPGKF-NH_2 concentration is in M and thrombin concentration is shown as units. ($n = 4$).

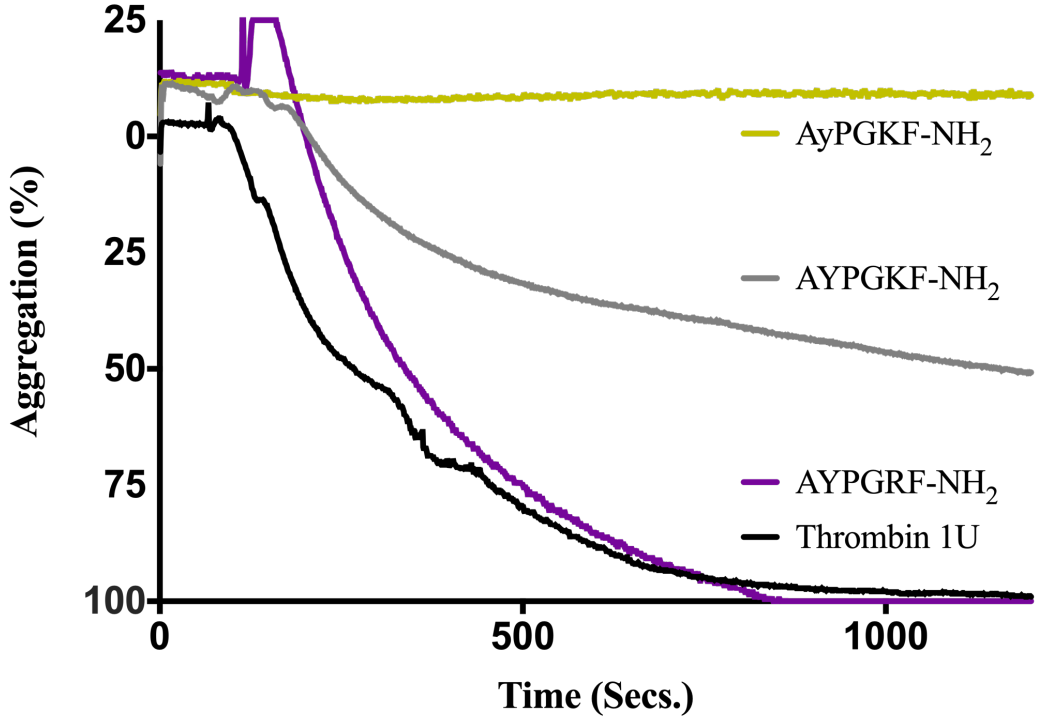

1335 **Figure 14. PAR4 agonist-mediated platelet aggregation.** Both thrombin (1 unit/mL; shown
1336 in black) and AYPGKF-NH_2 (100 µM; shown in grey) initiated PAR4-dependent rat platelet
1337 aggregation. We observed that stimulation of washed platelet samples with a calcium signalling
1338 null, β-arrestin biased peptide, AyPGKF-NH_2 (100 µM; shown in yellow) did not stimulate
1339 platelet aggregation. Further, stimulation of washed platelets with the peptide agonist
1340 AYPGRF-NH_2 (100 µM; shown in purple), caused a robust platelet aggregation comparable to
1341 the response with 1unit/mL thrombin response (*n = 2-4*).

References.

Adams MN, Ramachandran R, Yau M-K, Suen JY, Fairlie DP, Hollenberg MD, Hooper JD. 2011. Structure, function and pathophysiology of protease activated receptors. *Pharmacology & therapeutics* **130**:248–282.

Al-Ani B, Saifeddine M, Kawabata A, Hollenberg MD. 1999. Proteinase activated receptor 2: Role of extracellular loop 2 for ligand-mediated activation. *Br J Pharmacol* **128**:1105–1113.

Al-Ani B, Wijesuriya SJ, Hollenberg MD. 2002. Proteinase-activated receptor 2: differential activation of the receptor by tethered ligand and soluble peptide analogs. *The Journal of pharmacology and experimental therapeutics* **302**:1046–1054.

Bar-Shavit R, Maoz M, Kancharla A, Jaber M, Agranovich D, Grisaru-Granovsky S, Uziely B. 2016. Protease-activated receptors (PARs) in cancer: Novel biased signaling and targets for therapy. *Methods in cell biology* **132**:341–358. doi:10.1016/bs.mcb.2015.11.006

Blackhart BD, Emilsson K, Nguyen D, Teng W, Martelli AJ, Nystedt S, Sundelin J, Scarborough RM. 1996. Ligand cross-reactivity within the protease-activated receptor family. *The Journal of biological chemistry* **271**:16466–16471.

Boitano S, Flynn AN, Schulz SM, Hoffman J, Price TJ, Vagner J. 2011. Potent Agonists of the Protease Activated Receptor 2 (PAR2). *J Med Chem* **54**:1308–1313. doi:10.1021/jm1013049

Cheng RKY, Fiez-Vandal C, Schlenker O, Edman K, Aggeler B, Brown DG, Brown GA, Cooke RM, Dumelin CE, Doré AS, Geschwindner S, Grebner C, Hermansson N-O, Jazayeri A, Johansson P, Leong L, Prihandoko R, Rappas M, Soutter H, Snijder A, Sundström L, Tehan B, Thornton P, Troast D, Wiggin G, Zhukov A, Marshall FH, Dekker N. 2017. Structural insight into allosteric modulation of protease-activated receptor 2. *Nature* **545**:112–115. doi:10.1038/nature22309

Chidiac P. 2016. RGS proteins destroy spare receptors: Effects of GPCR-interacting proteins and signal deamplification on measurements of GPCR agonist potency. *Methods* **92**:87–93. doi:10.1016/j.ymeth.2015.08.011

Coughlin SR. 2005. Protease-activated receptors in hemostasis, thrombosis and vascular biology. *J Thromb Haemost* **3**:1800–1814.

Coughlin SR. 1999. How the protease thrombin talks to cells. *Proceedings of the National Academy of Sciences of the United States of America* **96**:11023–11027.

Covic L, Misra M, Badar J, Singh C, Kuliopulos A. 2002. Pepducin-based intervention of thrombin-receptor signaling and systemic platelet activation. *Nature Medicine* **8**:1161–1165.

Dolinsky TJ, Nielsen JE, McCammon JA, Baker NA. 2004. PDB2PQR: an automated pipeline for the setup of Poisson-Boltzmann electrostatics calculations. *Nucleic Acids Res* **32**:W665-667. doi:10.1093/nar/gkh381

Edelstein LC, Simon LM, Lindsay CR, Kong X, Teruel-Montoya R, Tourdot BE, Chen ES, Ma L, Coughlin S, Nieman M, Holinstat M, Shaw CA, Bray PF. 2014. Common variants in the human platelet PAR4 thrombin receptor alter platelet function and differ by race. *Blood* **124**:3450–3458. doi:10.1182/blood-2014-04-572479

Erlandson SC, McMahon C, Kruse AC. 2018. Structural Basis for G Protein–Coupled Receptor Signaling. *doi.org* **47**:annurev–biophys–070317–032931.

Faruqi TR, Weiss EJ, Shapiro MJ, Huang W, Coughlin SR. 2000. Structure-function analysis of protease-activated receptor 4 tethered ligand peptides. Determinants of specificity and utility in assays of receptor function. *The Journal of biological chemistry* **275**:19728–19734.

Ferguson SSG, Caron MG. 2004. Green Fluorescent Protein-Tagged β-Arrestin Translocation as a Measure of G Protein-Coupled Receptor Activation In: Smrcka AV, editor. G Protein Signaling: Methods and Protocols, Methods in Molecular Biology™. Totowa, NJ: Humana Press. pp. 121–126. doi:10.1385/1-59259-430-1:121

1395 Fredriksson R, Schioth HB. 2005. The repertoire of G-protein-coupled receptors in fully
1396 sequenced genomes. *Molecular pharmacology* **67**:1414–1425.
1397 doi:10.1124/mol.104.009001
1398 French SL, Hamilton JR. 2016. Protease-activated receptor 4: from structure to function and
1399 back again. *Br J Pharmacol* **173**:2952–2965. doi:10.1111/bph.13455
1400 Gerszten RE, Chen J, Ishii M, Ishii K, Wang L, Nanevicz T, Turck CW, Vu TK, Coughlin SR.
1401 1994. Specificity of the thrombin receptor for agonist peptide is defined by its
1402 extracellular surface. *Nature* **368**:648–651.
1403 Graham FL, van der Eb AJ. 1973. A new technique for the assay of infectivity of human
1404 adenovirus 5 DNA. *Virology* **52**:456–467.
1405 Hilger D, Masureel M, Kobilka BK. 2018. Structure and dynamics of GPCR signaling
1406 complexes. *Nature structural & molecular biology* **25**:4–12. doi:10.1038/s41594-017-
1407 0011-7
1408 Hoffmann W, Langenhan J, Huhmann S, Moschner J, Chang R, Accorsi M, Seo J,
1409 Rademann J, Meijer G, Koksch B, Bowers MT, von Helden G, Pagel K. 2019. An
1410 Intrinsic Hydrophobicity Scale for Amino Acids and Its Application to Fluorinated
1411 Compounds. *Angewandte Chemie International Edition* **58**:8216–8220.
1412 doi:10.1002/anie.201813954
1413 Holinstat M, Voss B, Bilodeau ML, McLaughlin JN, Cleator J, Hamm HE. 2006. PAR4, but
1414 not PAR1, signals human platelet aggregation via Ca2+ mobilization and synergistic
1415 P2Y12 receptor activation. *The Journal of biological chemistry* **281**:26665–26674.
1416 Hollenberg MD. 2003. Proteinase-activated receptors: Tethered ligands and receptor-
1417 activating peptides. *Drug Dev Res* **59**:336–343. doi:10.1002/ddr.10301
1418 Hollenberg MD, Mihara K, Polley D, Suen JY, Han A, Fairlie DP, Ramachandran R. 2014.
1419 Biased signalling and proteinase-activated receptors (PARs): targeting inflammatory
1420 disease. *British journal of pharmacology* **171**:1180–1194.
1421 Ishihara H, Connolly AJ, Zeng D, Kahn ML, Zheng YW, Timmons C, Tram T, Coughlin SR.
1422 1997. Protease-activated receptor 3 is a second thrombin receptor in humans.
1423 *Nature* **386**:502–506.
1424 Jacques SL, Kuliopulos A. 2003. Protease-activated receptor-4 uses dual prolines and an
1425 anionic retention motif for thrombin recognition and cleavage. *The Biochemical*
1426 *journal* **376**:733–740.
1427 Jacques SL, LeMasurier M, Sheridan PJ, Seeley SK, Kuliopulos A. 2000. Substrate-assisted
1428 catalysis of the PAR1 thrombin receptor. Enhancement of macromolecular
1429 association and cleavage. *The Journal of biological chemistry* **275**:40671–40678.
1430 Jean-Charles P-Y, Kaur S, Shenoy SK. 2017. GPCR signaling via β-arrestin-dependent
1431 mechanisms. *J Cardiovasc Pharmacol* **70**:142–158.
1432 doi:10.1097/FJC.0000000000000482
1433 Kahn ML, Zheng YW, Huang W, Bigornia V, Zeng D, Moff S, Farese RVJ, Tam C, Coughlin
1434 SR. 1998. A dual thrombin receptor system for platelet activation. *Nature* **394**:690–
1435 694.
1436 Khan A, Li D, Ibrahim S, Smyth E, Woulfe DS. 2014. The Physical Association of the P2Y12
1437 Receptor with PAR4 Regulates Arrestin-Mediated Akt Activation. *Molecular*
1438 *pharmacology* **86**:1–11.
1439 Kim BH, Wang FI, Pereverzev A, Chidiac P, Dixon SJ. 2019. Toward Defining the
1440 Pharmacophore for Positive Allosteric Modulation of PTH1 Receptor Signaling by
1441 Extracellular Nucleotides. *ACS Pharmacol Transl Sci* **2**:155–167.
1442 doi:10.1021/acsptsci.8b00053
1443 Lee H, Heo L, Lee MS, Seok C. 2015. GalaxyPepDock: a protein–peptide docking tool
1444 based on interaction similarity and energy optimization. *Nucleic Acids Res* **43**:W431–
1445 W435. doi:10.1093/nar/gkv495
1446 Lerner DJ, Chen M, Tram T, Coughlin SR. 1996. Agonist recognition by proteinase-activated
1447 receptor 2 and thrombin receptor. Importance of extracellular loop interactions for
1448 receptor function. *The Journal of biological chemistry* **271**:13943–13947.

1449 Li D, D'Angelo L, Chavez M, Woulfe DS. 2011. Arrestin-2 differentially regulates PAR4 and
1450 ADP receptor signaling in platelets. *The Journal of biological chemistry* **286**:3805–
1451 3814.
1452 Liu LW, Vu TK, Esmon CT, Coughlin SR. 1991. The region of the thrombin receptor
1453 resembling hirudin binds to thrombin and alters enzyme specificity. *The Journal of*
1454 *biological chemistry* **266**:16977–16980.
1455 Madeira F, Park YM, Lee J, Buso N, Gur T, Madhusoodanan N, Basutkar P, Tivey ARN,
1456 Potter SC, Finn RD, Lopez R. 2019. The EMBL-EBI search and sequence analysis
1457 tools APIs in 2019. *Nucleic Acids Res* **47**:W636–W641. doi:10.1093/nar/gkz268
1458 Miller MM, Banville J, Friends T, Gagnon M, Hangeland JJ, Lavalee J-F, Martel A, O'Grady
1459 H, Remillard R, Ruediger EH, Tremblay F, Posy S, Allegretto N, Guarino VR, Harden
1460 D, Harper TW, Hartl K, Josephs J, Malmstrom S, Watson CA, Yang Y, Zhang G,
1461 Wong PC, Yang J, Bouvier M, Seiffert DA, Wexler RR, Lawrence RM, Priestley ES,
1462 Marinier A. 2019. Discovery of Potent Protease-Activated Receptor 4 Antagonists
1463 with in vivo Antithrombotic Efficacy. *J Med Chem*.
1464 doi:10.1021/acs.jmedchem.9b00186
1465 Morrow DA, Braunwald E, Bonaca MP, Ameriso SF, Dalby AJ, Fish MP, Fox KA, Lipka LJ,
1466 Liu X, Nicolau JC, Ophuis AJ, Paolasso E, Scirica BM, Spinar J, Theroux P, Wiviott
1467 SD, Strony J, Murphy SA. 2012. Vorapaxar in the secondary prevention of
1468 atherothrombotic events. *The New England journal of medicine* **366**:1404–1413.
1469 Morrow DA, Scirica BM, Fox KA, Berman G, Strony J, Veltri E, Bonaca MP, Fish P, McCabe
1470 CH, Braunwald E. 2009. Evaluation of a novel antiplatelet agent for secondary
1471 prevention in patients with a history of atherosclerotic disease: design and rationale
1472 for the Thrombin-Receptor Antagonist in Secondary Prevention of Atherothrombotic
1473 Ischemic Events (TRA 2 degrees P)-TIMI 50 trial. *Am Heart J* **158**:335–341 e3.
1474 Moschonas IC, Kellici TF, Mavromoustakos T, Stathopoulos P, Tsikaris V, Magafa V, Tzakos
1475 AG, Tselepis AD. 2017. Molecular requirements involving the human platelet
1476 protease-activated receptor-4 mechanism of activation by peptide analogues of its
1477 tethered-ligand. *Platelets* **28**:812–821. doi:10.1080/09537104.2017.1282607
1478 Nanevicz T, Ishii M, Wang L, Chen M, Chen J, Turck CW, Cohen FE, Coughlin SR. 1995.
1479 Mechanisms of thrombin receptor agonist specificity. Chimeric receptors and
1480 complementary mutations identify an agonist recognition site. *The Journal of*
1481 *biological chemistry* **270**:21619–21625.
1482 Nieman MT. 2008. Protease-Activated Receptor 4 Uses Anionic Residues To Interact with α-
1483 Thrombin in the Absence or Presence of Protease-Activated Receptor 1.
1484 *Biochemistry* **47**:13279–13286. doi:10.1021/bi801334s
1485 Nieman MT, Schmaier AH. 2007. Interaction of Thrombin with PAR1 and PAR4 at the
1486 Thrombin Cleavage Site. *Biochemistry* **46**:8603–8610. doi:10.1021/bi700597p
1487 Nystedt S, Emilsson K, Wahlestedt C, Sundelin J. 1994. Molecular cloning of a potential
1488 proteinase activated receptor. *Proceedings of the National Academy of Sciences of*
1489 *the United States of America* **91**:9208–9212.
1490 Pierce KL, Premont RT, Lefkowitz RJ. 2002. Seven-transmembrane receptors. *Nature*
1491 *Reviews Molecular Cell Biology* **3**:639–650.
1492 Ramachandran R, Mihara K, Thibeault P, Vanderboor CM, Petri B, Saifeddine M, Bouvier M,
1493 Hollenberg MD. 2017. Targeting a Proteinase-Activated Receptor 4 (PAR4) Carboxyl
1494 Terminal Motif to Regulate Platelet Function. *Molecular pharmacology* **91**:287–295.
1495 Rwibasira Rudinga G, Khan GJ, Kong Y. 2018. Protease-Activated Receptor 4 (PAR4): A
1496 Promising Target for Antiplatelet Therapy. *Int J Mol Sci* **19**.
1497 doi:10.3390/ijms19020573
1498 Sánchez Centellas D, Gudlur S, Vicente-Carrillo A, Ramström S, Lindahl TL. 2017. A cluster
1499 of aspartic residues in the extracellular loop II of PAR 4 is important for thrombin
1500 interaction and activation of platelets. *Thrombosis Research* **154**:84–92.
1501 doi:10.1016/j.thromres.2017.04.006
1502 Scarborough RM, Naughton MA, Teng W, Hung DT, Rose J, Vu TK, Wheaton VI, Turck CW,
1503 Coughlin SR. 1992. Tethered ligand agonist peptides. Structural requirements for

1504 thrombin receptor activation reveal mechanism of proteolytic unmasking of agonist
1505 function. *The Journal of biological chemistry* **267**:13146–13149.
1506 Schindelin J, Arganda-Carreras I, Frise E, Kaynig V, Longair M, Pietzsch T, Preibisch S,
1507 Rueden C, Saalfeld S, Schmid B, Tinevez J-Y, White DJ, Hartenstein V, Eliceiri K,
1508 Tomancak P, Cardona A. 2012. Fiji: an open-source platform for biological-image
1509 analysis. *Nature Methods* **9**:676–682. doi:10.1038/nmeth.2019
1510 Scirica BM, Bonaca MP, Braunwald E, De Ferrari GM, Isaza D, Lewis BS, Mehrhof F, Merlini
1511 PA, Murphy SA, Sabatine MS, Tendera M, Van de Werf F, Wilcox R, Morrow DA.
1512 2012. Vorapaxar for secondary prevention of thrombotic events for patients with
1513 previous myocardial infarction: a prespecified subgroup analysis of the TRA 2°P-TIMI
1514 50 trial. *The Lancet* **380**:1317–1324. doi:10.1016/S0140-6736(12)61269-0
1515 Seyedabadi M, Ghahremani MH, Albert PR. 2019. Biased signaling of G protein coupled
1516 receptors (GPCRs): Molecular determinants of GPCR/transducer selectivity and
1517 therapeutic potential. *Pharmacol Ther* **200**:148–178.
1518 doi:10.1016/j.pharmthera.2019.05.006
1519 Shapiro MJ, Weiss EJ, Faruqi TR, Coughlin SR. 2000. Protease-activated receptors 1 and 4
1520 are shut off with distinct kinetics after activation by thrombin. *The Journal of biological*
1521 *chemistry* **275**:25216–25221.
1522 Sievers F, Wilm A, Dineen D, Gibson TJ, Karplus K, Li W, Lopez R, McWilliam H, Remmert
1523 M, Söding J, Thompson JD, Higgins DG. 2011. Fast, scalable generation of high-
1524 quality protein multiple sequence alignments using Clustal Omega. *Molecular*
1525 *Systems Biology* **7**:539. doi:10.1038/msb.2011.75
1526 Soh UJ, Dores MR, Chen B, Trejo J. 2010. Signal transduction by protease-activated
1527 receptors. *British journal of pharmacology* **160**:191–203.
1528 Sriram K, Insel PA. 2018. G Protein-Coupled Receptors as Targets for Approved Drugs:
1529 How Many Targets and How Many Drugs? *Molecular pharmacology* **93**:251–258.
1530 Tourdot BE, Stoveken H, Trumbo D, Yeung J, Kanthi Y, Edelstein LC, Bray PF, Tall GG,
1531 Holinstat M. 2018. Genetic Variant in Human PAR (Protease-Activated Receptor) 4
1532 Enhances Thrombus Formation Resulting in Resistance to Antiplatelet Therapeutics.
1533 *Arterioscler Thromb Vasc Biol* **38**:1632–1643. doi:10.1161/ATVBAHA.118.311112
1534 Venkatakrishnan AJ, Deupi X, Lebon G, Tate CG, Schertler GF, Babu MM. 2014. Molecular
1535 signatures of G-protein-coupled receptors. *Nature* **494**:185–194.
1536 doi:10.1038/nature11896
1537 Vu TK, Hung DT, Wheaton VI, Coughlin SR. 1991. Molecular cloning of a functional
1538 thrombin receptor reveals a novel proteolytic mechanism of receptor activation. *Cell*
1539 **64**:1057–1068.
1540 Webb B, Sali A. 2017. Protein Structure Modeling with MODELLERFunctional Genomics.
1541 New York, NY: Humana Press, New York, NY. pp. 39–54. doi:10.1007/978-1-4939-
1542 7231-9_4
1543 Wheatley M, Wootten D, Conner MT, Simms J, Kendrick R, Logan RT, Poyner DR, Barwell
1544 J. 2012. Lifting the lid on GPCRs: the role of extracellular loops. *Br J Pharmacol*
1545 **165**:1688–1703. doi:10.1111/j.1476-5381.2011.01629.x
1546 Wilson SJ, Ismat FA, Wang Z, Cerra M, Narayan H, Raftis J, Gray TJ, Connell S, Garonzik
1547 S, Ma X, Yang J, Newby DE. 2017. PAR4 (Protease-Activated Receptor 4)
1548 Antagonism With BMS-986120 Inhibits Human Ex Vivo Thrombus Formation.
1549 *Arteriosclerosis, Thrombosis, and Vascular Biology* ATVBAHA.117.310104.
1550 doi:10.1161/ATVBAHA.117.310104
1551 Wong PC, Seiffert D, Bird JE, Watson CA, Bostwick JS, Giancarli M, Allegretto N, Hua J,
1552 Harden D, Guay J, Callejo M, Miller MM, Lawrence RM, Banville J, Guy J, Maxwell
1553 BD, Priestley ES, Marinier A, Wexler RR, Bouvier M, Gordon DA, Schumacher WA,
1554 Yang J. 2017. Blockade of protease-activated receptor-4 (PAR4) provides robust
1555 antithrombotic activity with low bleeding. *Science translational medicine* **9**:eaaf5294.
1556 doi:10.1126/scitranslmed.aaf5294
1557 Woolley MJ, Conner AC. 2017. Understanding the common themes and diverse roles of the
1558 second extracellular loop (ECL2) of the GPCR super-family. *Molecular and Cellular*

1559 *Endocrinology*, Pleiotropic GPCR signaling in health and disease **449**:3–11.
1560 doi:10.1016/j.mce.2016.11.023
1561 Wu CC, Huang SW, Hwang TL, Kuo SC, Lee FY, Teng CM. 2000. YD-3, a novel inhibitor of
1562 protease-induced platelet activation. *Br J Pharmacol* **130**:1289–1296.
1563 Xu WF, Andersen H, Whitmore TE, Presnell SR, Yee DP, Ching A, Gilbert T, Davie EW,
1564 Foster DC. 1998. Cloning and characterization of human protease-activated receptor
1565 4. *Proceedings of the National Academy of Sciences of the United States of America*
1566 **95**:6642–6646.
1567 Young SE, Duvernay MT, Schulte ML, Nance KD, Melancon BJ, Engers J, Wood MR,
1568 Hamm HE, Lindsley CW. 2010. A Novel and Selective PAR4 Antagonist:
1569 ML354Probe Reports from the NIH Molecular Libraries Program. Bethesda (MD):
1570 National Center for Biotechnology Information (US).
1571

1572 # Supplemental tables and figures:

1573

1574 **Table S1: MS data of synthesized peptides.**

1575

Compound	Molecular Formula (M)	Calc. $[M+H]^+$ (*m/z*)	Found $[M+H]^+$ (*m/z*)
Ac-AYPGKF-NH$_2$	$C_{36}H_{50}N_8O_8$	723.38	723.43
AAPGKF-NH$_2$	$C_{28}H_{44}N_8O_6$	589.35	589.30
AYAGKF-NH$_2$	$C_{32}H_{46}N_8O_7$	655.36	655.43
AYPAKF-NH$_2$	$C_{35}H_{50}N_8O_7$	695.39	695.46
AYPGAF-NH$_2$	$C_{31}H_{41}N_7O_7$	624.31	625.36
AYPGKA-NH$_2$	$C_{28}H_{44}N_8O_7$	605.34	606.42
aYPGKF-NH$_2$	$C_{34}H_{48}N_8O_7$	681.37	681.44
AyPGKF-NH$_2$	$C_{34}H_{48}N_8O_7$	681.37	681.44
AYPGkF-NH$_2$	$C_{34}H_{48}N_8O_7$	681.37	681.46
AYPGKf-NH$_2$	$C_{34}H_{48}N_8O_7$	681.37	681.48
Aib-YPGKF-NH$_2$	$C_{35}H_{50}N_8O_7$	695.39	695.49
Sar-YPGKF-NH$_2$	$C_{34}H_{48}N_8O_7$	681.37	681.38
Inp-YPGKF-NH$_2$	$C_{37}H_{52}N_8O_7$	721.40	721.50
betaAla-YPGKF-NH$_2$	$C_{34}H_{48}N_8O_7$	681.37	681.46
A-Tyr(Me)-PGKF-NH$_2$	$C_{35}H_{50}N_8O_7$	695.39	695.48
A-F(4-fluoro)-PGKF-NH$_2$	$C_{34}H_{47}N_8O_6F$	683.37	683.36
AY-Pip-GKF-NH$_2$	$C_{35}H_{50}N_8O_7$	695.39	695.39
AY-Nip-GKF-NH$_2$	$C_{35}H_{50}N_8O_7$	695.39	695.39
AYP-Sar-KF-NH$_2$	$C_{35}H_{50}N_8O_7$	695.39	695.39
AYP-betaAla-KF-NH$_2$	$C_{35}H_{50}N_8O_7$	695.39	695.48
AYPGK-1Nal-NH$_2$	$C_{38}H_{50}N_8O_7$	731.38	731.48
AYPGK-2Nal-NH$_2$	$C_{38}H_{50}N_8O_7$	731.38	731.50
AYPGK-F(4-fluoro)-NH$_2$	$C_{34}H_{47}N_8O_7F$	699.36	699.38
AYPGK-F(4-Me)-NH$_2$	$C_{35}H_{50}N_8O_7$	695.39	695.39
AYpGKF-NH$_2$	$C_{34}H_{48}N_8O_7$	681.37	681.37
AYPGK-(*N*-Me-F)-NH$_2$	$C_{35}H_{50}N_8O_7$	695.39	695.39
AYPG-(N_α-Me-K)-F-NH$_2$	$C_{35}H_{50}N_8O_7$	695.39	695.39
A-(*N*-Me-Y)-PGKF-NH$_2$	$C_{35}H_{50}N_8O_7$	695.39	695.39
(*N*-Me-A)-YPGKF-NH$_2$	$C_{35}H_{50}N_8O_7$	695.39	695.39
VYPGKF-NH$_2$	$C_{36}H_{52}N_8O_7$	709.40	709.40
(*N*-Me-S)-YPGKF-NH$_2$	$C_{35}H_{50}N_8O_8$	711.38	711.38
Nle-YPGKF-NH$_2$	$C_{37}H_{54}N_8O_7$	723.42	723.42
AYPGRF-NH$_2$	$C_{34}H_{48}N_{10}O_7$	709.38	709.38
AYPGOF-NH$_2$	$C_{33}H_{46}N_8O_7$	667.36	667.36
AYPG-Cit-F-NH$_2$	$C_{34}H_{47}N_9O_8$	710.36	710.36
AYPG-(N_ε-Me-K)-F-NH$_2$	$C_{35}H_{50}N_8O_7$	695.39	695.39
AYPGKY-NH$_2$	$C_{34}H_{48}N_8O_8$	697.37	697.37

1576

Figure S1: Analytical RP-HPLC UV detection chromatograms of synthesized peptides. Purity of all peptides are > 95% as determined by analytical RP-HPLC UV detection (see traces below).

Ac-AYPGKF-NH_2:

t_R = 10.50 min; gradient = 10% to 50% (solvent A in solvent B, 0 to 10 min)

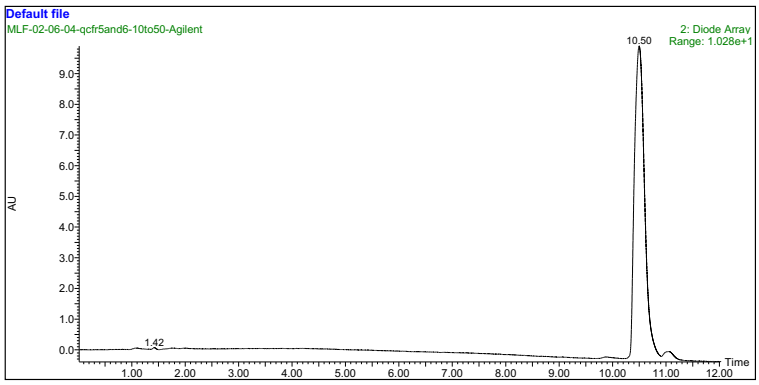

AAPGKF-NH_2:

t_R = 8.08 min; gradient = 10% to 70% (solvent A in solvent B, 0 to 10 min)

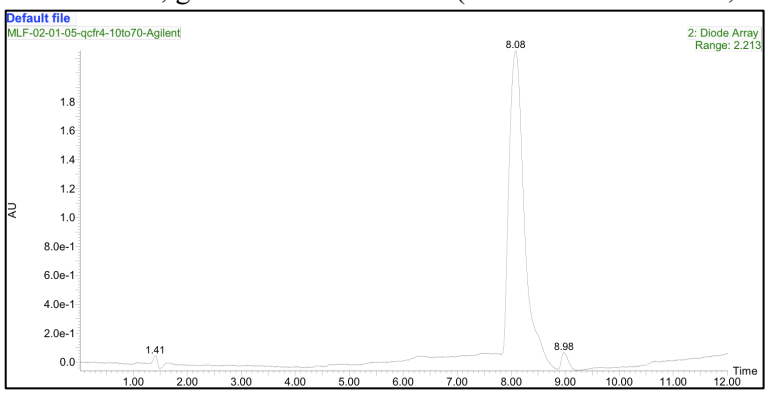

AYAGKF-NH_2:

t_R = 9.14 min; gradient = 10% to 60% (solvent A in solvent B, 0 to 10 min)

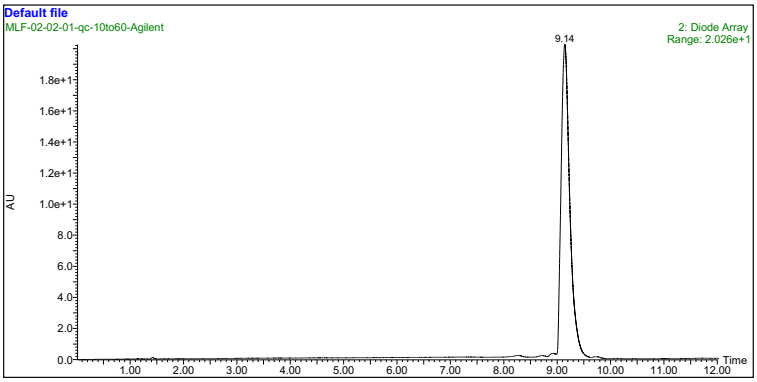

AYPAKF-NH_2:

t_R = 10.53 min; gradient = 10% to 50% (solvent A in solvent B, 0 to 10 min)

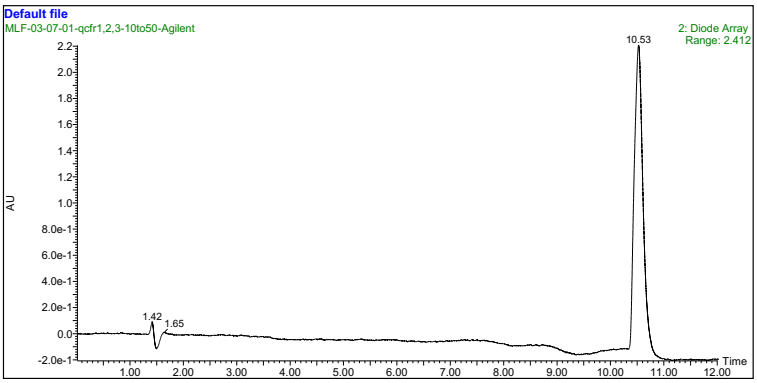

AYPGAF-NH_2:

t_R = 10.83 min; gradient = 10% to 50% (solvent A in solvent B, 0 to 10 min)

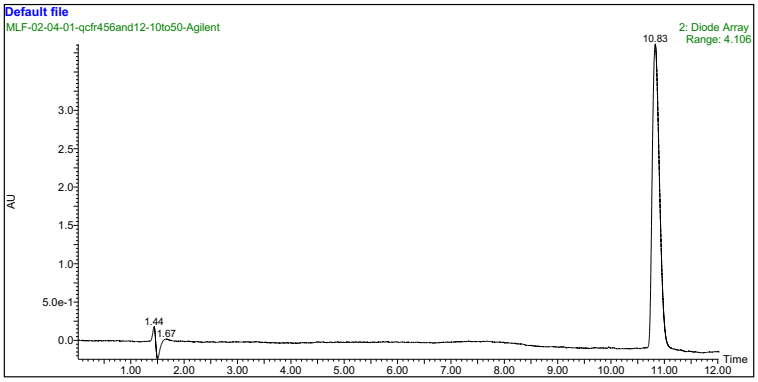

AYPGKA-NH_2:

t_R = 9.71 min; gradient = 5% to 30% (solvent A in solvent B, 0 to 10 min)

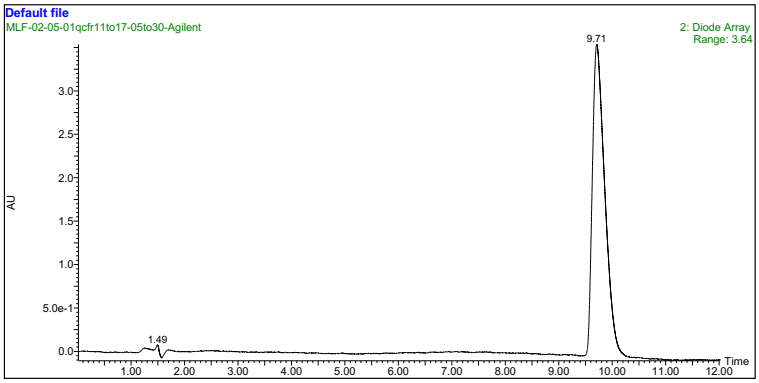

aYPGKF-NH_2:

t_R = 10.06 min; gradient = 10% to 50% (solvent A in solvent B, 0 to 10 min)

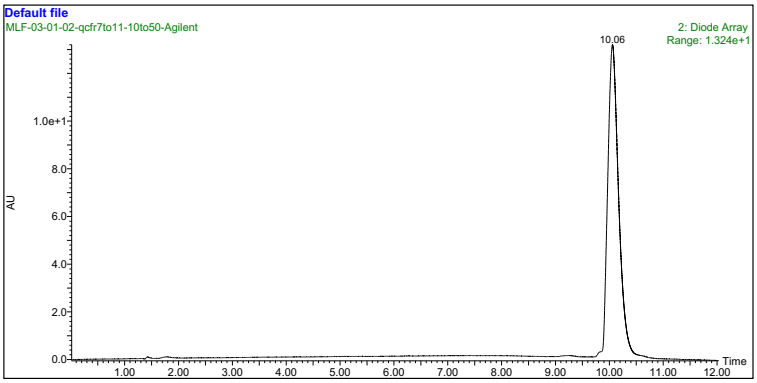

AyPGKF-NH_2:

t_R = 9.49 min; gradient = 15% to 50% (solvent A in solvent B, 0 to 10 min)

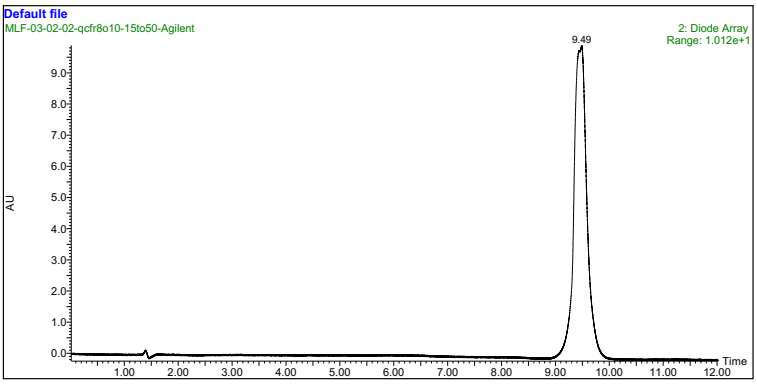

AYPGkF-NH_2:

t_R = 9.17 min; gradient = 10% to 70% (solvent A in solvent B, 0 to 10 min)

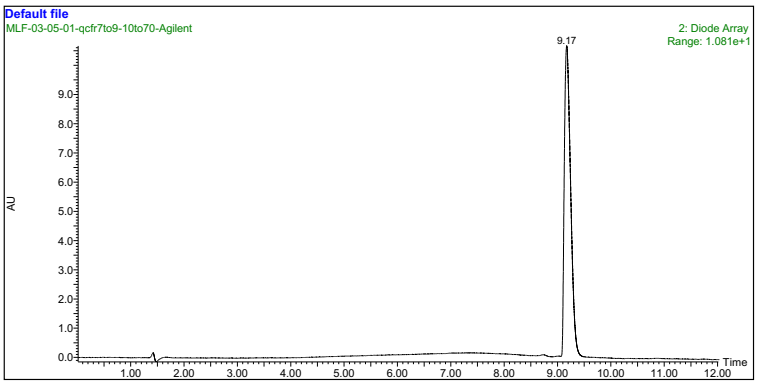

AYPGKf-NH_2:

t_R = 9.04 min; gradient = 10% to 70% (solvent A in solvent B, 0 to 10 min)

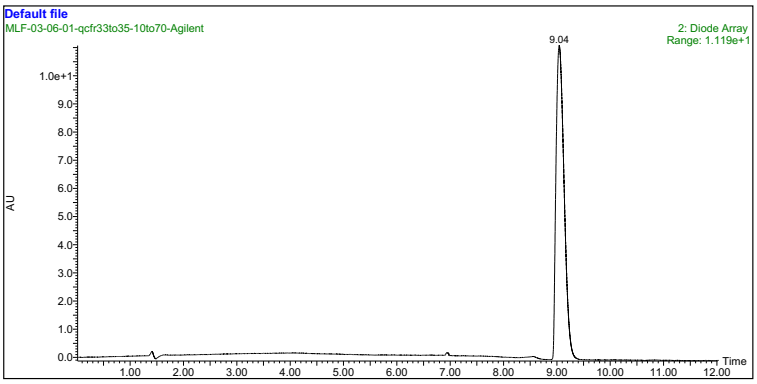

Aib-YPGKF-NH_2:

t_R = 9.35 min; gradient = 10% to 70% (solvent A in solvent B, 0 to 10 min)

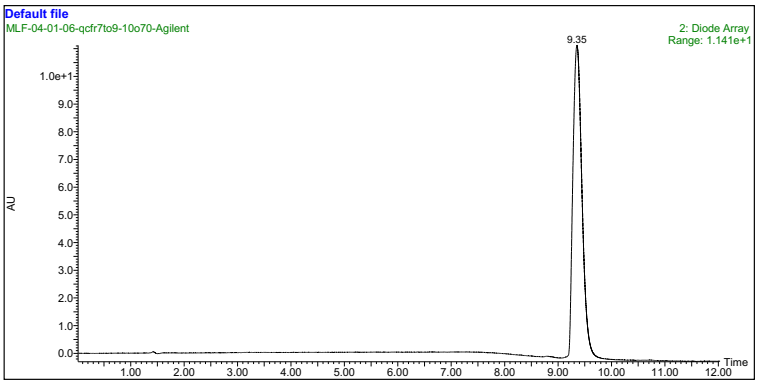

Sar-YPGKF-NH_2:

t_R = 9.23 min; gradient = 10% to 70% (solvent A in solvent B, 0 to 10 min)

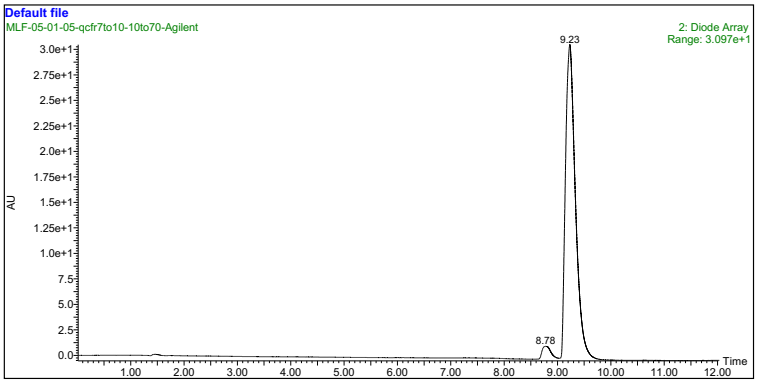

Inp-YPGKF-NH_2:

t_R = 9.26 min; gradient = 10% to 70% (solvent A in solvent B, 0 to 10 min)

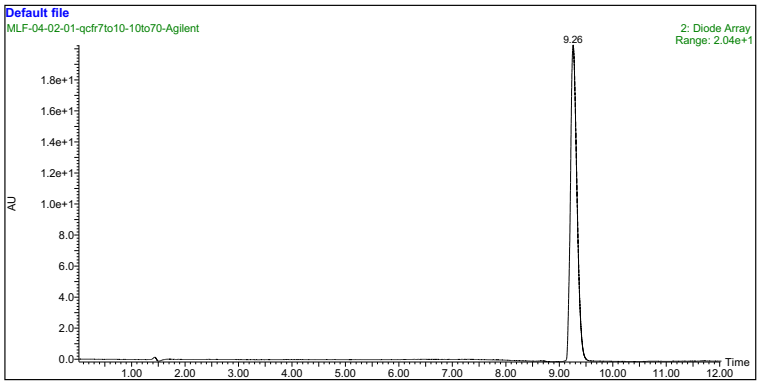

betaAla-YPGKF-NH_2:

t_R = 9.34 min; gradient = 10% to 70% (solvent A in solvent B, 0 to 10 min)

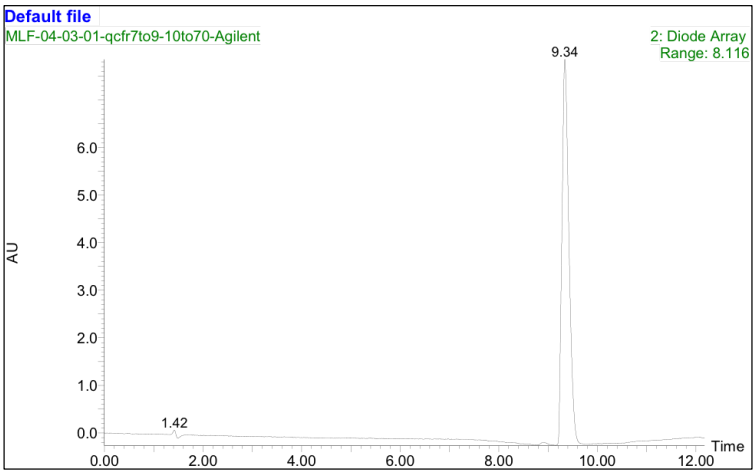

A-Tyr(Me)-PGKF-NH_2:

t_R = 9.57 min; gradient = 13% to 70% (solvent A in solvent B, 0 to 10 min)

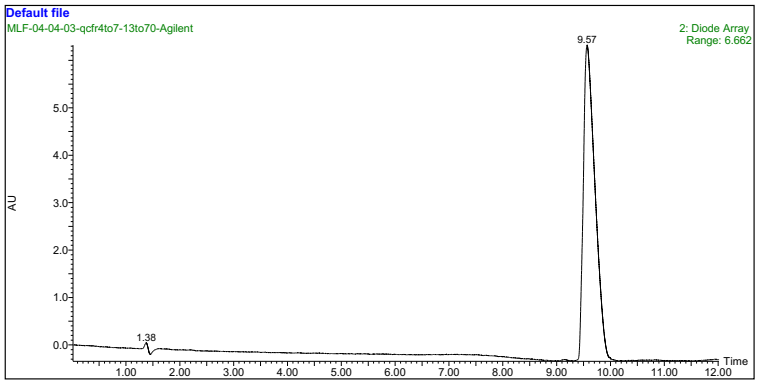

A-F(4-fluoro)-PGKF-NH_2:

t_R = 9.63 min; gradient = 13% to 70% (solvent A in solvent B, 0 to 10 min)

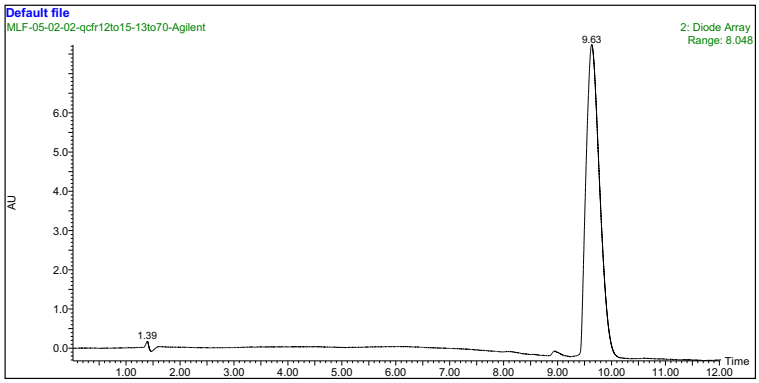

AY-Pip-GKF-NH_2:

t_R = 9.25 min; gradient = 13% to 70% (solvent A in solvent B, 0 to 10 min)

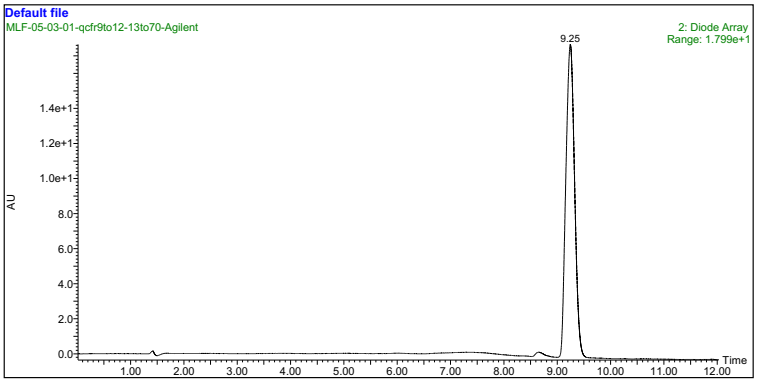

AY-Nip-GKF-NH_2:

t_R = 8.77 min; gradient = 13% to 70% (solvent A in solvent B, 0 to 10 min)

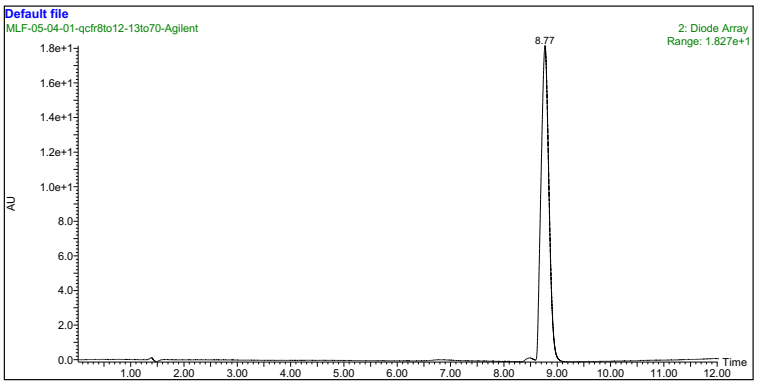

AYP-Sar-KF-NH_2:

t_R = 9.56 min; gradient = 10% to 60% (solvent A in solvent B, 0 to 10 min)

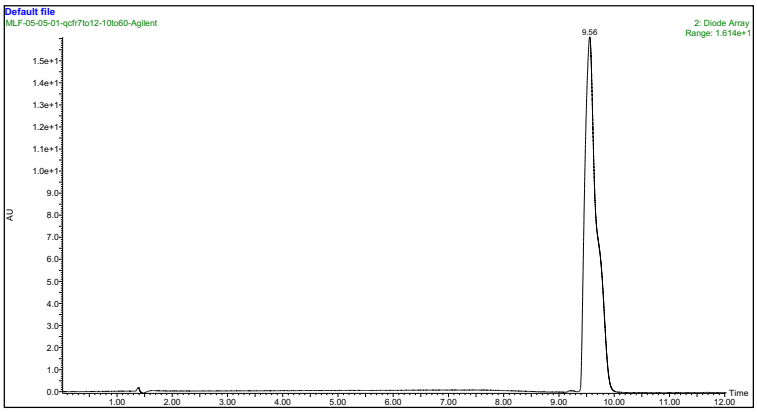

AYP-betaAla-KF-NH_2:

t_R = 9.38 min; gradient = 10% to 70% (solvent A in solvent B, 0 to 10 min)

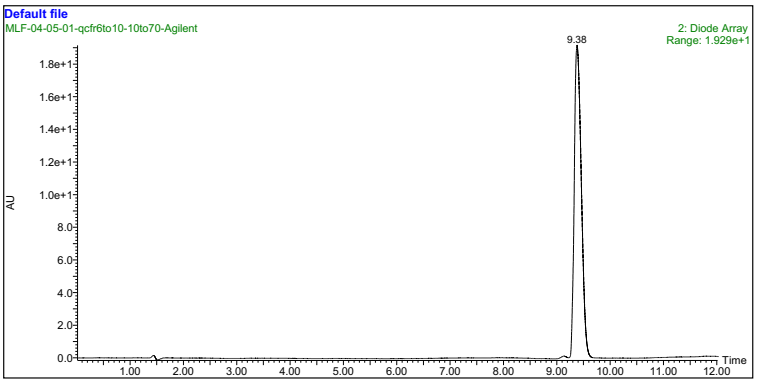

AYPGK-1Nal-NH_2:

t_R = 9.71 min; gradient = 13% to 70% (solvent A in solvent B, 0 to 10 min)

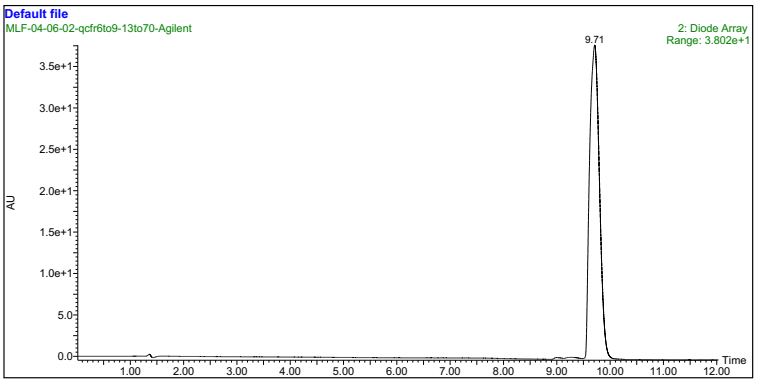

AYPGK-2Nal-NH_2:

t_R = 9.72 min; gradient = 13% to 70% (solvent A in solvent B, 0 to 10 min)

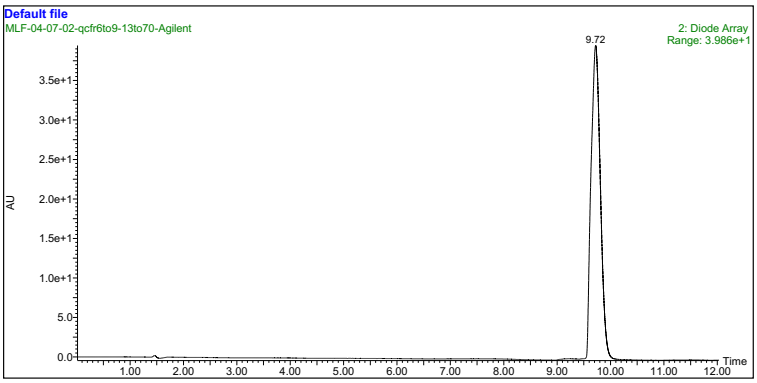

AYPGK-F(4-fluoro)-NH_2:

t_R = 8.91 min; gradient = 13% to 70% (solvent A in solvent B, 0 to 10 min)

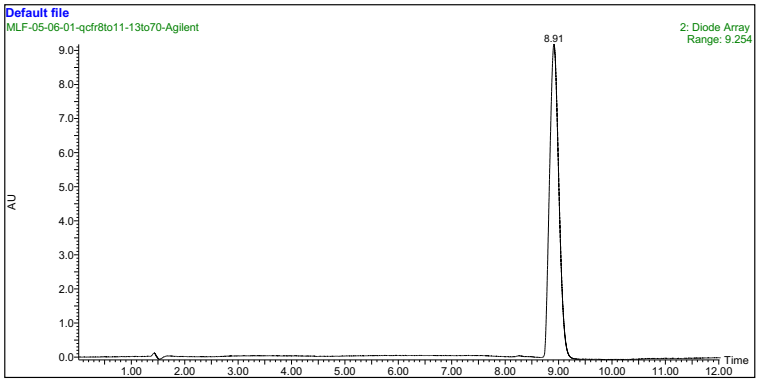

AYPGK-F(4-Me)-NH_2:

t_R = 9.32 min; gradient = 13% to 70% (solvent A in solvent B, 0 to 10 min)

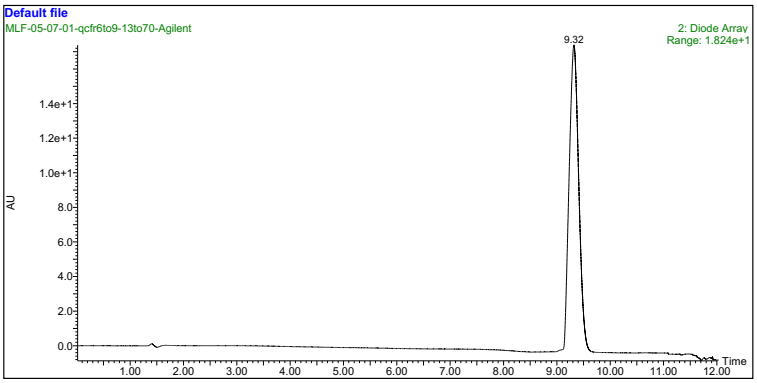

AYpGKF-NH_2:

t_R = 9.02 min; gradient = 12% to 75% (solvent A in solvent B, 0 to 10 min)

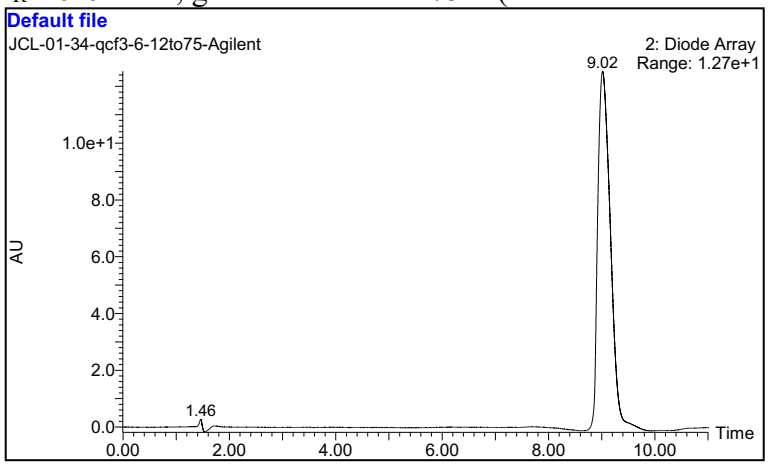

AYPGK-(*N*-Me-F)-NH_2:

t_R = 8.73 min; gradient = 12% to 80% (solvent A in solvent B, 0 to 10 min)

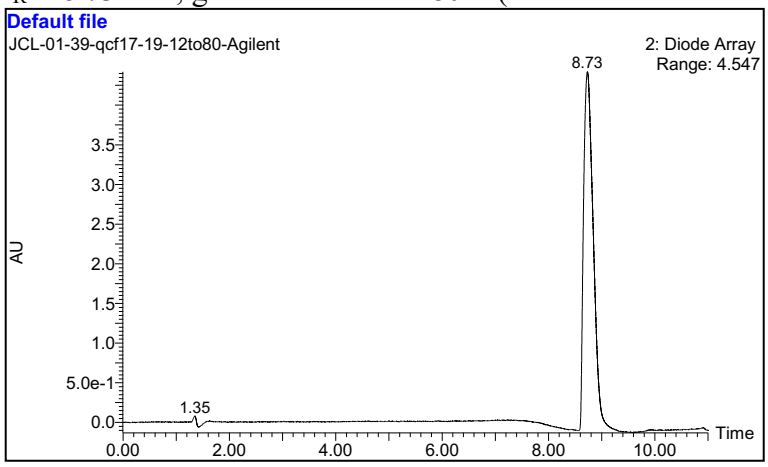

AYPG-(N_α-Me-K)-F-NH_2:

t_R = 8.33 min; gradient = 15% to 70% (solvent A in solvent B, 0 to 10 min)

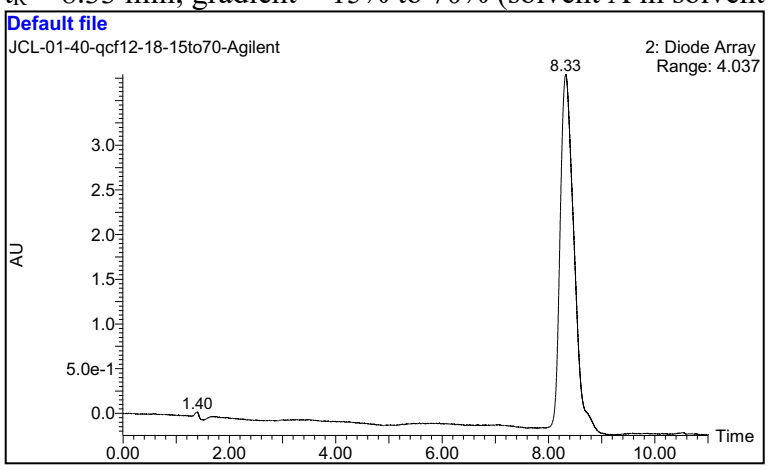

1757 A-(*N*-Me-Y)-PGKF-NH_2:

1758 t_R = 8.74 min; gradient = 12% to 70% (solvent A in solvent B, 0 to 10 min)

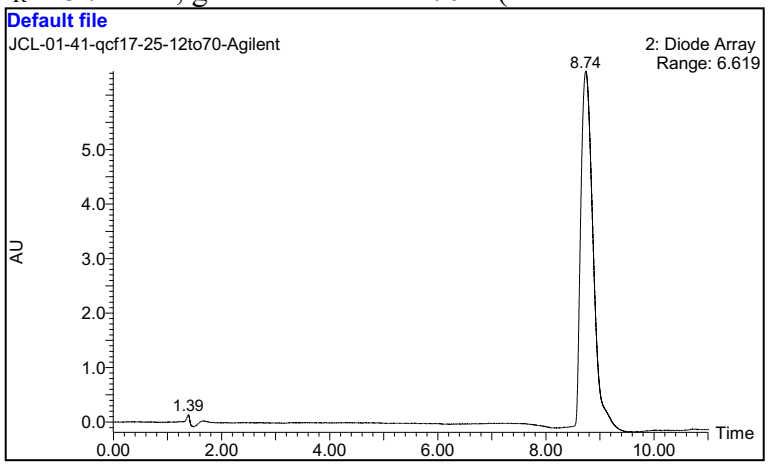

1759

1760

1761 (*N*-Me-A)-YPGKF-NH_2:

1762 t_R = 8.88 min; gradient = 12% to 70% (solvent A in solvent B, 0 to 10 min)

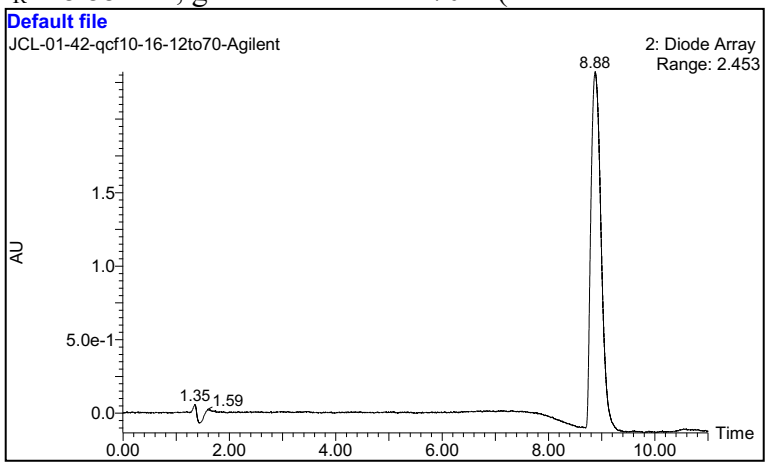

1763

1764

1765 VYPGKF-NH_2:

1766 t_R = 8.90 min; gradient = 12% to 70% (solvent A in solvent B, 0 to 10 min)

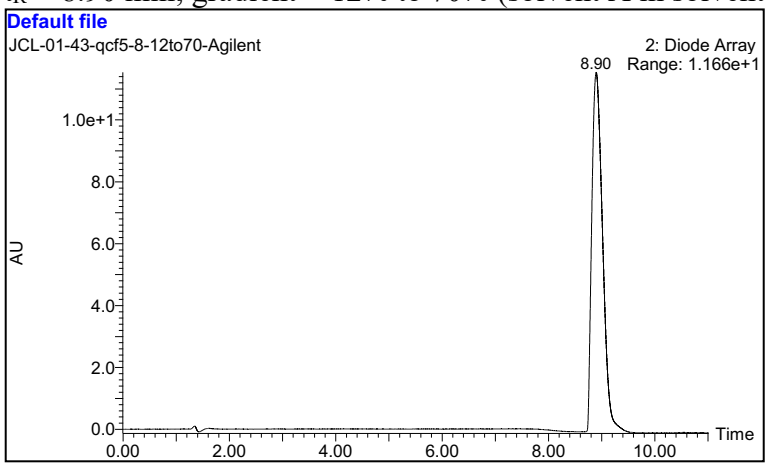

1767

1768

1769

1770

1771

1772

1773 (*N*-Me-S)-YPGKF-NH_2:

1774 t_R = 9.00 min; gradient = 13% to 70% (solvent A in solvent B, 0 to 10 min)

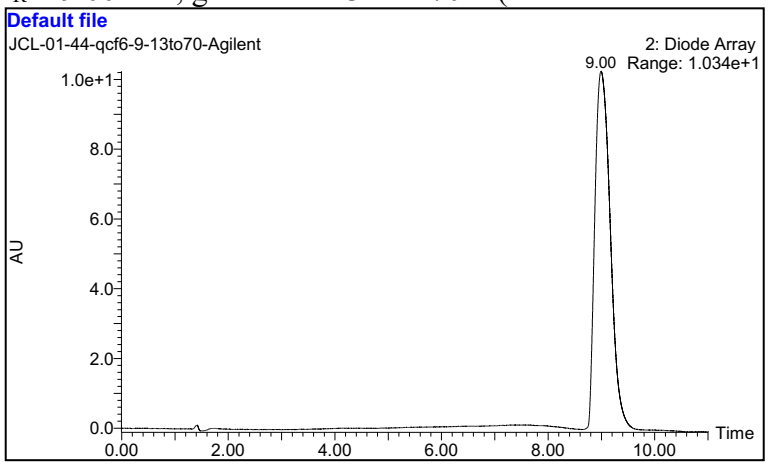

1775
1776

1777 Nle-YPGKF-NH_2:

1778 t_R = 8.88 min; gradient = 15% to 70% (solvent A in solvent B, 0 to 10 min)

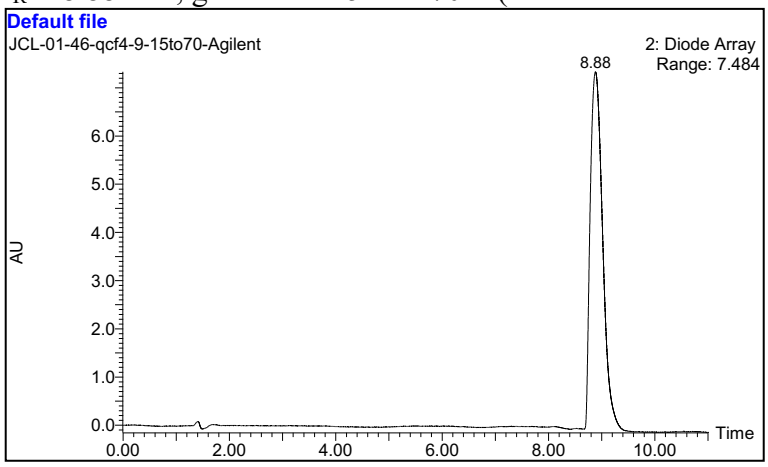

1779
1780

1781 AYPGRF-NH_2:

1782 t_R = 8.73 min; gradient = 13% to 70% (solvent A in solvent B, 0 to 10 min)

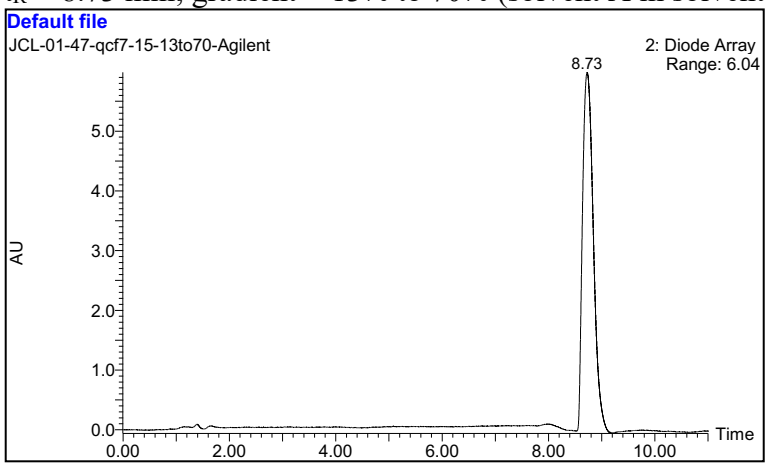

1783
1784
1785
1786
1787
1788

AYPGOF-NH_2:

t_R = 9.16 min; gradient = 12% to 80% (solvent A in solvent B, 0 to 10 min)

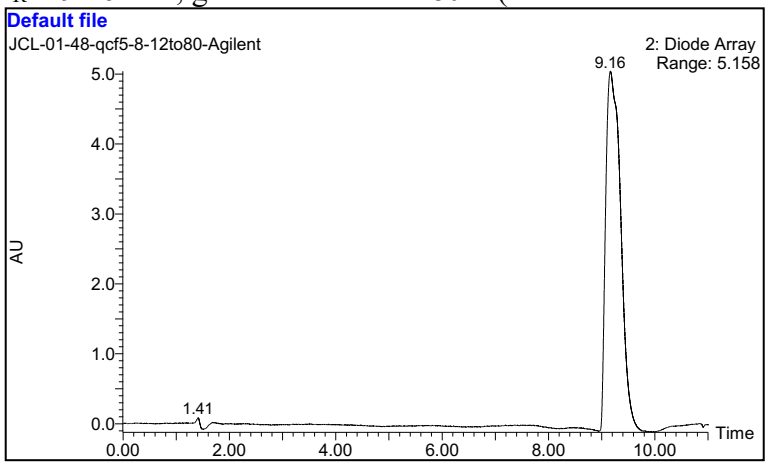

AYPG-Cit-F-NH_2:

t_R = 8.82 min; gradient = 13% to 80% (solvent A in solvent B, 0 to 10 min)

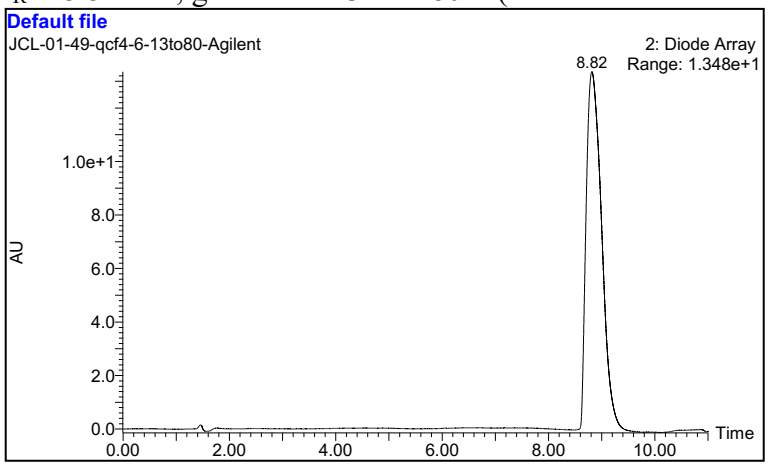

AYPG-(N_ε-Me-K)-F-NH_2:

t_R = 8.74 min; gradient = 12% to 70% (solvent A in solvent B, 0 to 10 min)

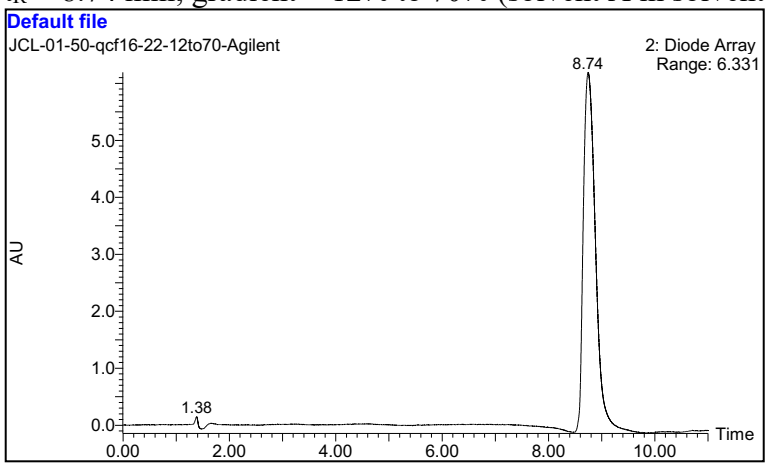

AYPGKY-NH_2:

t_R = 8.88 min; gradient = 8% to 80% (solvent A in solvent B, 0 to 10 min)

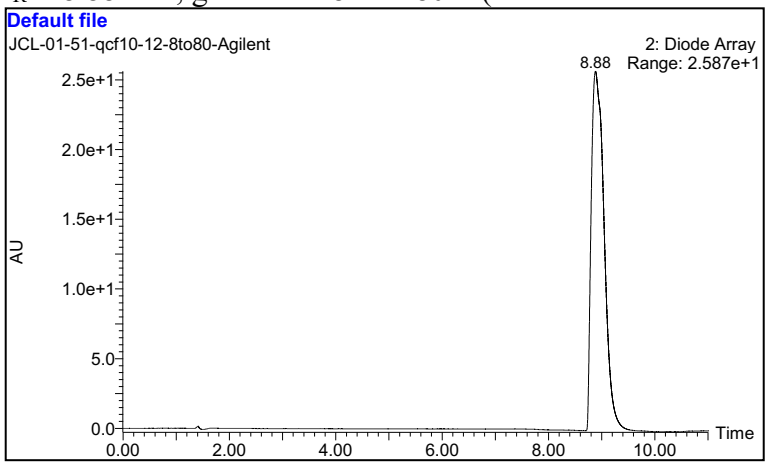

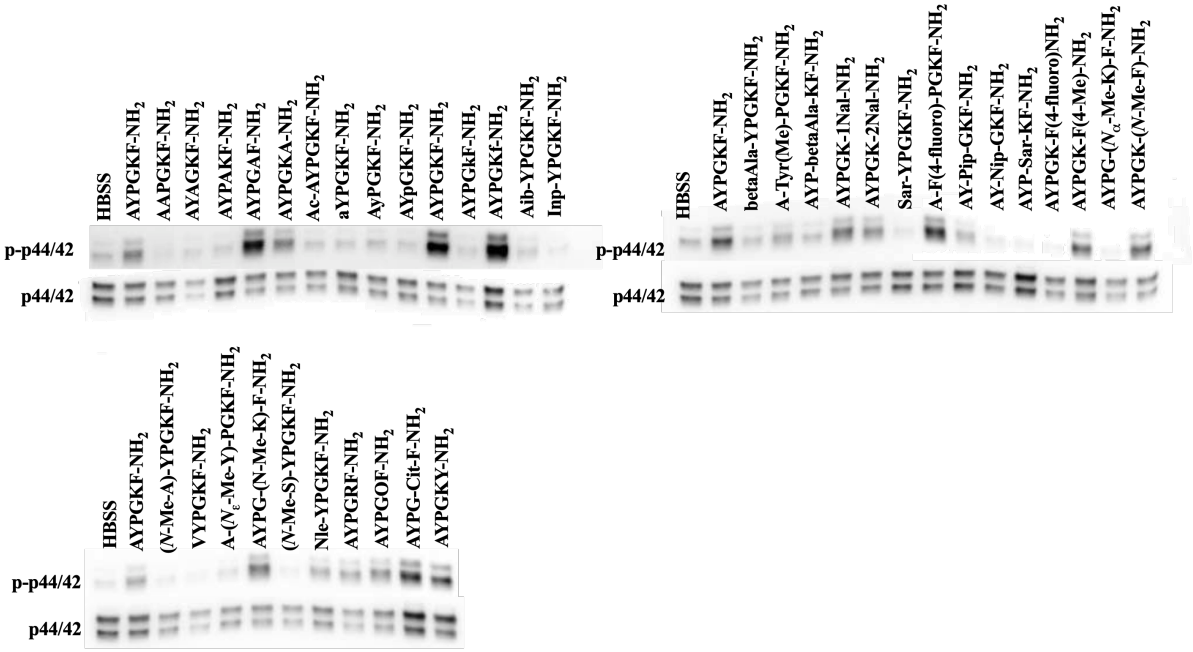

Figure S2. Representative blots of ERK phosphorylation in response to 100 μM of AYPGKF-NH_2 and derivative peptides. Data are summarized in figure 10.

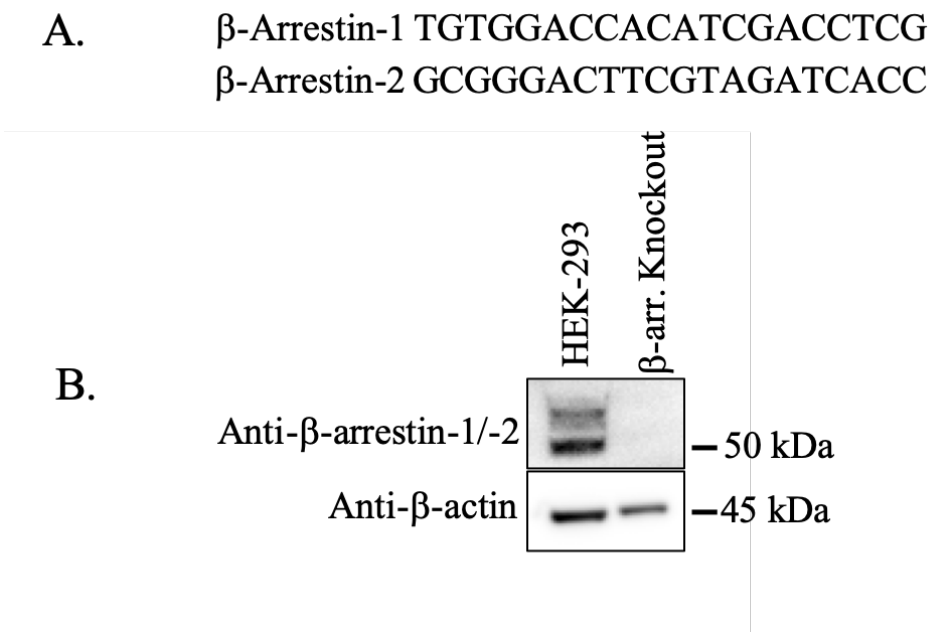

1810 **Figure S3. (A) Guide RNA sequences designed to target either β-arrestin-1 or -2. (B)**
1811 **Representative blots of β-arrestin-1/-2 protein from HEK-293 and β-arrestin-1/-2 double**
1812 **knockout HEK-293 (β-arr. Knockout) cells.** We observe no β-arrestin-1/-2 protein in the β-
1813 arr. knockout HEK-293 cell line.

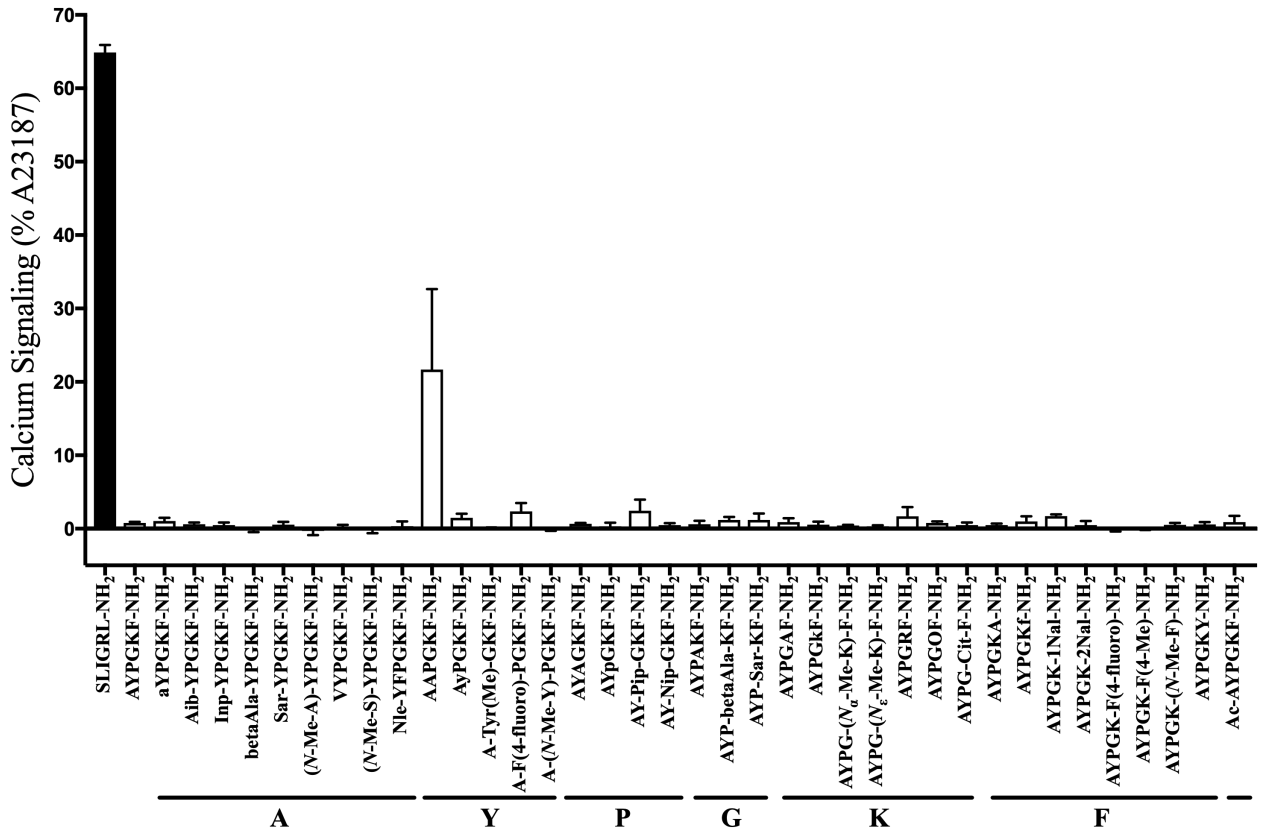

1814 **Figure S4. PAR4 peptide library is specific for PAR4 as shown by lack of calcium**
1815 **signalling in HEK-293 cells which do not endogenously express PAR4. Peptide AAPGKF-**
1816 **NH_2 was found to have basal fluorescence even in the absence of cells. (*n* = *3*)**

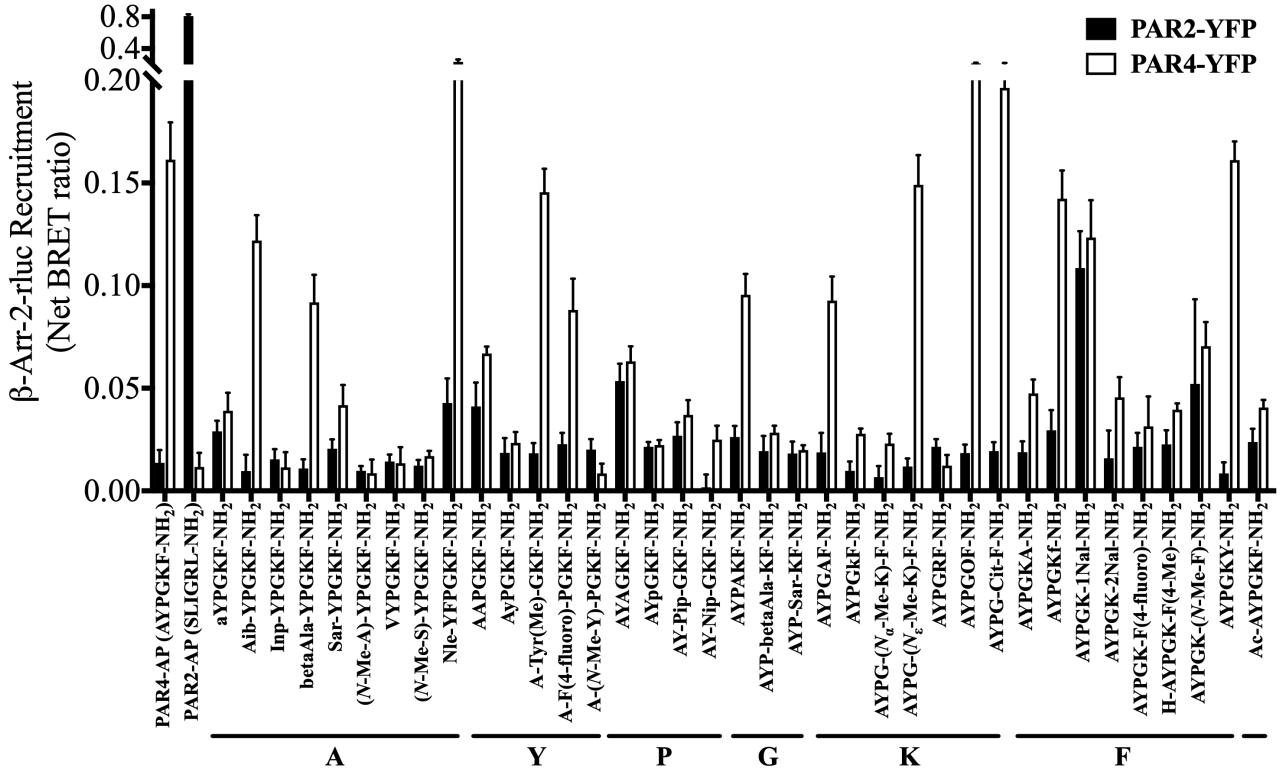

Figure S5. PAR4 peptide library is specific for PAR4 and does not cause recruitment of β-arrestin-2 to PAR2 (shown as black bars) at 100 µM, with the exception of AYPGK-1Nal-NH_2 which shows some β-arrestin recruitment to PAR2. BRET ratios obtained with the parental peptides for both PAR4 (AYPGKF-NH_2) and PAR2 (SLIGRL-NH_2) are shown. (*n* = *3*)